Final Report

A STUDY OF THE APPLICABILITY OF SOLAR ELECTRIC PROPULSION

F. I. Mann
J. L. Horsewood

Report No. 71-43
Contract NAS5-11364
December 1971

ANALYTICAL MECHANICS ASSOCIATES, INC.
10210 GREENBELT ROAD
SEABROOK, MARYLAND 20801

79

SUMMARY

This report summarizes the work performed under Contract NAS5-11364, which consisted of a one-year study to determine the applicability of solar-electric propulsion as a means of primary propulsion for the unmanned exploration of the solar system. Missions to a wide variety of solar system targets were investigated, including Venus, Mars, Jupiter, Saturn, Uranus, Neptune, Pluto, Ceres, Eros, Geographos, Icarus, D'Arrest, and Encke.

TABLE OF CONTENTS

Summary ii

I. INTRODUCTION 1

II. SOFTWARE DEVELOPMENT 2

III: NUMERICAL RESULTS 5

IV. NEW TECHNOLOGY 12

References 75

I. INTRODUCTION

This report summarizes the work performed under Contract NAS5-11364. The objective of this work is to expand our awareness of how solar-electric propulsion (SEP) can be used as a means of primary propulsion in the unmanned exploration of the solar system. This objective has been met by the publication of the numerical results of this report and the concurrent publication of [5], which augment the data previously published in [1, 2, 3, 4].

The numerical data presented in this report help to answer a wide variety of specific questions regarding the usefulness of solar-electric propulsion, in contrast to the data presented concurrently in [5], which represent a narrow but consistent view of SEP's usefulness for planetary exploration between 1975 and 1990.

This report features SEP performance requirements for Pluto missions (omitted from previous publications because of Pluto's relatively highly eccentric and inclined orbit), for missions to "new" targets (Eros, Geographos, Icarus) heretofore not investigated by the authors, and for missions using the small Delta launch vehicle. Also featured is a preliminary assessment of the penalties due to the spacecraft design constraints of a constant thrust-angle and a specified propulsion time.

Concurrent with the generation of new SEP data has been the task of updating and improving the associated computer software [6, 7, 8] and the implementation of computer graphics in the aid of SEP data generation [9]. Also, a study of the truncation effects in geopotential modeling was conducted and the results were applied to gravity anomaly data [10].

II. SOFTWARE DEVELOPMENT

Several modifications were made to the HILTOP computer program, and the report describing HILTOP has been updated and is being published concurrently [6]. The first part of this section sketches the basic program modifications made to HILTOP, and the reader is referred to [6] for the mathematical analysis and other details.

HILTOP's spacecraft model was altered to include the option of simulating optimum missions in which the spacecraft's thrust vector maintains a single, constant angle to the sun-spacecraft line throughout each trajectory. This constant thrust angle θ_T (also referred to as a thrust cone angle or a cone angle) may be held fixed or may be optimized. Some of the penalties associated with this spacecraft design constraint are given in the next section.

The capability of simulating optimum missions in which the total propulsion time t_p is constrained to be a specified value was incorporated into HILTOP. The basic penalties associated with this mission constraint are also given in the next section. Simulations of missions having the above two constraints required extensive modifications to the HILTOP program.

The capability of assessing the performance of orbiter missions in which the electric propulsion system provides the energy for the capture maneuver about the target planet has been added to HILTOP. The program was also modified to compute, for flyby missions, a ballistic swingby of the primary target followed by ballistic flight to an additional target. Such mission profiles are particularly useful for optimum SEP outer planet swingbys. Another capability was added in which launch-vehicle-independent data may be generated. Such data may then be related to any specific launch vehicle, which may lead to the optimum result of an off-loaded launch vehicle configuration, such that the full payload capability of the launch vehicle should not be used.

Fixed-conic ephemerides of several comets and asteroids have been added internally to the program, specifically Ceres, Icarus, Eros, Geographos, D'Arrest, and Encke. Also, several algorithms which help to circumvent the numerical difficulties associated with generating optimum electric propulsion trajectory data have been added to the program. Again, details concerning these features may be found in [6].

The SWINGBY computer program [7] has been modified to include the capability of integrating the differential equations by means of a seventh-order Runge-Kutta scheme. The basic lesson which has been learned regarding various integration schemes and optimal electric propulsion trajectory simulation is that predictor-corrector schemes tend to perform poorly due to the presence of several thrust switching points along a trajectory. Such points require restarting a predictor-corrector scheme, which introduces significant numerical noise into the two-point-boundary-value-problem, thereby preventing convergence in many instances. Runge-Kutta schemes, although generally slower and possibly even less accurate, do not suffer from this malady.

A technique has been developed in which the optimal electric propulsion trajectory problem may be solved with the aid of interactive computer graphics. This is described in a report which is being published concurrently [9]. Briefly, an appropriate two-dimensional projection of the trajectory is displayed on the computer's television screen, and a man-in-the-loop varies selected trajectory starting conditions in the fashion of a nonlinear walk until the viewed trajectory endpoint lies near a displayed target. Once global targeting is accomplished in this manner, program internal logic can easily handle local targeting to produce strong convergence.

The CHEBYTOP software package [8] has been acquired by AMA, Inc. and linked to a newly-created driver routine which optimizes several mission

parameters and can simulate round-trip, sample-return electric propulsion missions. The CHEBYTOP package combined with the AMA driver has been named AMATOP and is currently proving useful in generating crude mission mappings for defining general regions of interest.

A user's report was written for the ADMAP computer program [11]. This program, which generated the graphical presentation of [1, 2, 3], was modified to produce the format of the concurrently published report [5].

III. NUMERICAL RESULTS

As mentioned in the introduction, a concurrent report is being published [5] which presents a consistent view of SEP planetary mission possibilities between 1975 and 1990. That block of data consists of approximately 500 pages and is published separately from this report because it represents essentially a complete work in itself. The remainder of this section describes the graphical data presented in this report, which have been generated in response to specific requests for SEP information and also to satisfy specific contractual tasks.

Figures 1 through 6 present SEP performance requirements for Pluto missions (three-dimensional). Pluto opportunities occur every year, and 1980 was chosen as a representative year to investigate. The variation of performance requirements from opportunity to opportunity may be found in [5]. The powerplant specific mass α is 30 kg/kw and the tankage factor is .03 throughout this report unless specified otherwise. The launch vehicle assumed for Figures 1 through 5 is the Titan III B (core)/Centaur. For these Figures, the net spacecraft mass is maximized, and the parameters reference thrust acceleration, jet exhaust speed, departure date, and departure and arrival hyperbolic excess speeds are optimized. Normal projected state-of-the-art technology is assumed for the SEP spacecraft and trajectory model (see [5] for details). For orbiter missions, the SEP powerplant and tankage are jettisoned prior to orbit insertion, and a chemical retro stage performs an implicitly-optimal impulsive braking maneuver at the periapse of the capture orbit at a distance of 2 planet radii from the center of Pluto. The resulting capture orbit has an apoapse distance of 38 planet radii from the center of Pluto. The retro stage inert factor, k_r, is the same as in [1, 2, 3, 4, 5], specifically 0.11111. Pluto's gravitational constant is taken to be 3.317819×10^5 km^3/sec^2 and Pluto's radius is assumed to be 6349 km. The scaling factors following the name of each plotted quantity are easy to interpret. For instance, if a quantity has an apparent value of

2 and a scaling factor of 100, then its true value is 200. When the scaling factor is absent, it is assumed to be unity. The specific definitions of the spacecraft parameters and Lagrange multipliers may be found in [5]. The Mode A and Mode B missions correspond to approximately $\frac{1}{2}$ and $1\frac{1}{2}$ revolutions around the sun, respectively.

Figure 6 shows the variation of net spacecraft mass with reference power (power at 1 au from the sun) assuming fixed launch date, flight time, and specific impulse, and using a Titan III D/Centaur launch vehicle. (The Titan III D/Centaur is also called Titan III D(1205)/Centaur elsewhere in this report. These two names refer to the same launch vehicle.)

Figures 7 through 12 show performance requirements for SEP missions to the comet Encke in 1980 and 1984. Encke is assumed to be at perihelion on December 6, 1980 and February 7, 1984. These data augment the Encke data found in [3]. Figures 10 and 11 give launch-vehicle-independent performance requirements as functions of launch hyperbolic excess speed, and Figure 12 shows these data applied to the Titan III D/Centaur. The corners in the various curves are reflections of the corner in the propulsion time curve, which separates the regions of full-thrusting and partial-thrusting. In Figure 12, the net spacecraft mass curves cross over each other and the launch vehicle payload curves do likewise at the value of launch excess speed (about 7.8 km/sec) at which the optimum reference power equals 15 kw. The dashed curves should actually not extend to the right of this cross-over point. The actual initial mass (launch vehicle payload) and net spacecraft mass may be obtained from Figure 10 simply by multiplying the curves by the desired SEP reference power. The resulting curve for initial mass may then be compared to any desired launch vehicle performance curves, such as those found in [12], to determine if a given launch vehicle can deliver a specified net spacecraft mass to Encke. This same analysis can be carried out for the curves of Figure 13. Figures 13 through 15 are similar to

Figures 10 through 12 except for the mission investigated, which is a representative Jupiter flyby mission. The data of Figures 10 through 15 have been previously presented in [13].

Figures 16 through 19 are designed to show the effect which limiting the propulsion time has on representative outer planet missions. Jupiter and Neptune flybys and orbiters were investigated. These data were generated under the same general assumptions as the data of Figures 1 through 5, and the graphs are of a similar format except that the independent variable is propulsion time rather than flight time. The launch vehicle is the Titan III B(core)/Centaur, the trajectories are three dimensional, and the orbiter missions assume 2 x 38 planet-radii capture orbits with jettisoning of SEP powerplant and tankage. The Jupiter missions are 1000 days and the Neptune missions are 5000 days, and all missions begin in late 1979 or early 1980. The rightmost end of the plotted curves (tic marks) represent the optimum propulsion time. The separately plotted points correspond to optimum burn time for constant, optimized thrust angle. An obvious conclusion derivable from these data is that the propulsion time can be substantially reduced for direct outer planet SEP missions without incurring a significant net spacecraft mass penalty. Also, such missions do not seem to be greatly affected by the constant thrust angle constraint. It also appears that the arrival SEP thrusting phase for outer planet orbiter missions may be discarded.

Figure 20 shows the effect of imposing the spacecraft design constraint of a constant thrust angle on a Mode A Jupiter flyby mission. The data were generated under the assumption of circular, coplanar orbits for Earth and Jupiter. The optimum constant thrust angle in this particular case is about 68°, at which point the net spacecraft mass is about 260 kg, which is about 18% below the optimum variable thrust angle value of about 315 kg. Some penalties associated with the constant thrust angle constraint may be seen in Figure 6, Figures 16 through 19, Figure 20 and Figure 25.

Figures 21 through 23 characterize the SEP Jupiter flyby "mission windows" for the 1978 and 1984 launch opportunities. The Titan III D(1205)/Centaur was assumed as the launch vehicle, and the SEP spacecraft was constrained to have a specific impulse of 3000 seconds and a reference power of 25 kilowatts. The SEP thrust vector was optimized along the trajectory, and only mission durations of 800 days were considered. The CHEBYTOP [8] computer program was used in the generation of these data. This computer program does not consider the possibility of departure asymptote declinations which might violate the due-east ETR launch of the launch vehicle model. However, some spot-checks using the HILTOP [6] trajectory program indicate that for Jupiter flybys the departure asymptote declination is always sufficiently small to allow due-east ETR launches.

Figures 21 and 22 present the net spacecraft mass as functions of Julian launch date for the 1978 and 1984 opportunities. The large peaks are the $\frac{1}{2}$-revolution class of trajectories (Mode A) and the smaller peaks are the $1\frac{1}{2}$-revolution class of trajectories (Mode B). The interesting thing about solar electric propulsion is that missions are always performable, whereas it is assumed that all-ballistic missions using the same launch vehicle would produce a net spacecraft mass curve lying beneath the Mode A portion of the SEP curve but dropping to zero somewhat symmetrically on either side of the peak.

The 1978 and 1984 curves are very similar, the only basic difference being the slightly greater net spacecraft masses in 1984. The 1978 peak mass is 1940 kg with 700 kg being launchable at any time, and the 1984 peak mass is 2120 kg with 850 kg being launchable at any time. The corresponding net mass penalties for assuming a perpetually launchable payload are 64% in 1978 and 60% in 1984.

Figure 23 was obtained from Figures 21 and 22 and presents the mission window widths for specified net spacecraft masses. Although these

data were generated for a specific mission duration, launch vehicle, and SEP parameters, their general form is considered to be representative of a broad range of SEP missions.

Figure 24 presents SEP mission performance capabilities for ten different missions and for four launch vehicles. The SEP reference power is given in parentheses. The Jupiter swingby mission consists of a ballistic continuation to Saturn. The current Delta vehicle is the TAT(3C)/Delta/TE364(1440) with a performance curve as given in [12].

Figure 25 presents Delta launch vehicle mission penalties compared to the all-optimized missions. Delta launch vehicle missions using SEP spacecraft having an optimized fixed thrust angle yield net spacecraft masses in the 50 to 150 kg. range with a spacecraft reference power level in the 2 to 3 kw. range. Such missions are economically feasible and might represent logical first steps in the evolution of SERT II technology for the exploration of the solar system.

Figures 26 through 33 show the trajectory profiles for the missions of Figure 24 (except the Jupiter missions). The data presented in Figures 24 through 33 were previously presented in [14].

Figures 34 through 38 pertain to 1400 day Saturn missions using the Titan III D/Centaur launch vehicle, including missions having a gravity-assist supplied by Jupiter. Figure 34 depicts a general swingby trajectory profile, and Figure 35 displays an actual Jupiter swingby to Saturn trajectory profile using solar electric propulsion and fully-optimized by the SWINGBY computer program [7]. Figure 36 gives comparative net spacecraft masses for 1400 day Saturn missions with and without an optimized Jupiter swingby maneuver. Numbers in parentheses are optimum SEP reference power in kw, and masses are in kg. Orbiter missions assume 2 x 38 capture orbits with SEP jettisoning.

Since the optimum reference power is greater than zero, inclusion of SEP always increases the net spacecraft mass compared to the corresponding all-ballistic mission. However, for the particular mission considered, it is not always advantageous to include a gravity-assist maneuver, as the orbiter results indicate. Only the Saturn flyby mission yields higher net spacecraft mass when the Jupiter gravity-assist is included.

Figures 37 and 38 illustrate the highly nonlinear nature of the optimum SEP swingby trajectory two-point-boundary-value-problem. Figure 37 indicates that it is optimal in terms of increasing net spacecraft mass to turn on the SEP engine for a very short period of time at Jupiter closest approach. However, the penalty due to discarding this small thrust phase is negligible, so that the SEP system may be conveniently discarded at 383 days into the mission.

The SWINGBY program was also used to investigate an optimum SEP Venus swingby to Mercury mission, but since optimum SEP swingby results are so difficult to obtain at present, only one mission opportunity could be investigated. This mission opportunity was a "fast" Venus swingby to Mercury, having a relatively short travel angle, and the SWINGBY program led to a local optimum solution requiring no SEP system, that is, an all-ballistic mission. It is therefore felt that fast Venus swingbys to Mercury will generally not require electric propulsion, and SEP will become advantageous only for missions having longer flight times and correspondingly larger travel angles.

Also accomplished as a task of the subject contract was a study leading to the concurrent publication of a scientific report "Truncation Effects in Geopotential Modeling" [10]. Part I is subtitled "Back to Page 1" and Part II is subtitled "Application to Gravity Anomaly Data".

In Part I, the effects of computational error inherently present in a least square fit of a geopotential model to a finite set of data points are studied.

It is shown that not only these errors, but also the determinacy of the model coefficients, depend on the number and distribution of the data points. Formulas which can be used for providing estimates of the computational error are given for a few distributions. A "good" distribution of data points, the Gaussian grid, is analysed in some detail. The fit to the Gaussian grid is carried out by weighted least squares; the weight factors may be thought of as a means of partially compensating for computational error.

In Part II, a study is made of the application of gravity anomaly data to geopotential modeling. The analysis differs from that of Part I, where least square fits of the geopotential to a finite number of data points were investigated. Here we consider instead a least square fit of gravity anomaly over the continuum of points on a sphere. The resulting integrals are approximated in various ways by sums over a finite number of area blocks. The results of the analysis are similar to those of Part I; the determinacy of the model, and the computational error incurred in the coefficients depend on the number, size and structure of the area blocks. No analogue of the Gaussian grid has been found, but the possibility of introducting weighting to compensate for the computational error is discussed. Some effects of systematic and random errors in the data on the analysis are described.

IV. NEW TECHNOLOGY

Reviews of the work carried out under the subject contract, which is summarized in the above sections, were conducted periodically during the course of the contract by the Principal Investigator with particular attention being given to possible contributions to New Technology. It is believed that significant advances have been made during the course of this work in the fields of electric propulsion mission and trajectory analysis and data generation and also in the field of geopotential field modeling. Steps are being taken to disseminate the new information to persons working in the respective fields. It is believed, however, that applications of the study results outside the fields of study is unlikely.

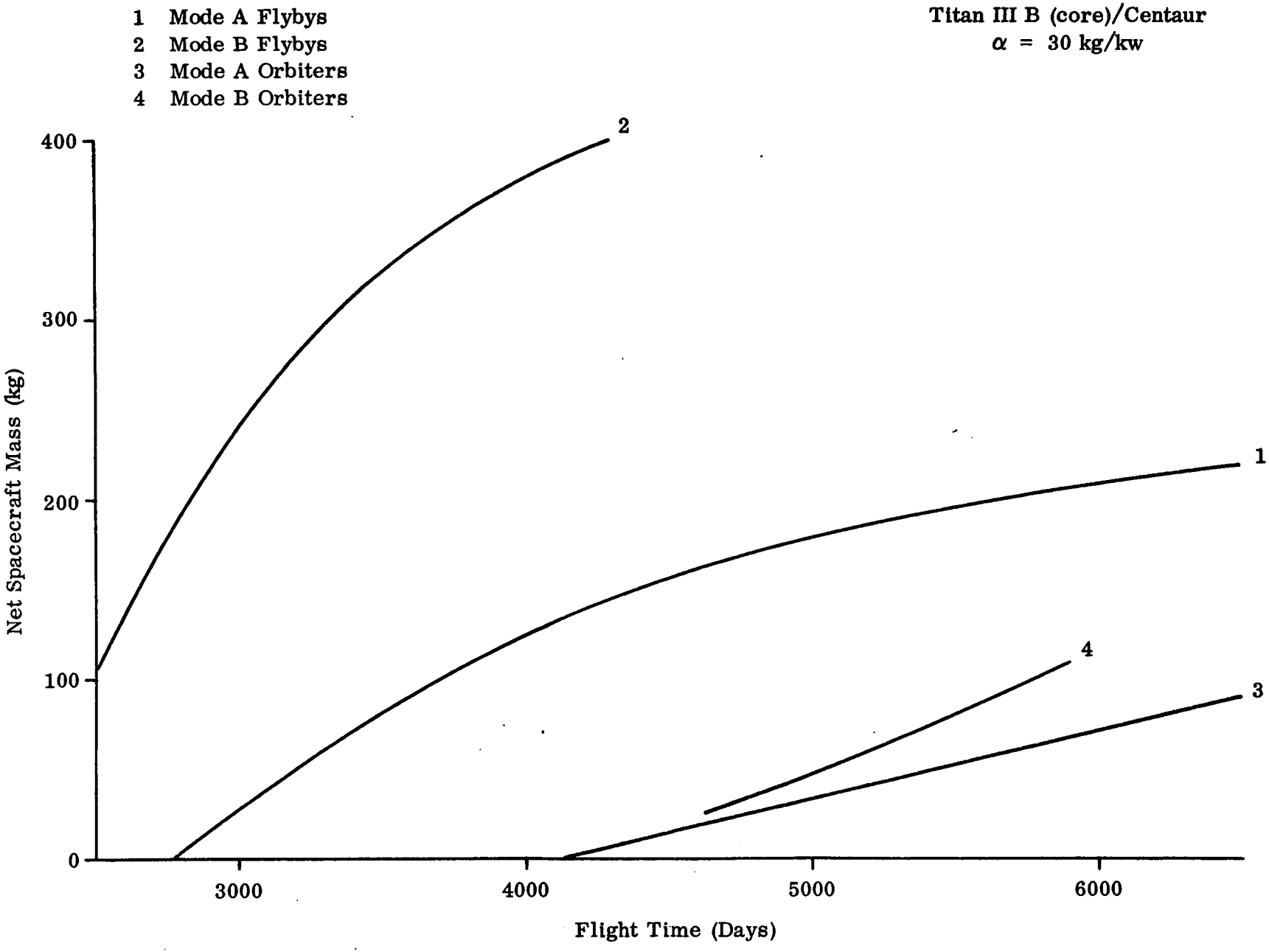

Fig. 1 1980 Pluto Missions Net Spacecraft Mass Summary

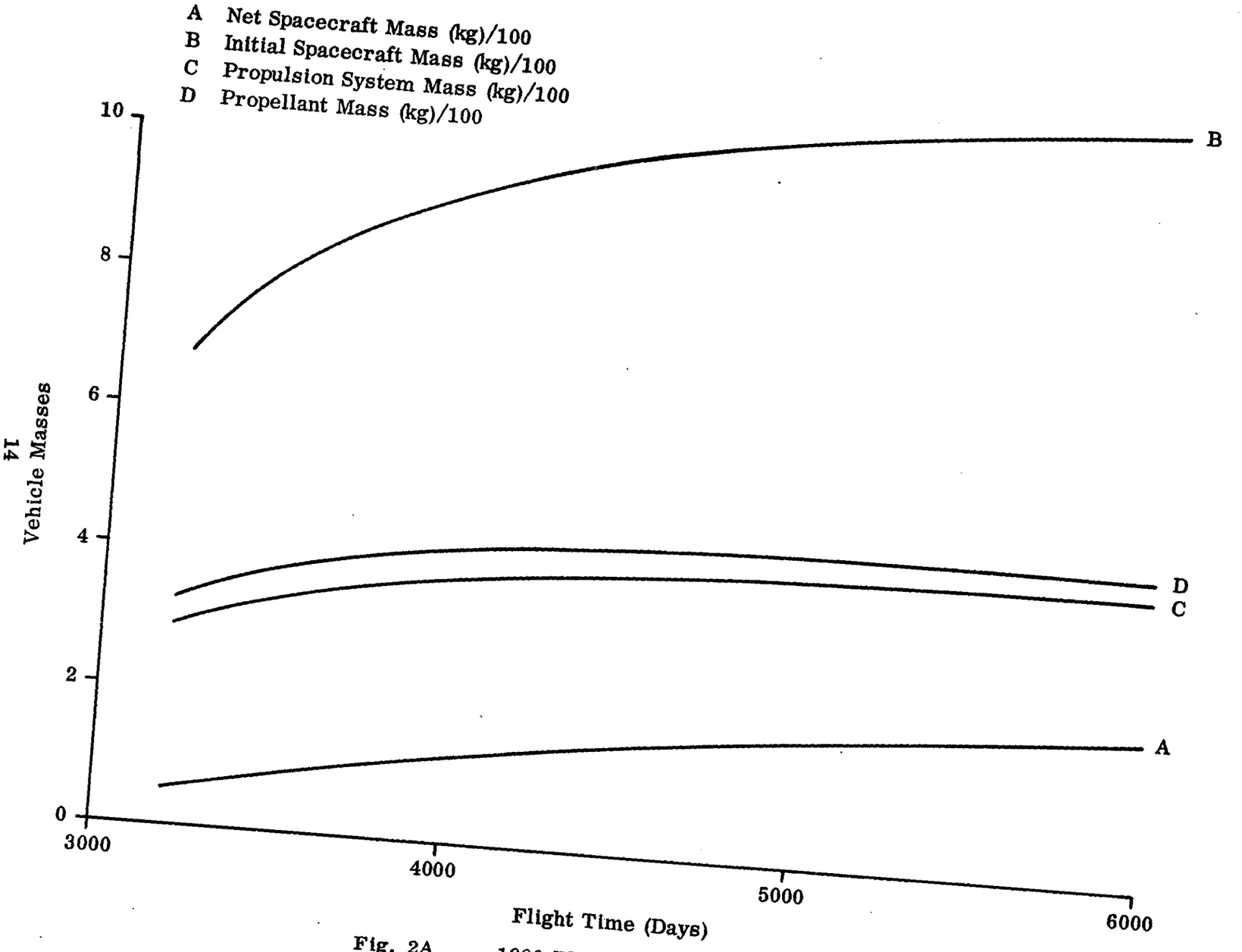

Fig. 2A 1980 Pluto Mode A Flyby Missions

F Reference Power (kw)/10
G Maximum Power (kw)/10
H Jet Exhaust Speed (m/sec)/10000
I Reference Thrust (newtons)/1. E-1
J Propulsion Time (days)/1000

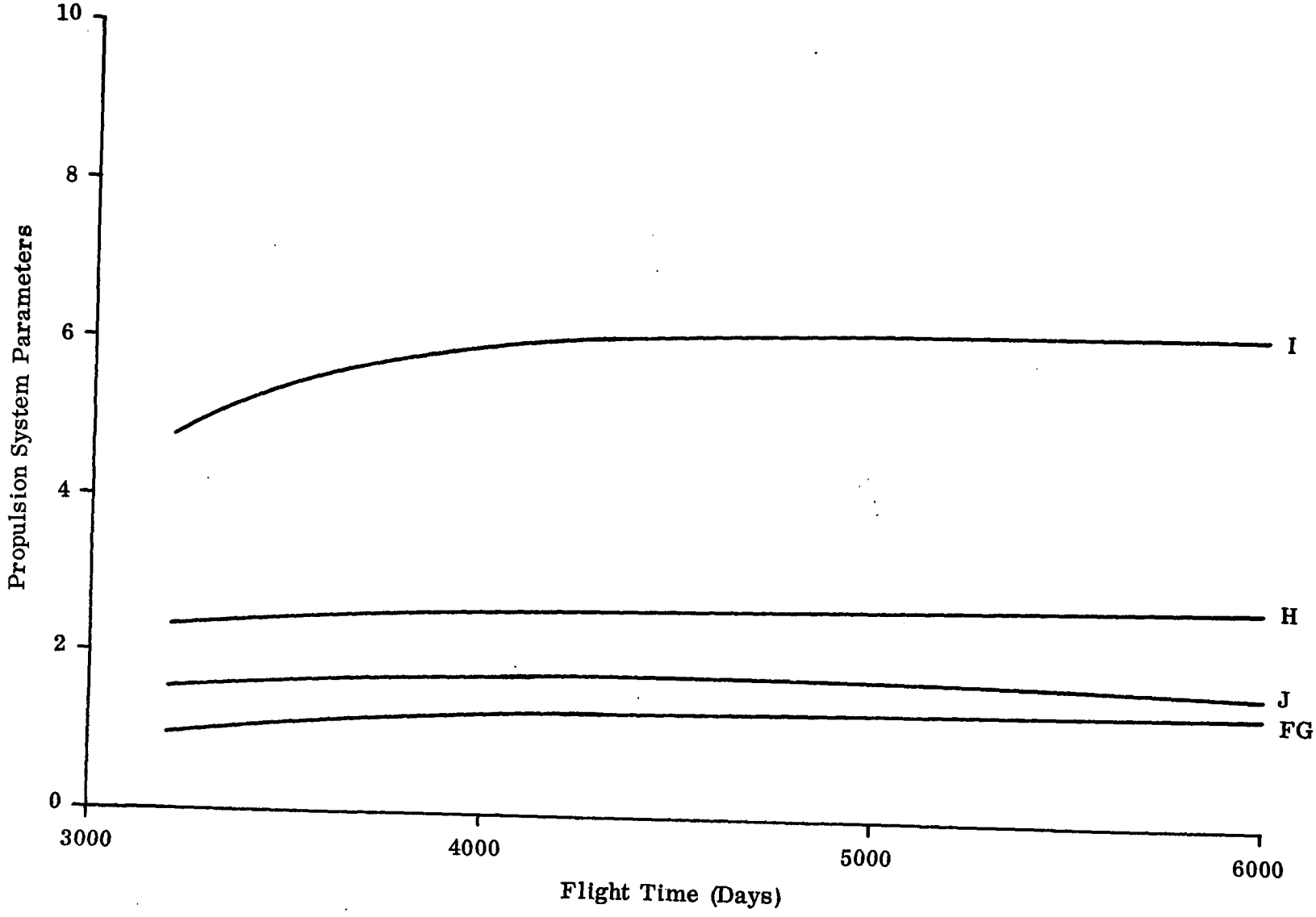

Fig. 2B 1980 Pluto Mode A Flyby Missions

K Maximum Solar Distance (au)/10
L Minimum Solar Distance (au)
M Heliocentric Travel Angle (deg)/100
N Launch Excess Speed (m/sec)/1000
O Arrival Excess Speed (m/sec)/10000
R Launch Date (Days from 2444487)/10

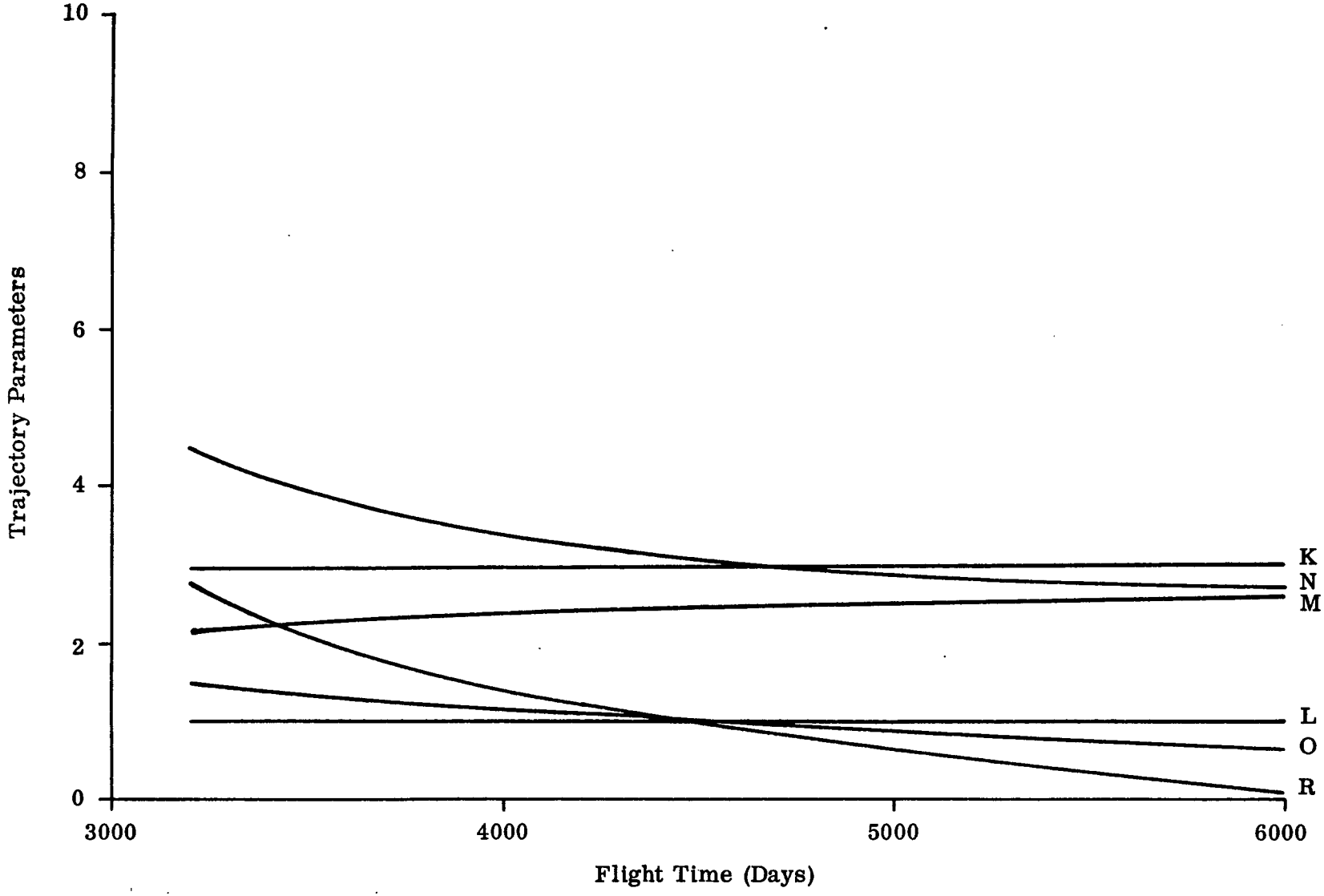

Fig. 2C 1980 Pluto Mode A Flyby Missions

U X-Component of Primer
V Y-Component of Primer
W Z-Component of Primer
X X-Component of Primer Derivative
Y Y-Component of Primer Derivative
Z Z-Component of Primer Derivative

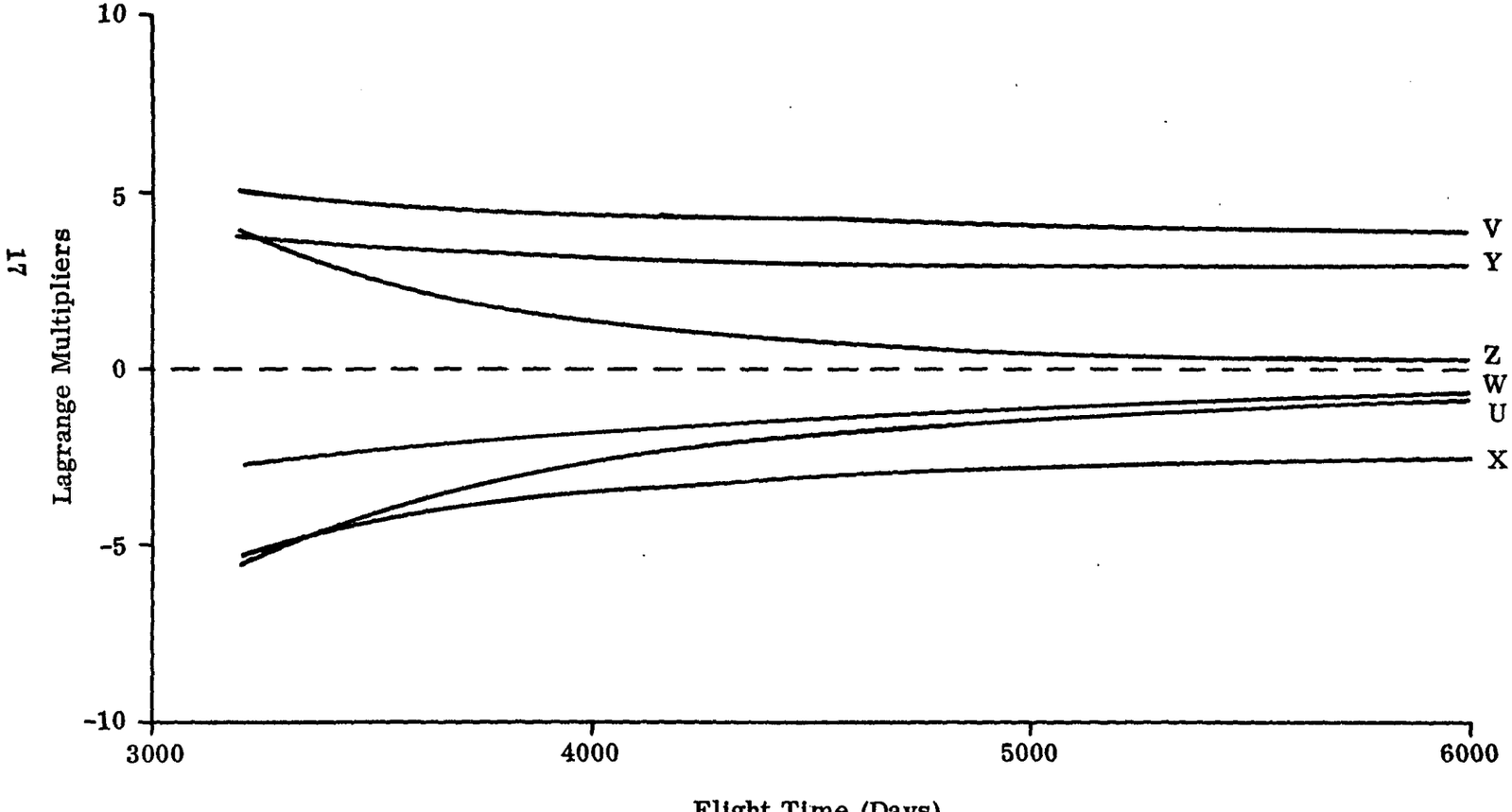

Fig. 2D 1980 Pluto Mode A Flyby Missions

A Net Spacecraft Mass (kg)/100
B Initial Spacecraft Mass (kg)/1000
C Propulsion System Mass (kg)/100
D Propellant Mass (kg)/100

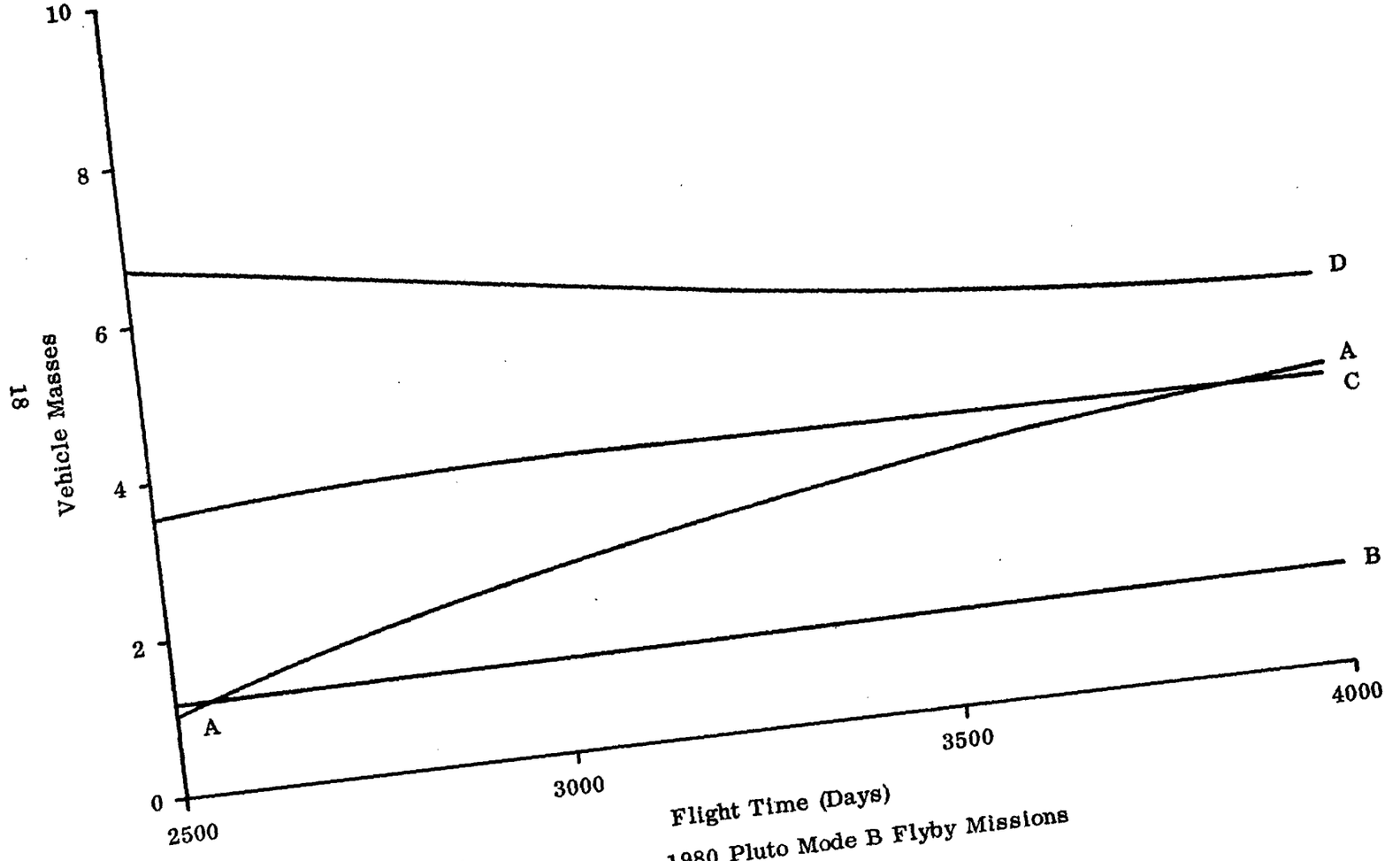

Fig. 3A 1980 Pluto Mode B Flyby Missions

F Reference Power (kw)/10
G Maximum Power (kw)/10
H Jet Exhaust Speed (m/sec)/10000
I Reference Thrust (newtons)/1.E-1
J Propulsion Time (days)/1000

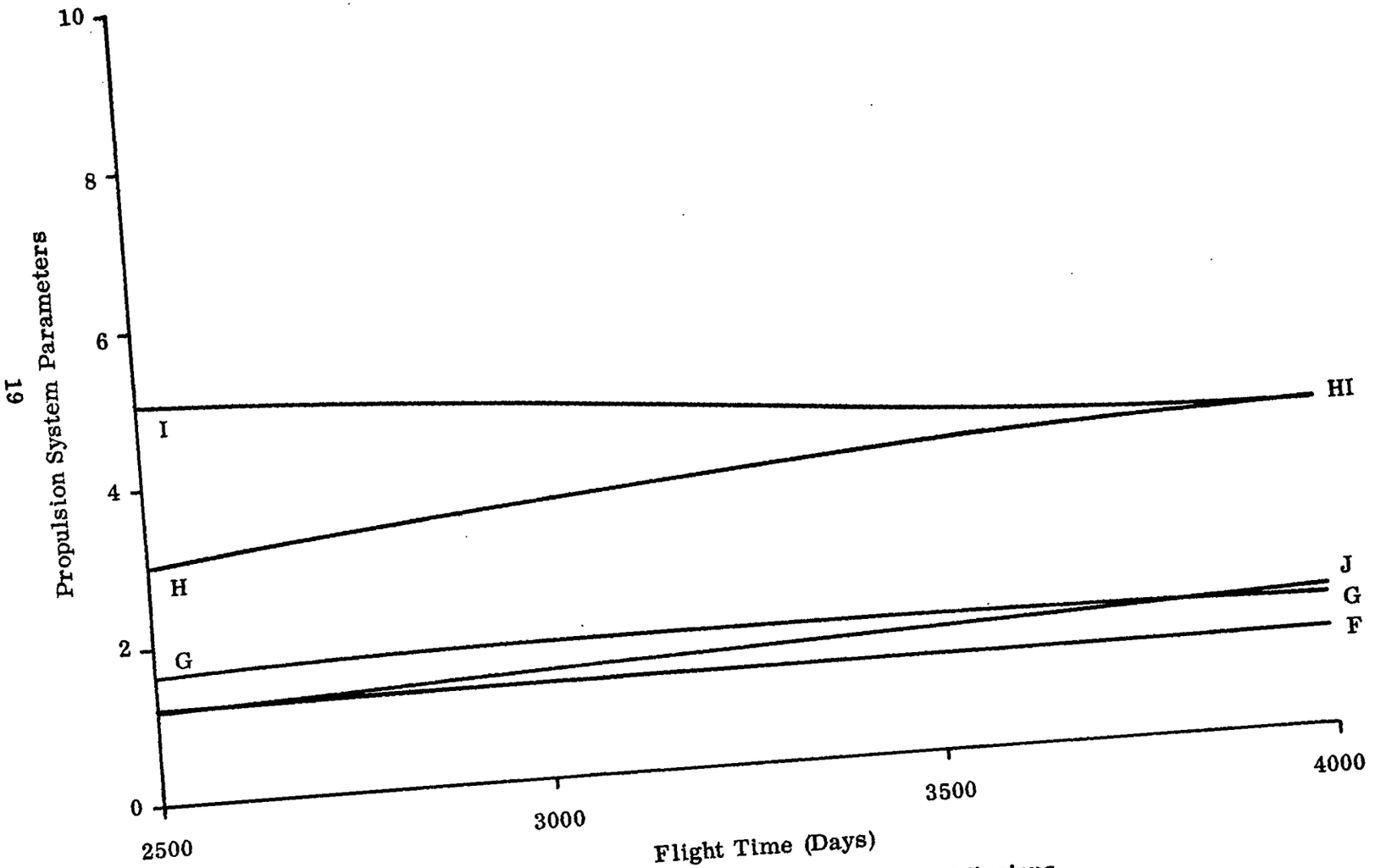

Fig. 3B 1980 Pluto Mode B Flyby Missions

K Maximum Solar Distance (au)/10
L Minimum Solar Distance (au)/1. E-1
M Heliocentric Travel Angle (deg)/100
N Launch Excess Speed (m/sec)/1000
O Arrival Excess Speed (m/sec)/10000
R Launch Date (Days from 2444511)/10

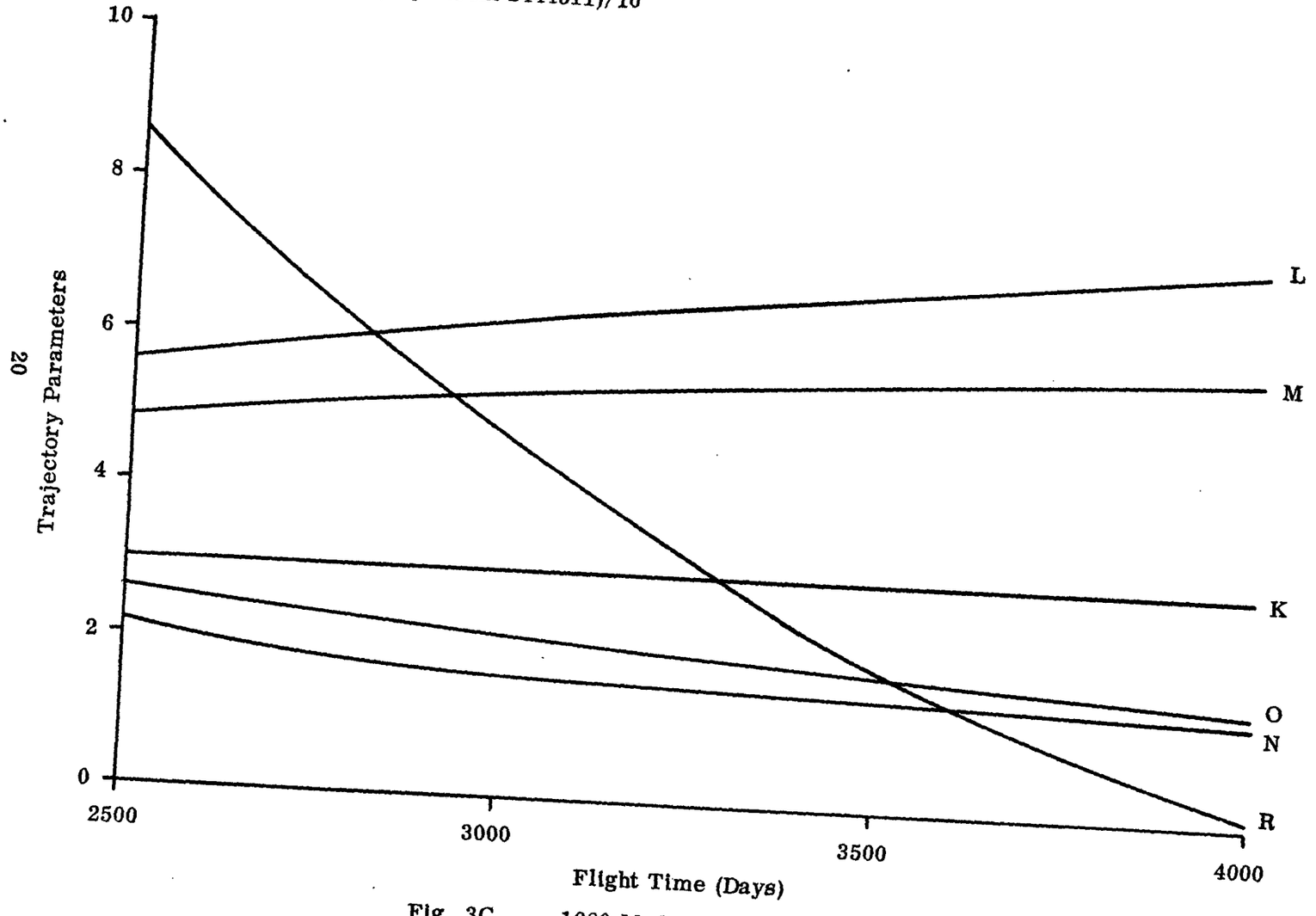

Fig. 3C 1980 Mode B Pluto Flyby Missions

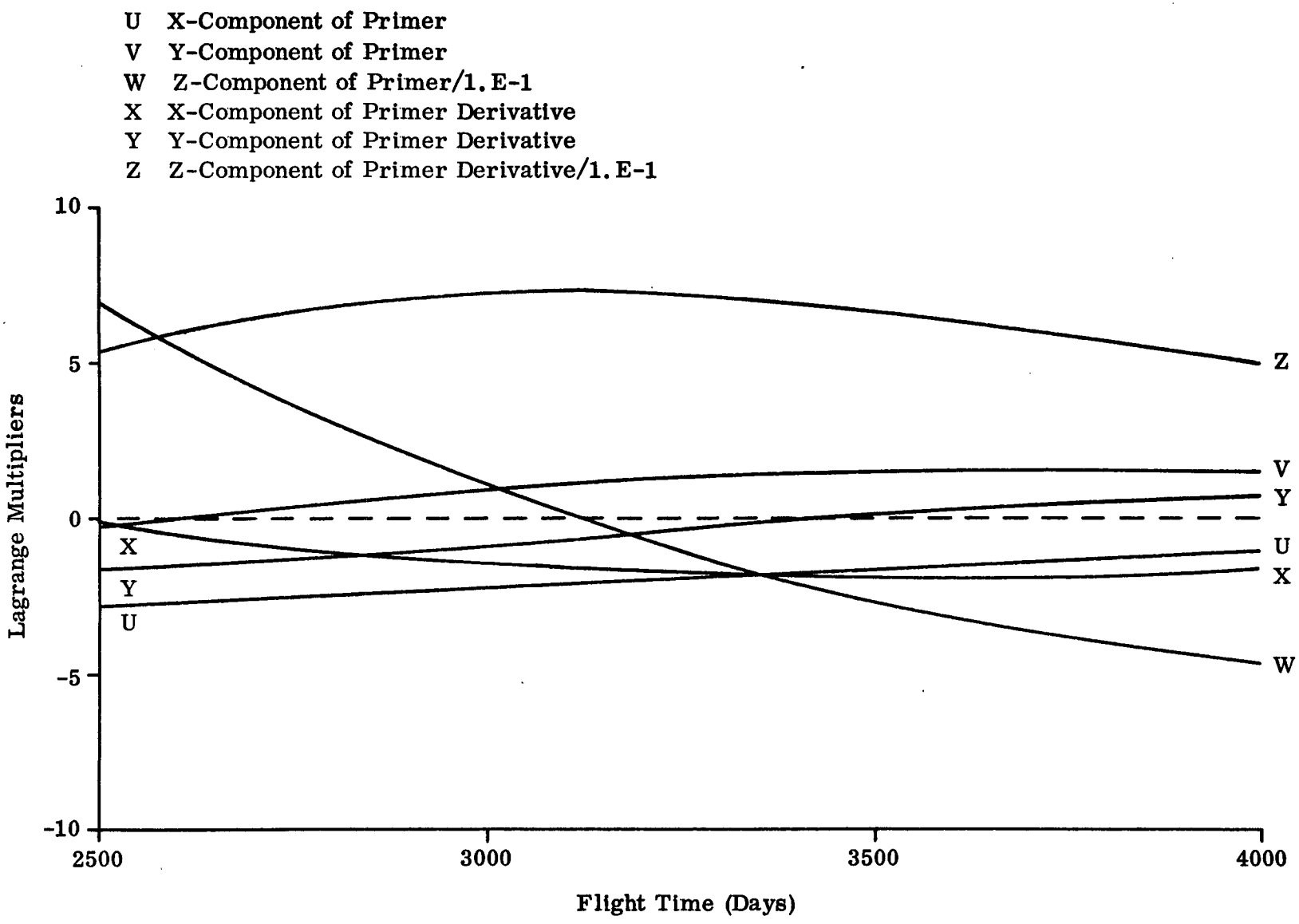

Fig. 3D 1980 Pluto Mode B Flyby Missions

A Net Spacecraft Mass (kg)/10
B Initial Spacecraft Mass (kg)/1000
C Propulsion System Mass (kg)/100
D Propellant Mass (kg)/100
E Retro Propellant Mass (kg)/100

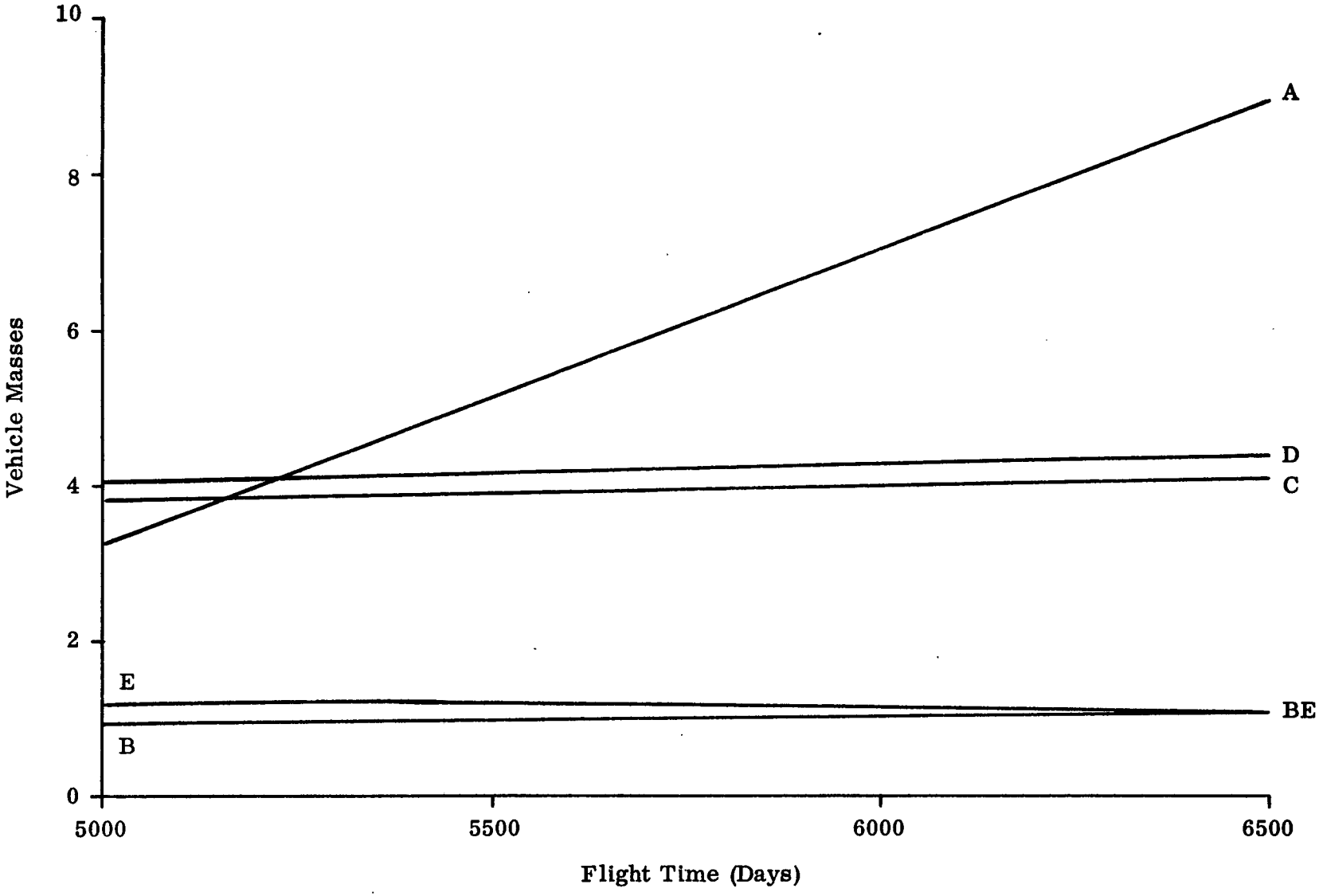

Fig. 4A 1980 Pluto Mode A Orbiter Missions

F Reference Power (kw)/10
G Maximum Power (kw)/10
H Jet Exhaust Speed (m/sec)/10000
I Reference Thrust (newtons)/1. E-1
J Propulsion Time (days)/1000

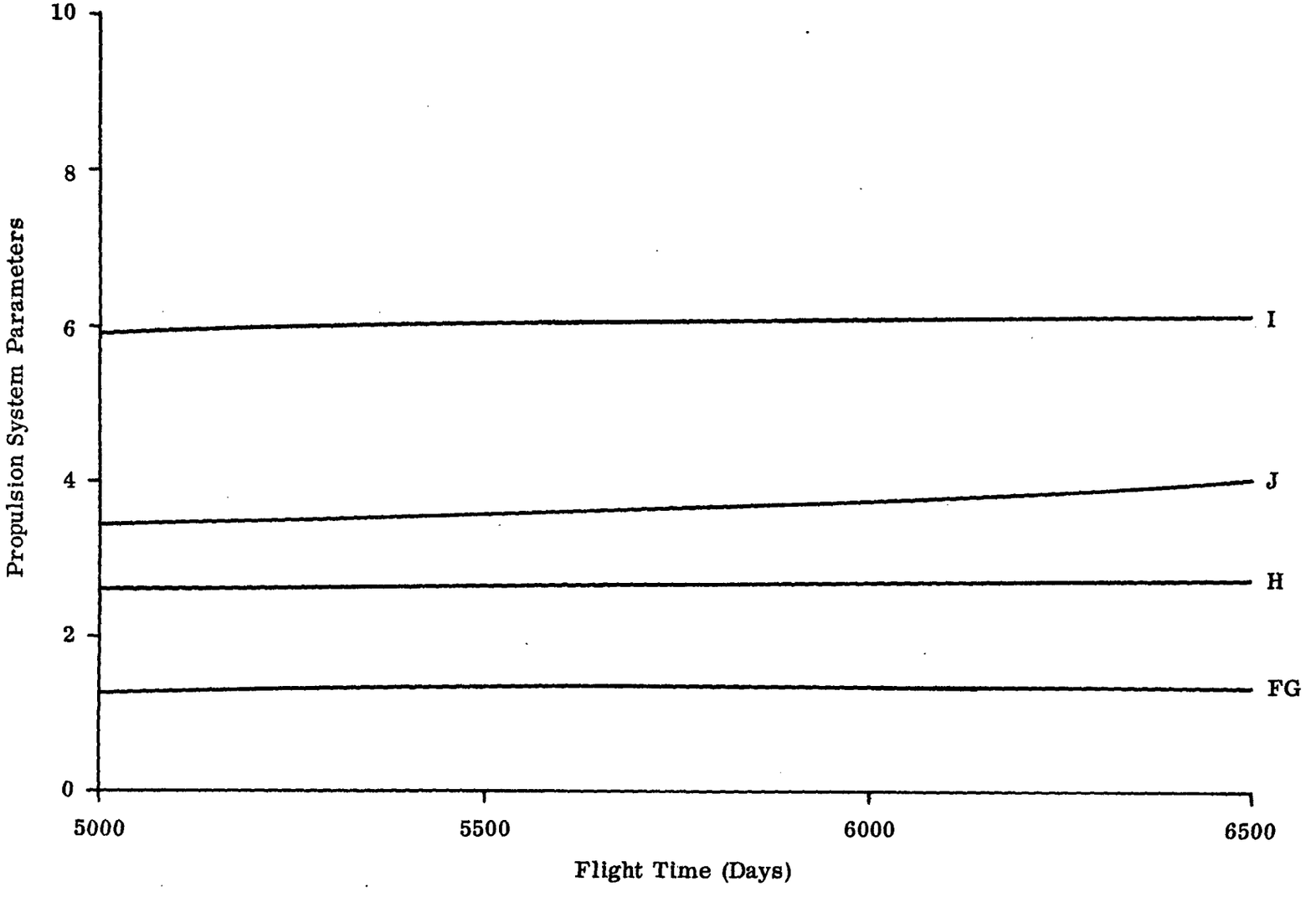

Fig. 4B 1980 Mode A Orbiter Missions

K Maximum Solar Distance (au)/10
L Minimum Solar Distance (au)
M Heliocentric Travel Angle (deg)/100
N Launch Excess Speed (m/sec)/1000
O Arrival Excess Speed (m/sec)/1000
P Retro Incremental Speed (m/sec)/1000
R Launch Date (Days from 2444489)/10

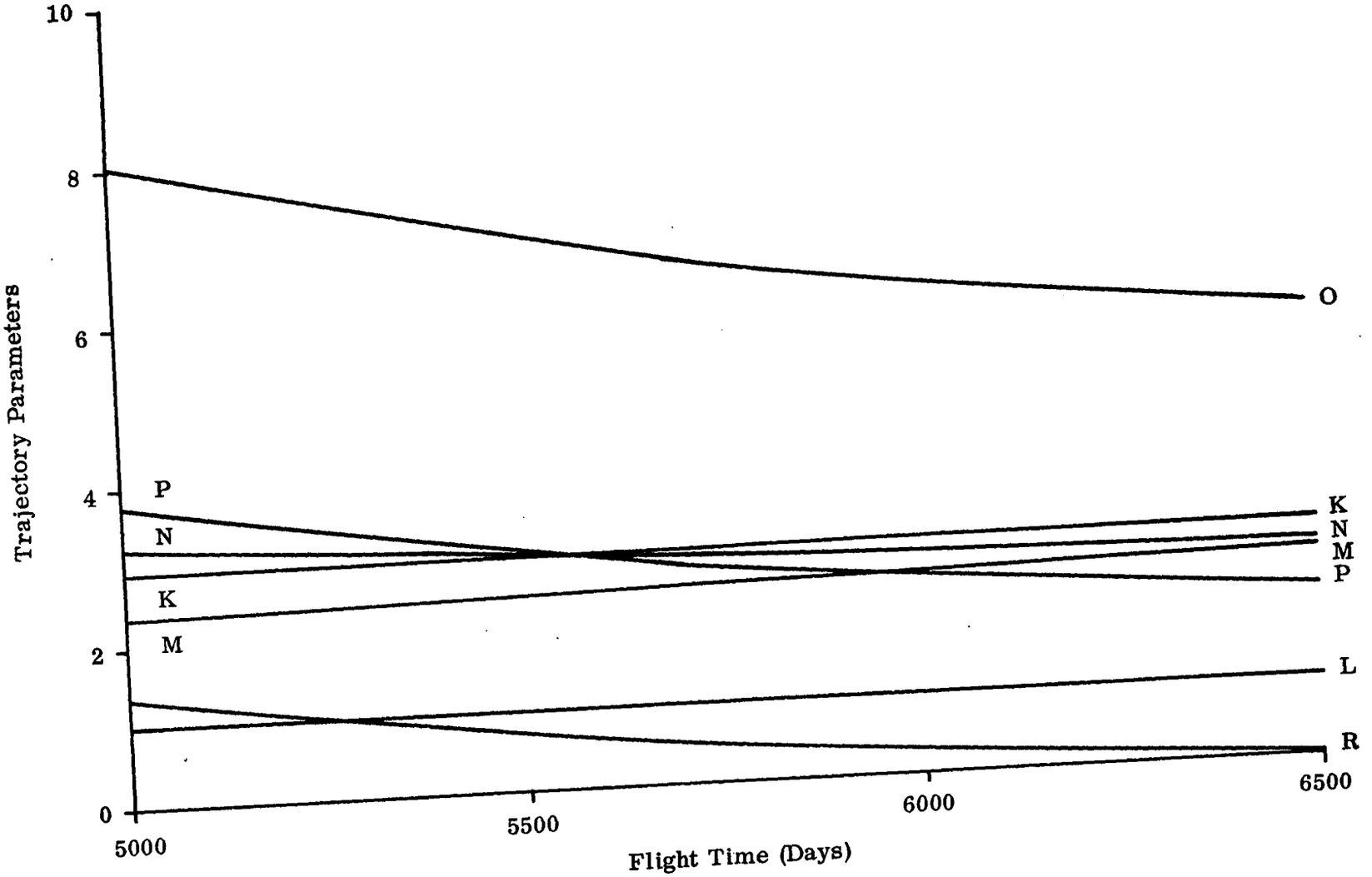

Fig. 4C 1980 Pluto Mode A Orbiter Missions

U X-Component of Primer
V Y-Component of Primer
W Z-Component of Primer
X X-Component of Primer Derivative
Y Y-Component of Primer Derivative
Z Z-Component of Primer Derivative/1.E-1

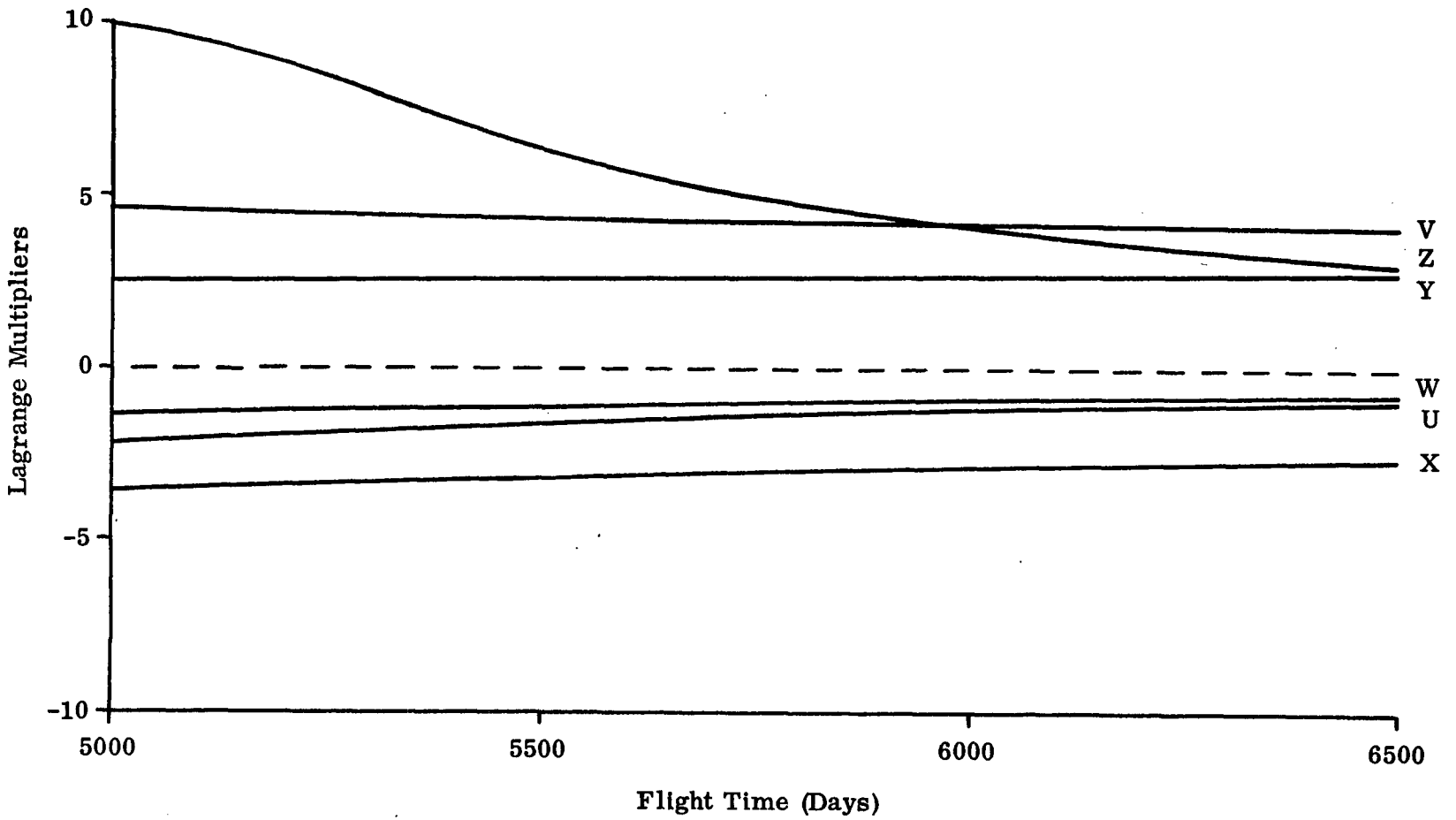

Fig. 4D 1980 Pluto Mode A Orbiter Missions

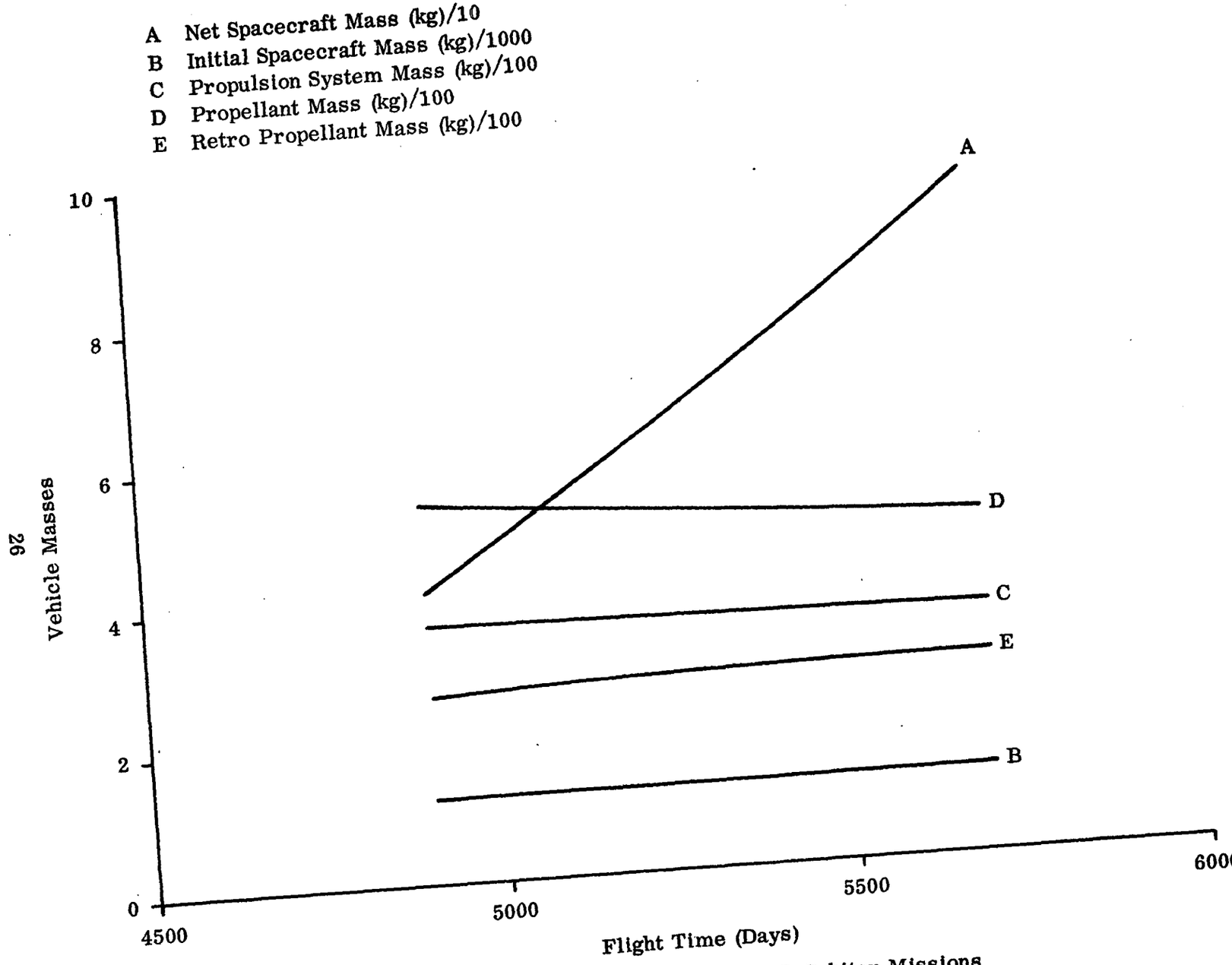

Fig. 5A 1980 Pluto Mode B Orbiter Missions

F Reference Power (kw)/10
G Maximum Power (kw)/10
H Jet Exhaust Speed (m/sec)/10000
I Reference Thrust (newtons)/1. E-1
J Propulsion Time (days)/1000

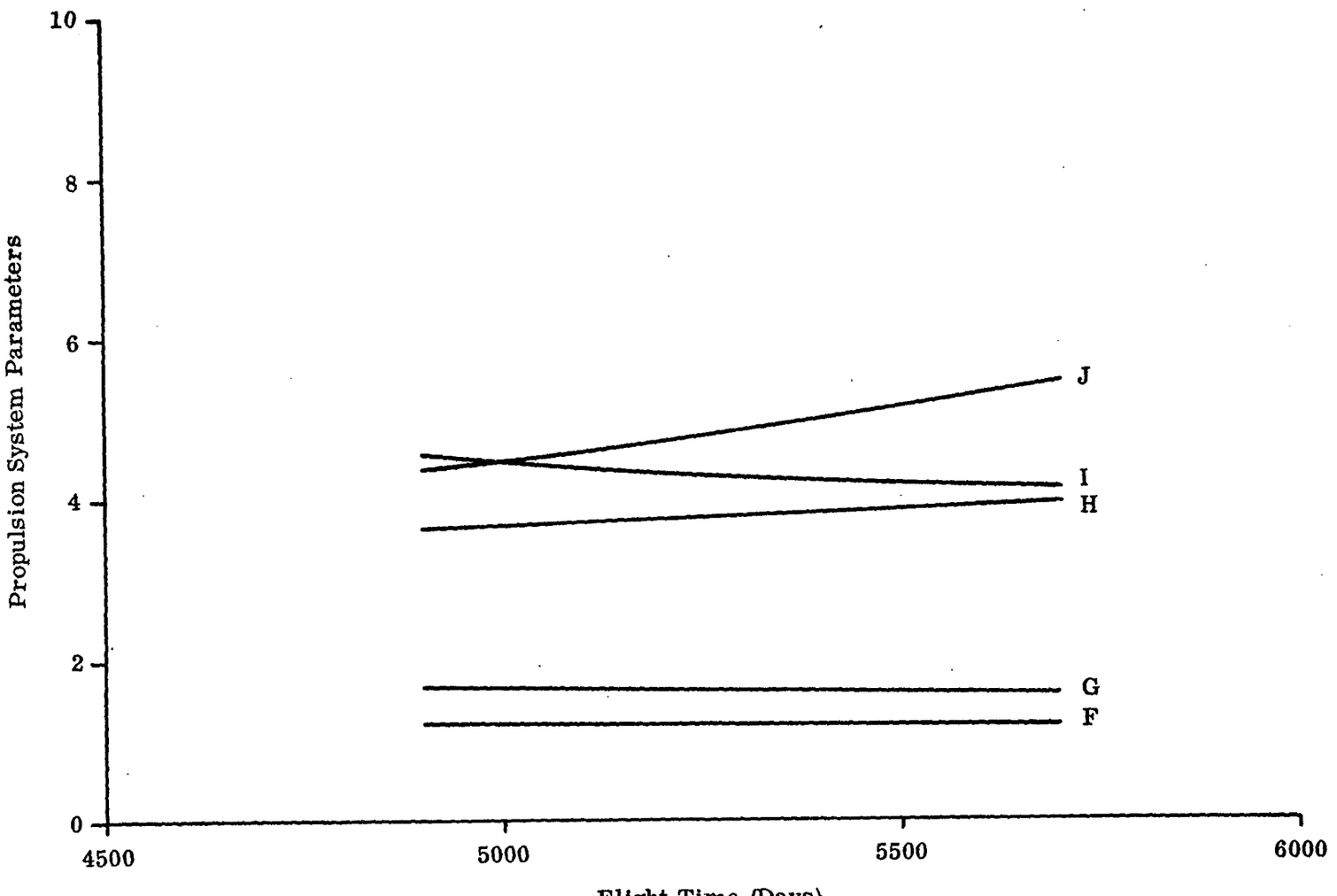

Fig. 5B 1980 Pluto Mode B Orbiter Missions

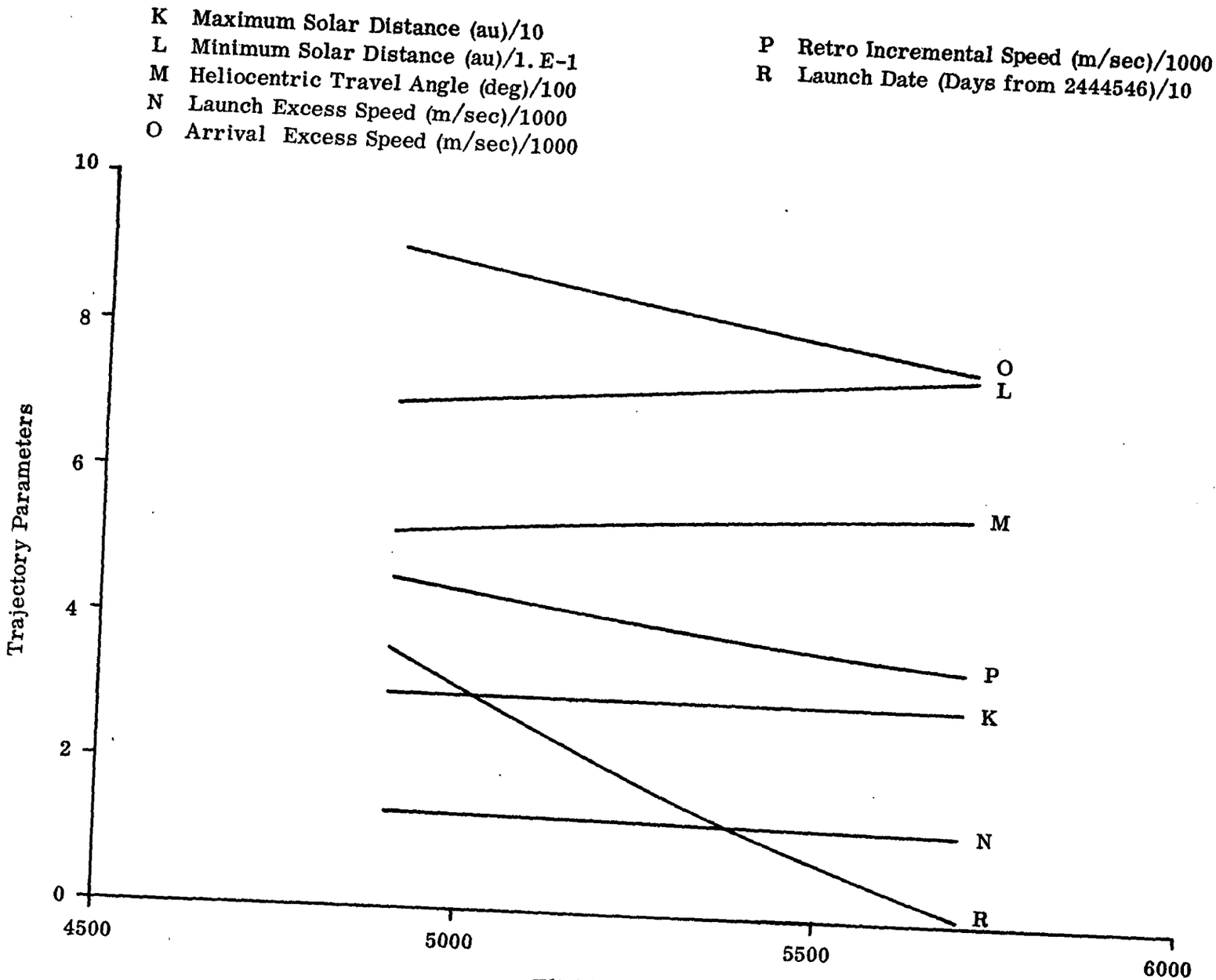

Fig. 5C 1980 Pluto Mode B Orbiter Missions

U X-Component of Primer
V Y-Component of Primer
W Z-Component of Primer/1.E-1
X X-Component of Primer Derivative/1.E-1
Y Y-Component of Primer Derivative/1.E-1
Z Z-Component of Primer Derivative/1.E-1

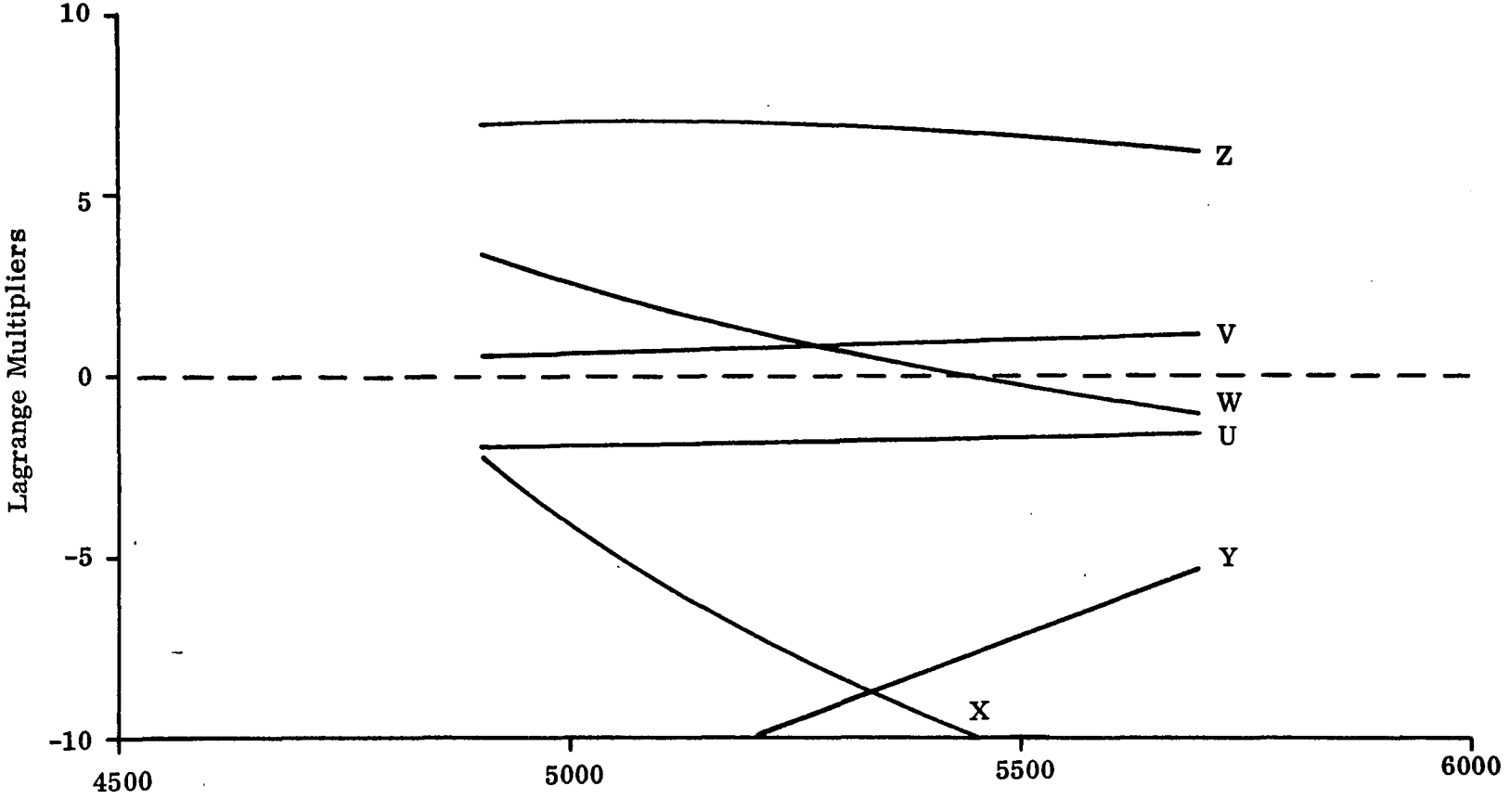

Fig. 5D 1980 Pluto Mode B Orbiter Missions

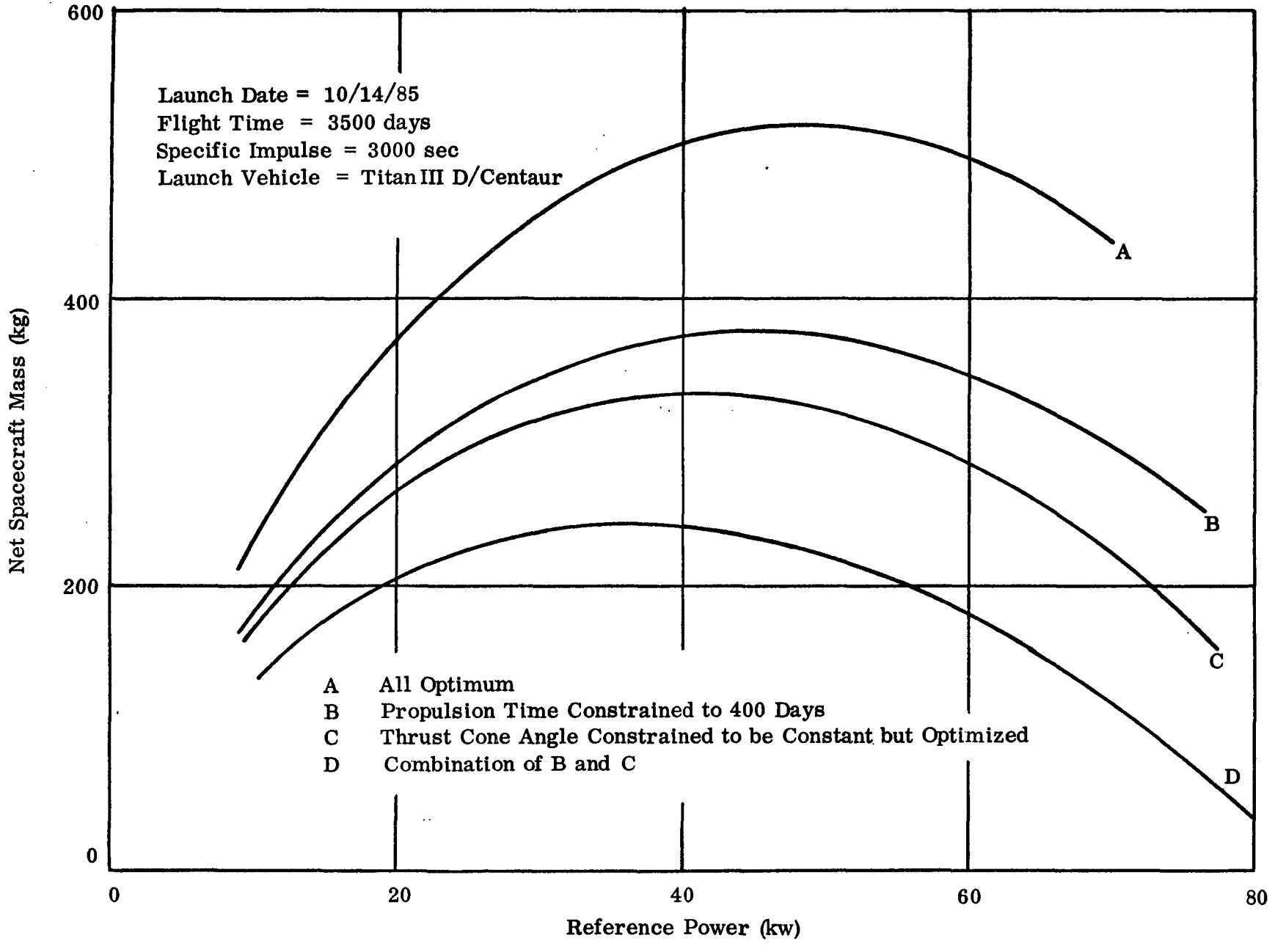

Fig. 6 1985 Pluto Mode A Flyby Missions

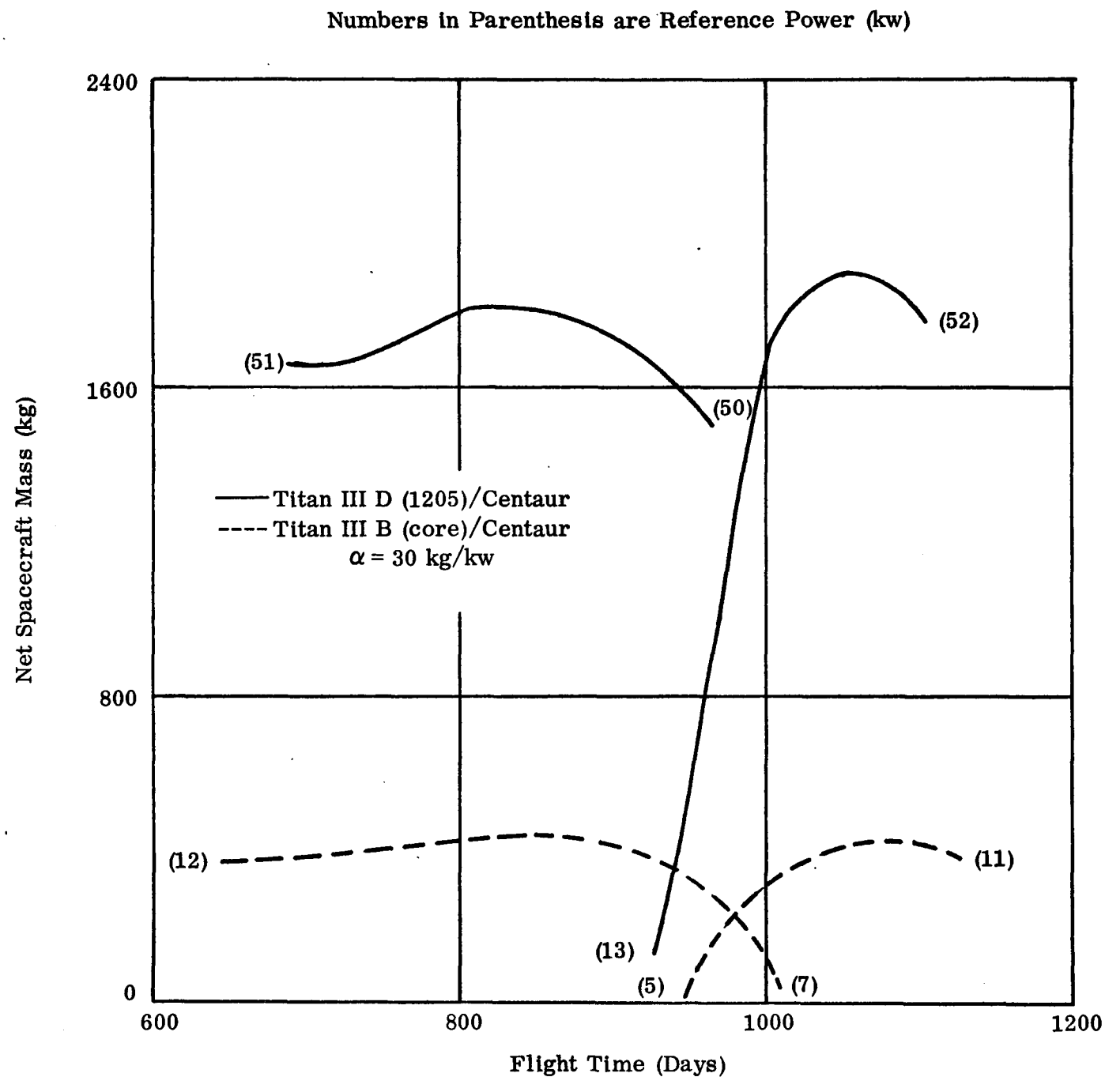

Fig. 7 1980 Encke Perihelion Rendezvous Missions.

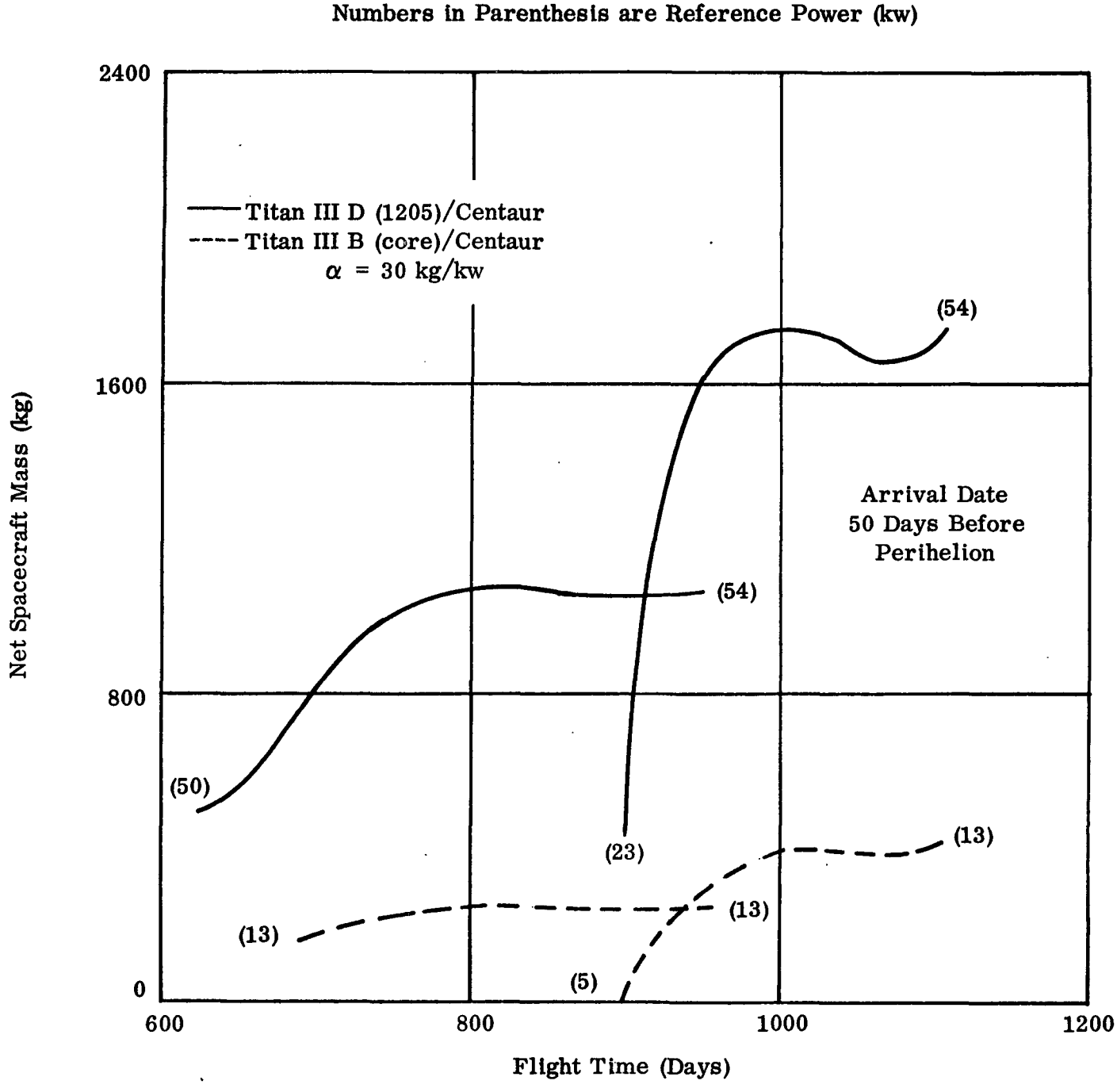

Fig. 8 1980 Encke Pre-Perihelion Rendezvous Missions

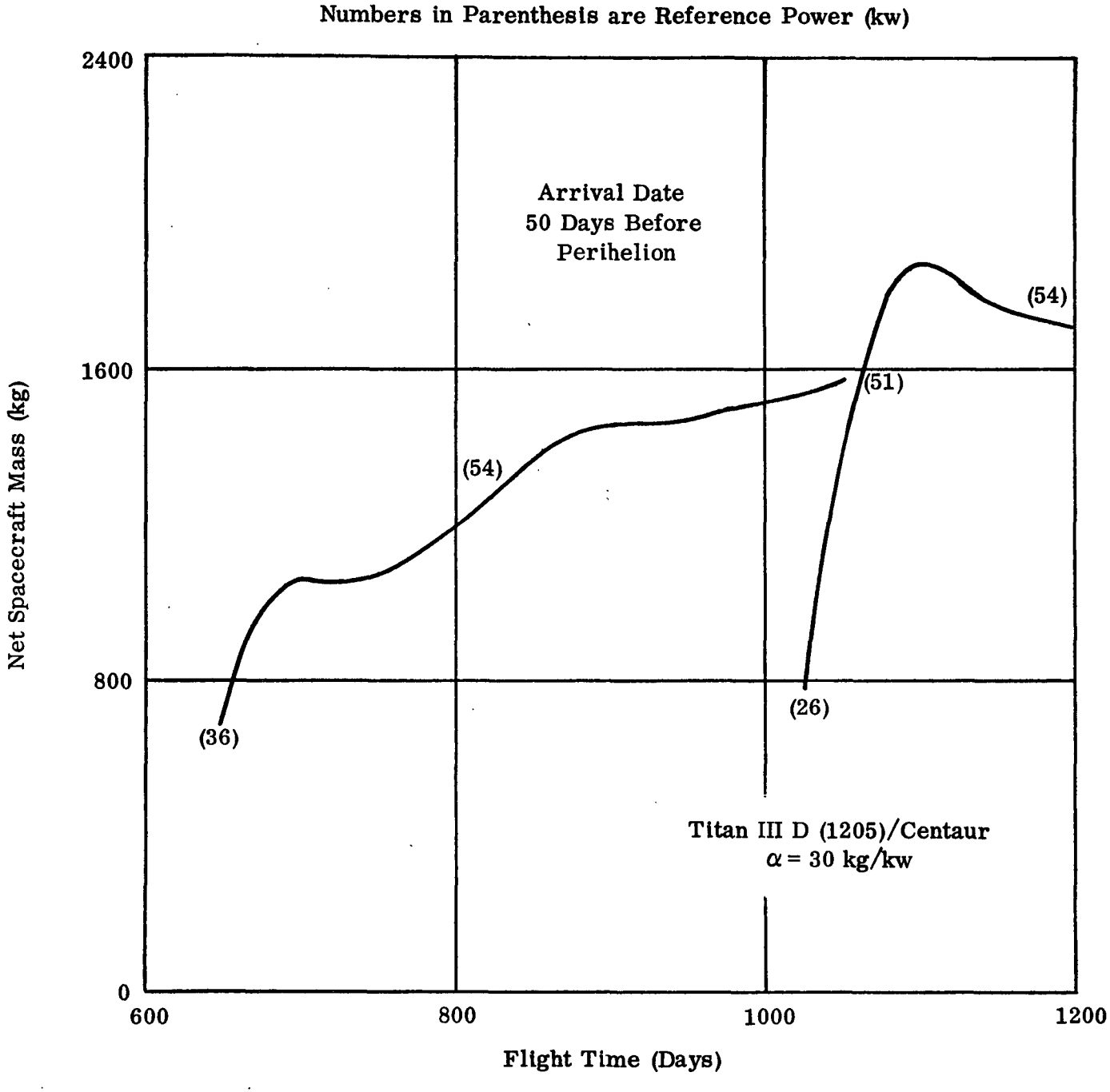

Fig. 9 1984 Encke Pre-Perihelion Rendezvous Missions

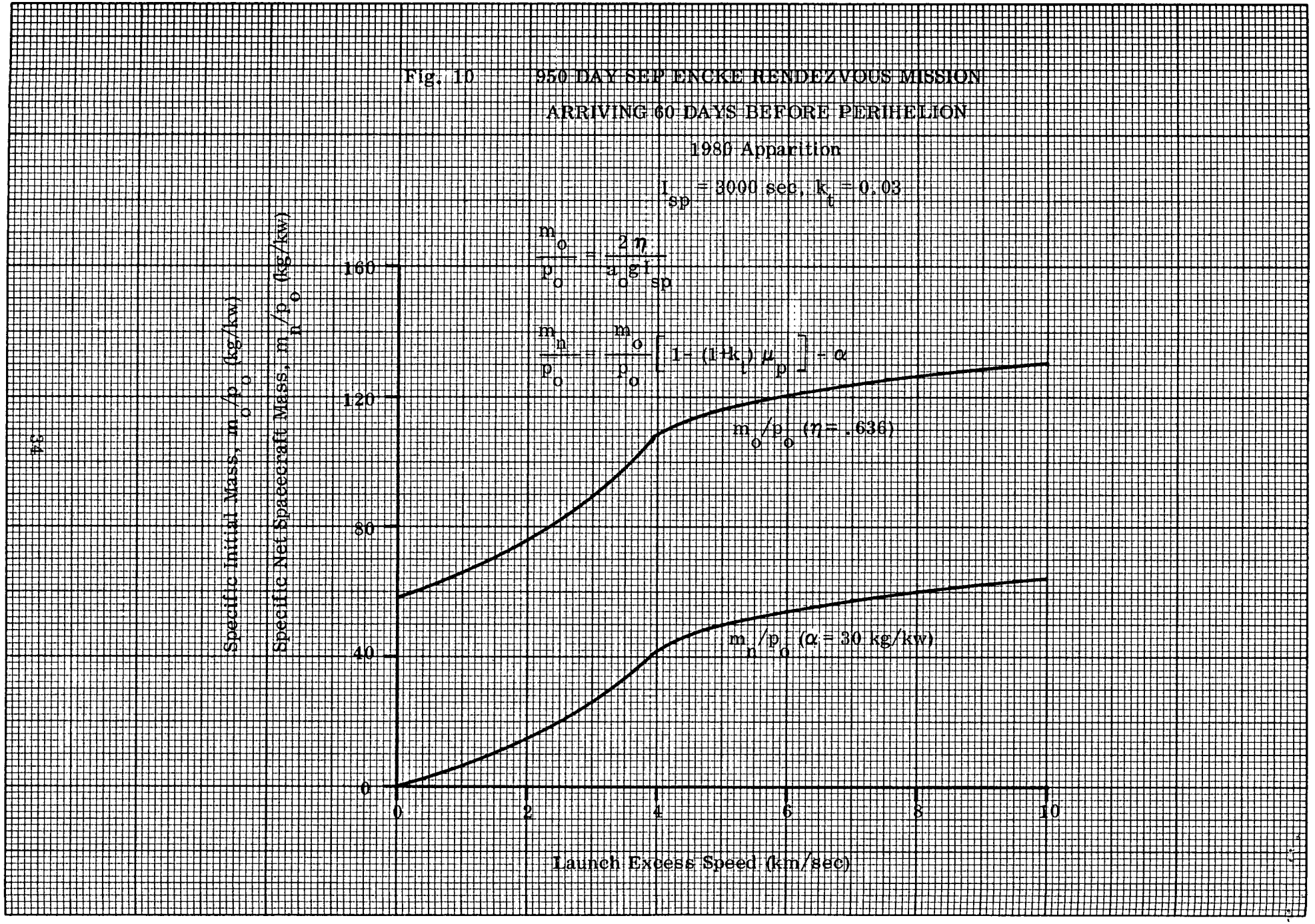

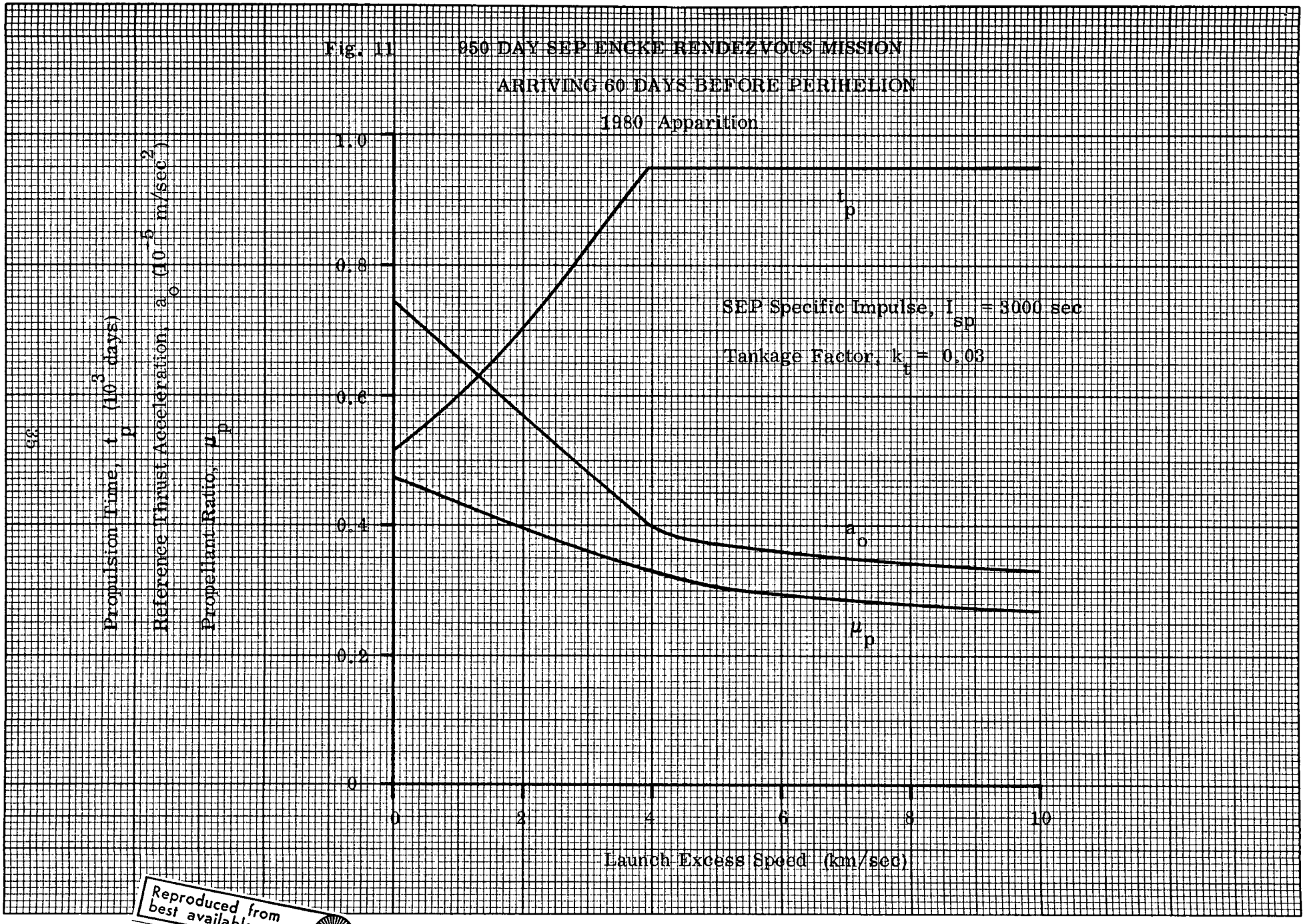

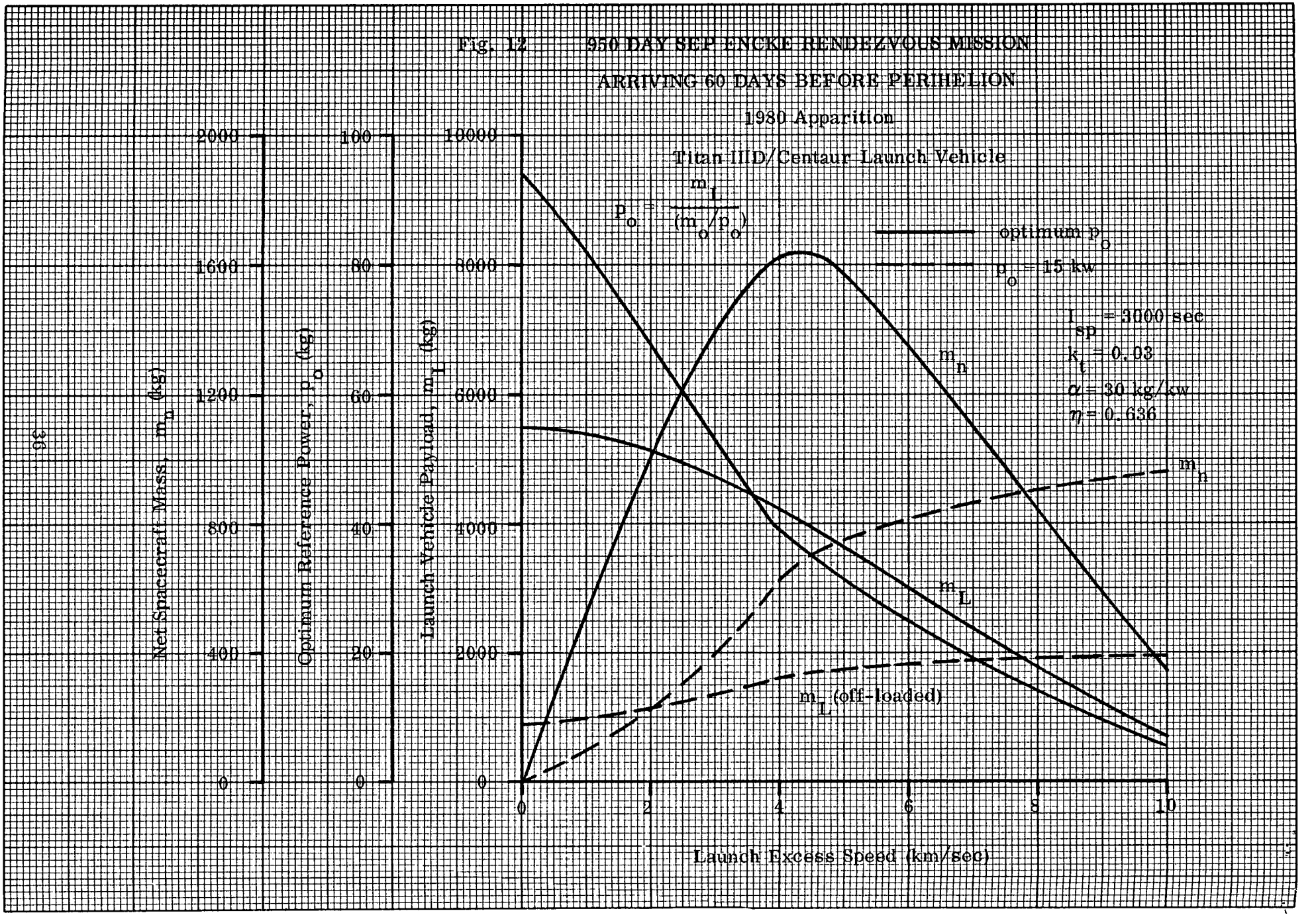

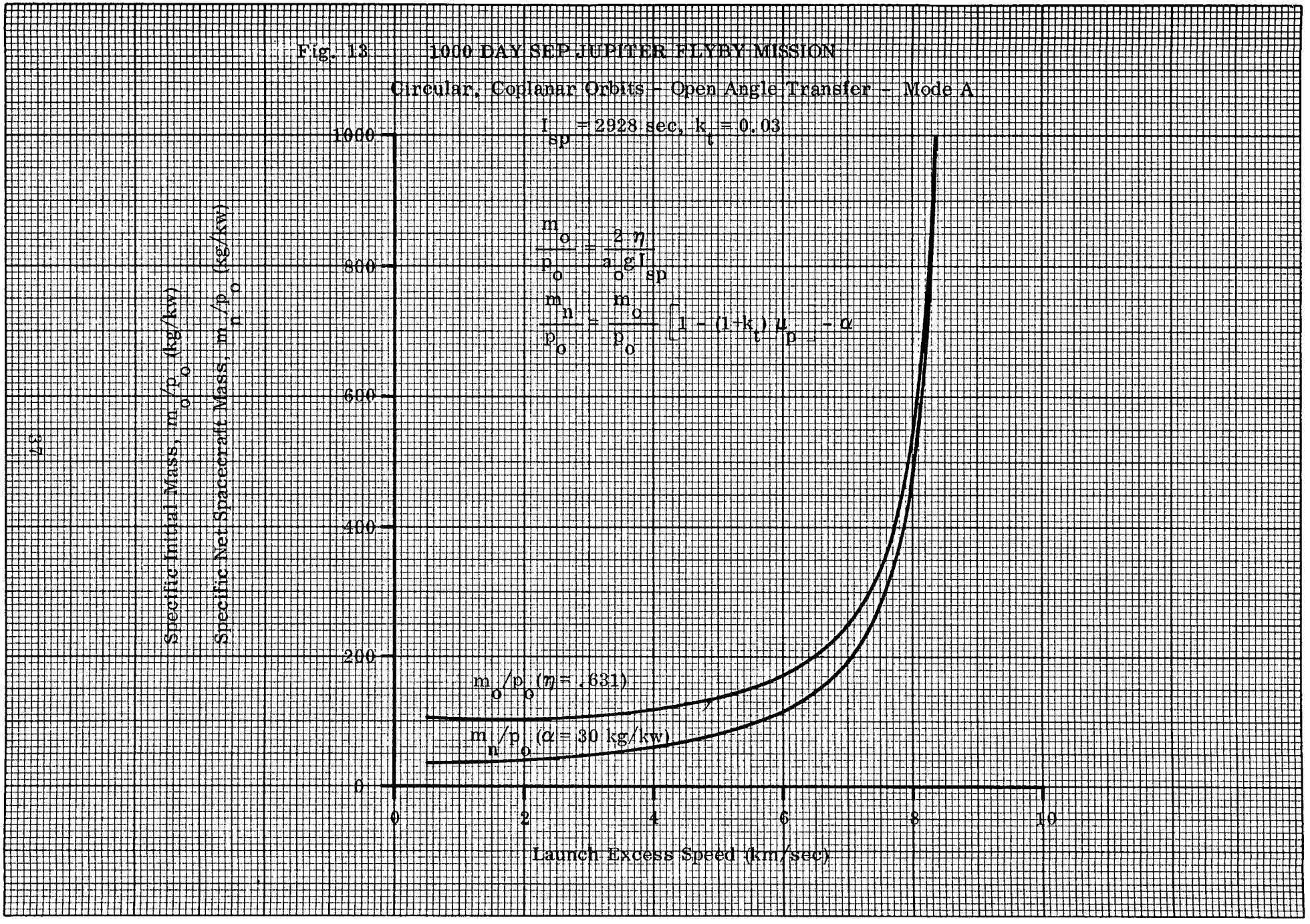

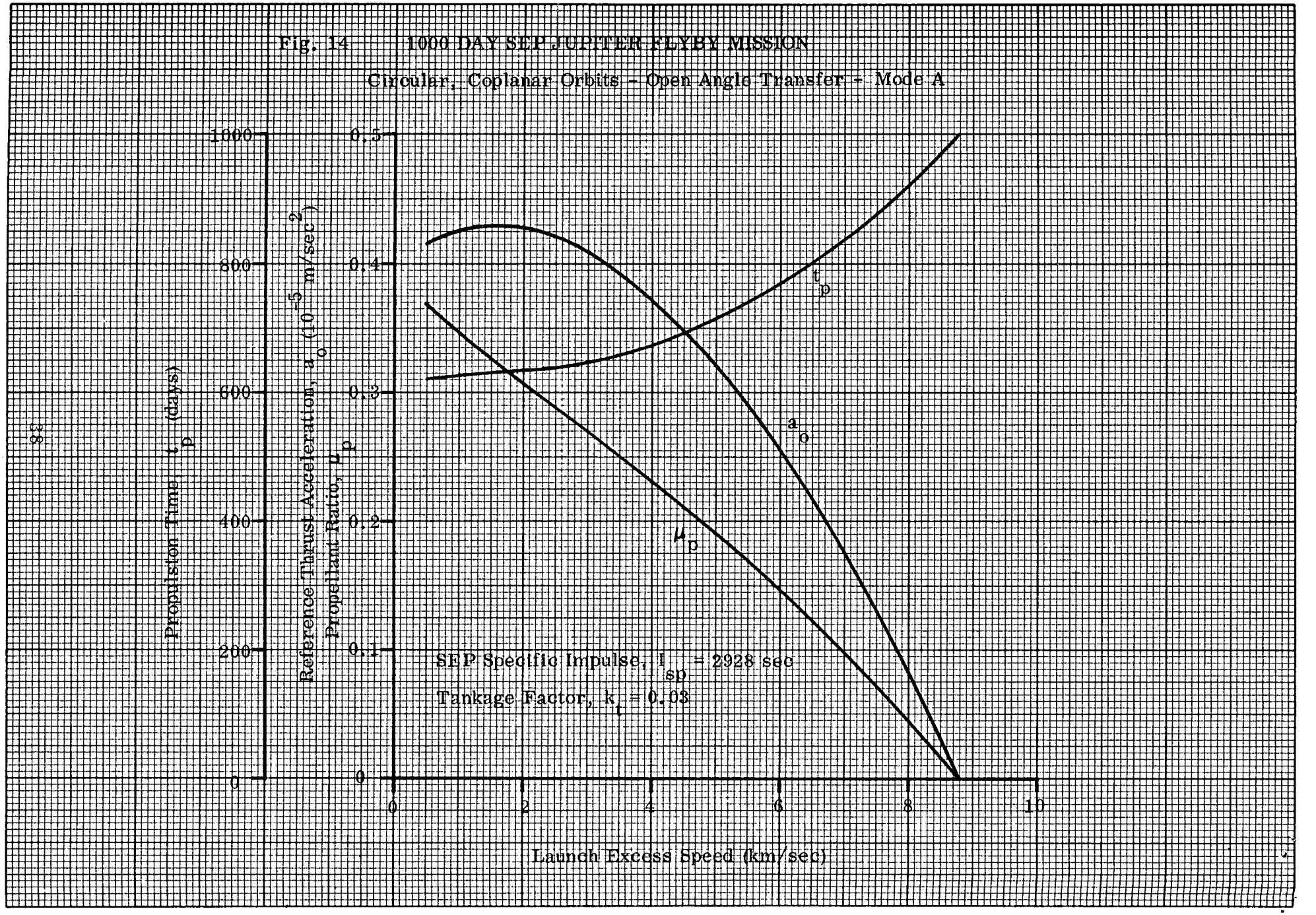

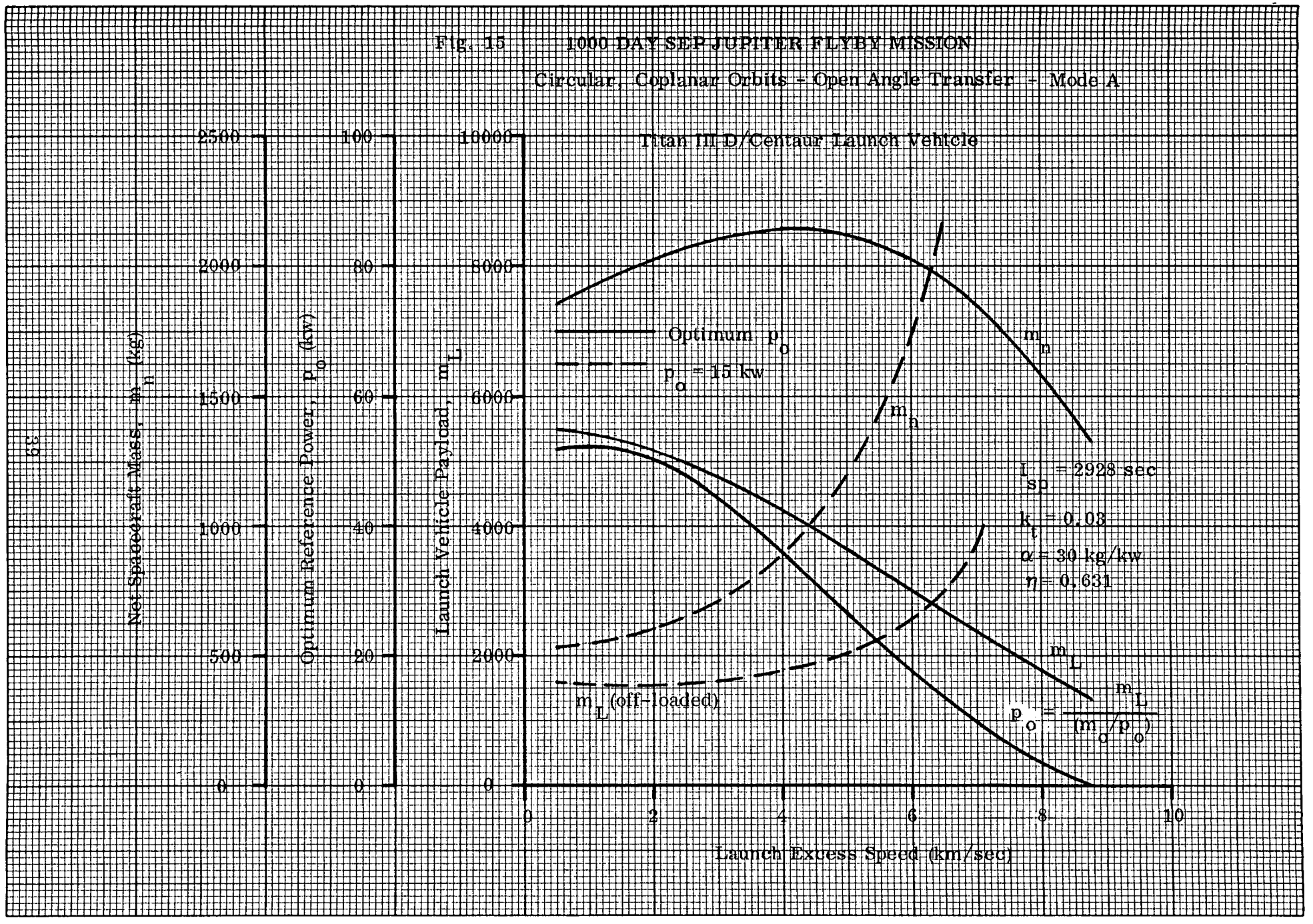

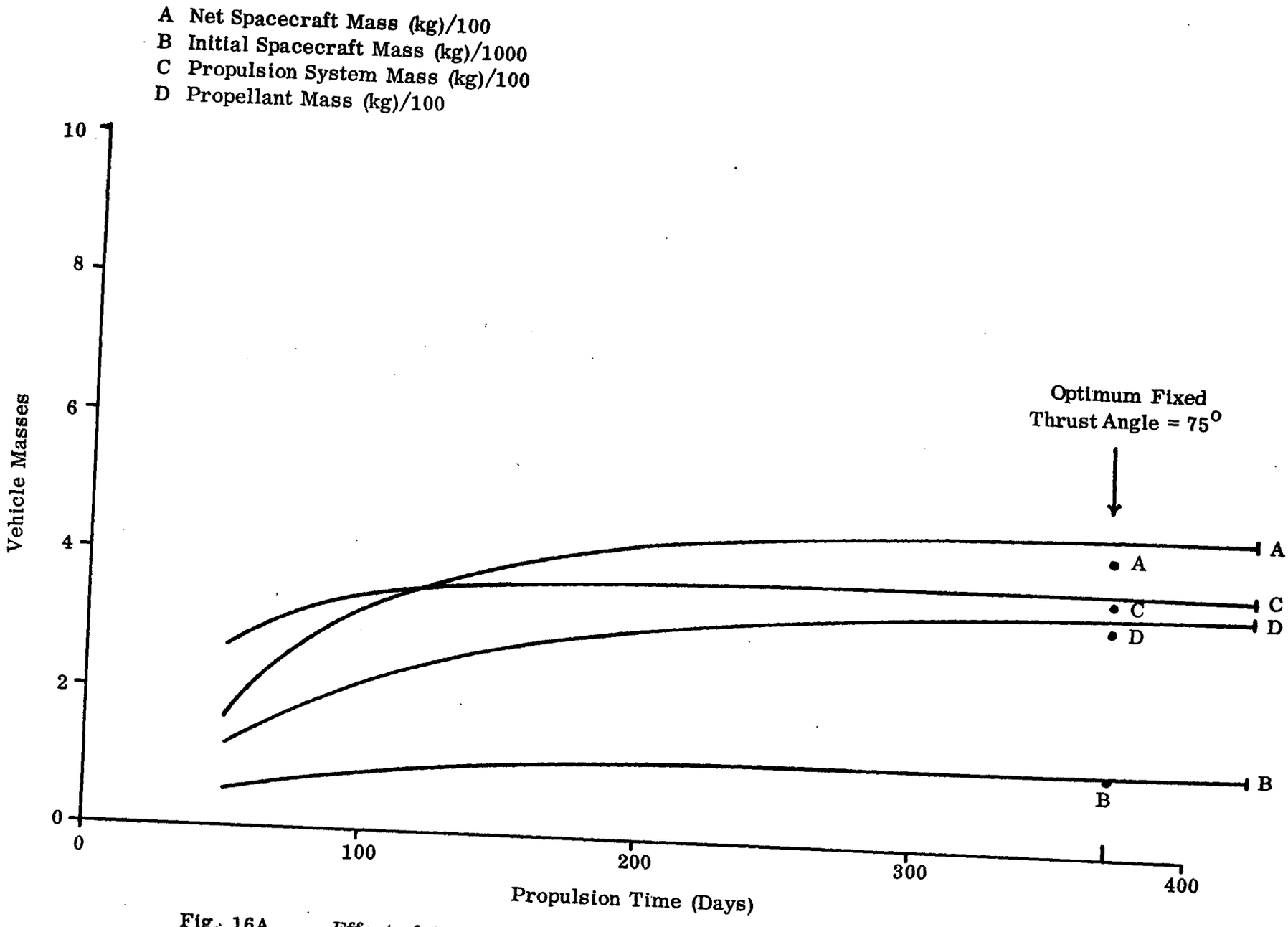

Fig. 16A Effect of Constrained Propulsion Time on Mode A Jupiter Flyby Mission

F Reference Power (kw)/10
G Maximum Power (kw)/10
H Jet Exhaust Speed (m/sec)/10000
I Reference Thrust Acceleration (m/sec/sec)/1. E-4

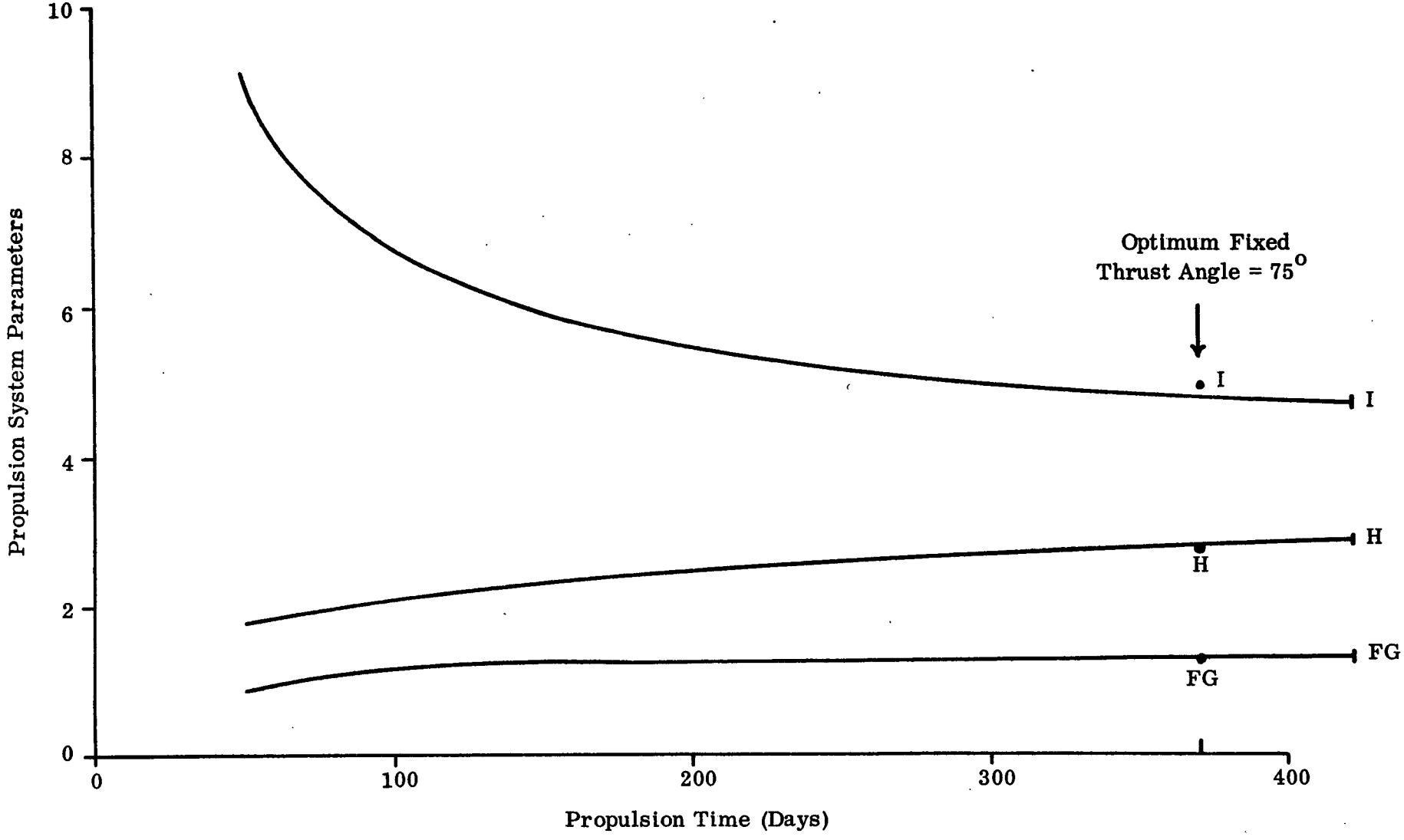

Fig. 16B Effect of Constrained Propulsion Time on Mode A Jupiter Flyby Mission

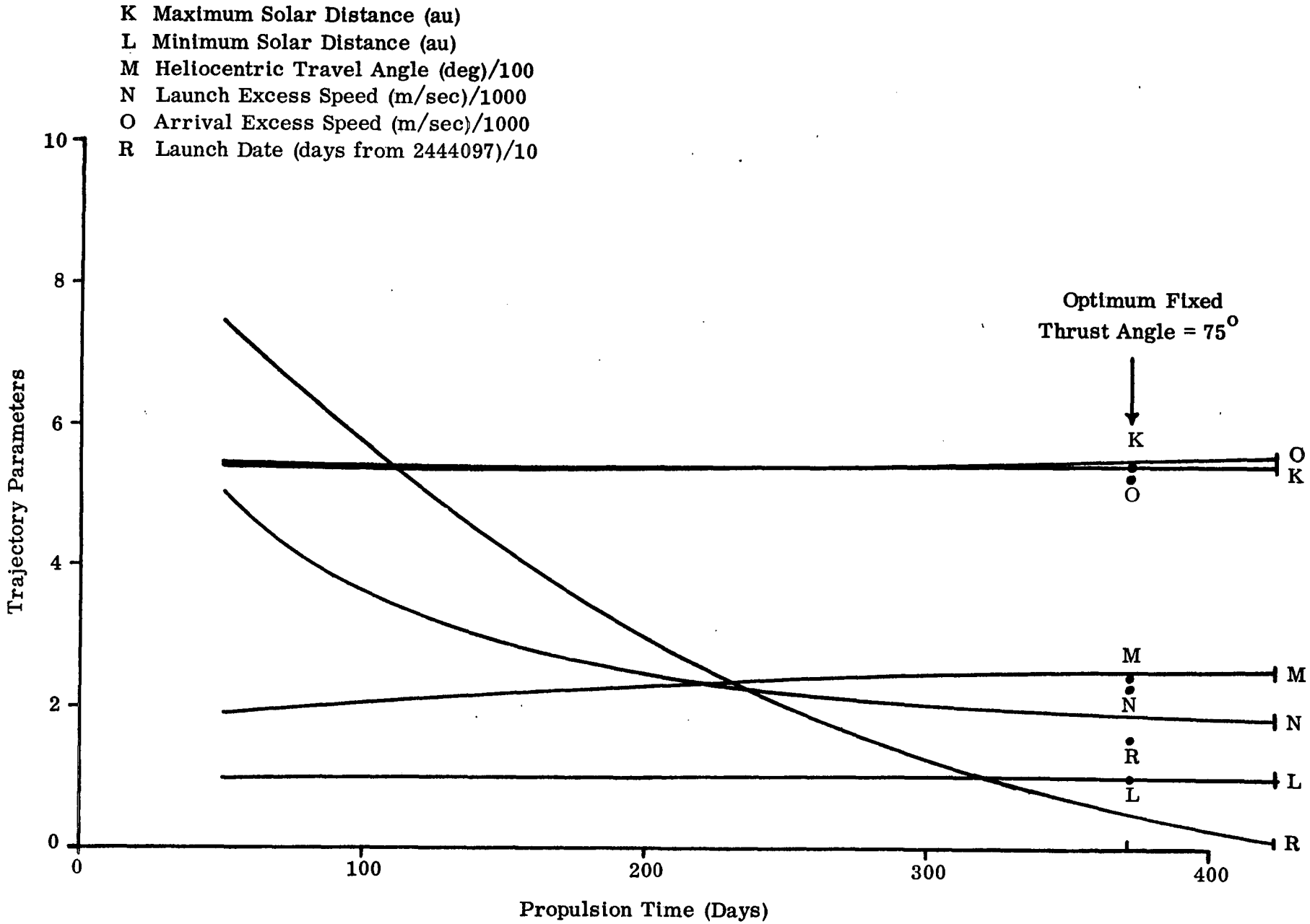

Fig. 16C Effect of Constrained Propulsion Time on Mode A Jupiter Flyby Mission

T Propulsion Time Multiplier/1.E-1
U X-Component of Primer
V Y-Component of Primer
W Z-Component of Primer/1.E-1
X X-Component of Primer Derivative
Y Y-Component of Primer Derivative
Z Z-Component of Primer Derivative

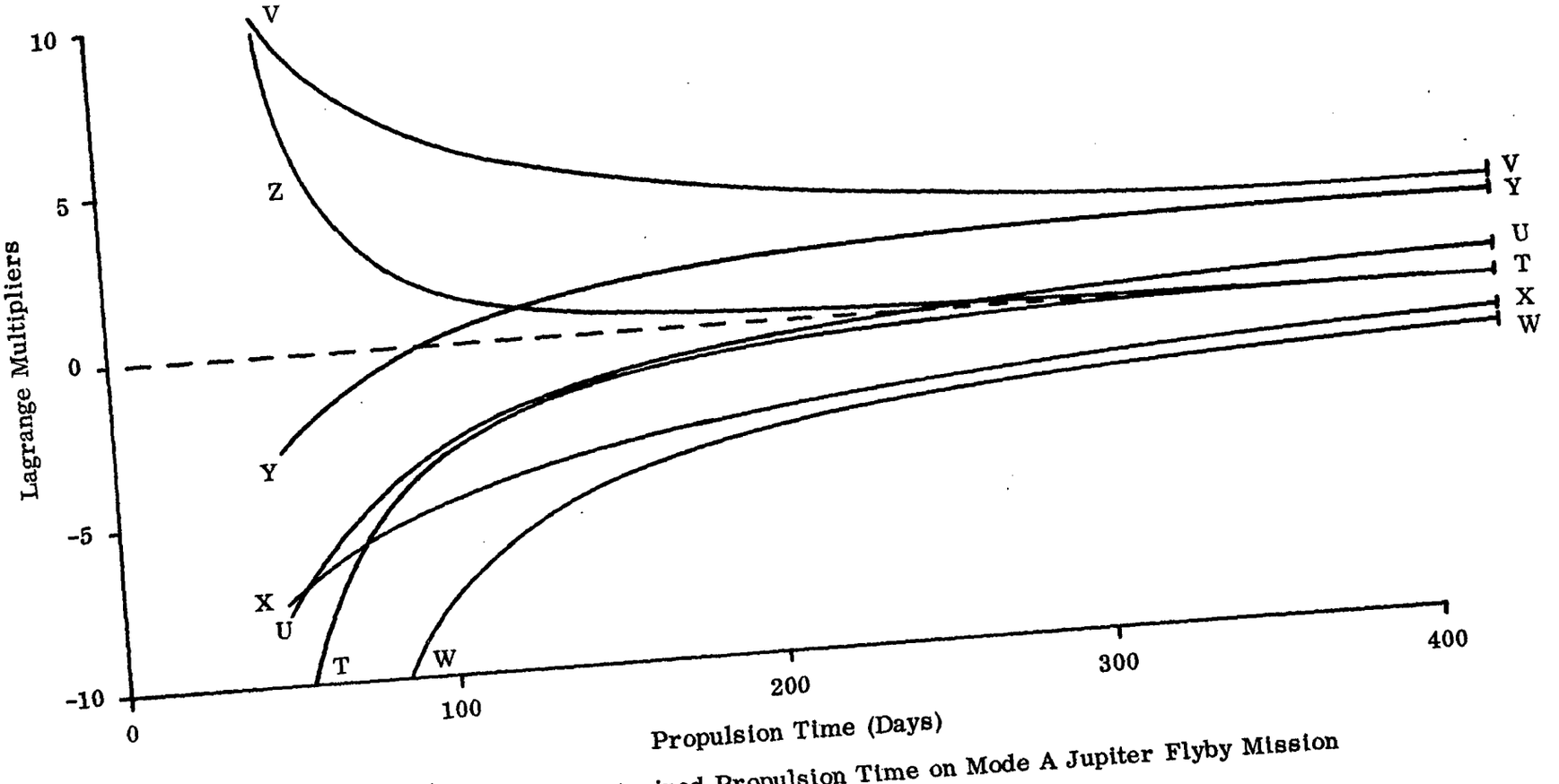

Fig. 16D Effect of Constrained Propulsion Time on Mode A Jupiter Flyby Mission

A Net Spacecraft Mass (kg)/100
B Initial Spacecraft Mass (kg)/1000
C Propulsion System Mass (kg)/100
D Propellant Mass (kg)/100
E Retro Propellant Mass (kg)/100

Note: All thrusting occurs during one thrust period commencing at Earth departure.

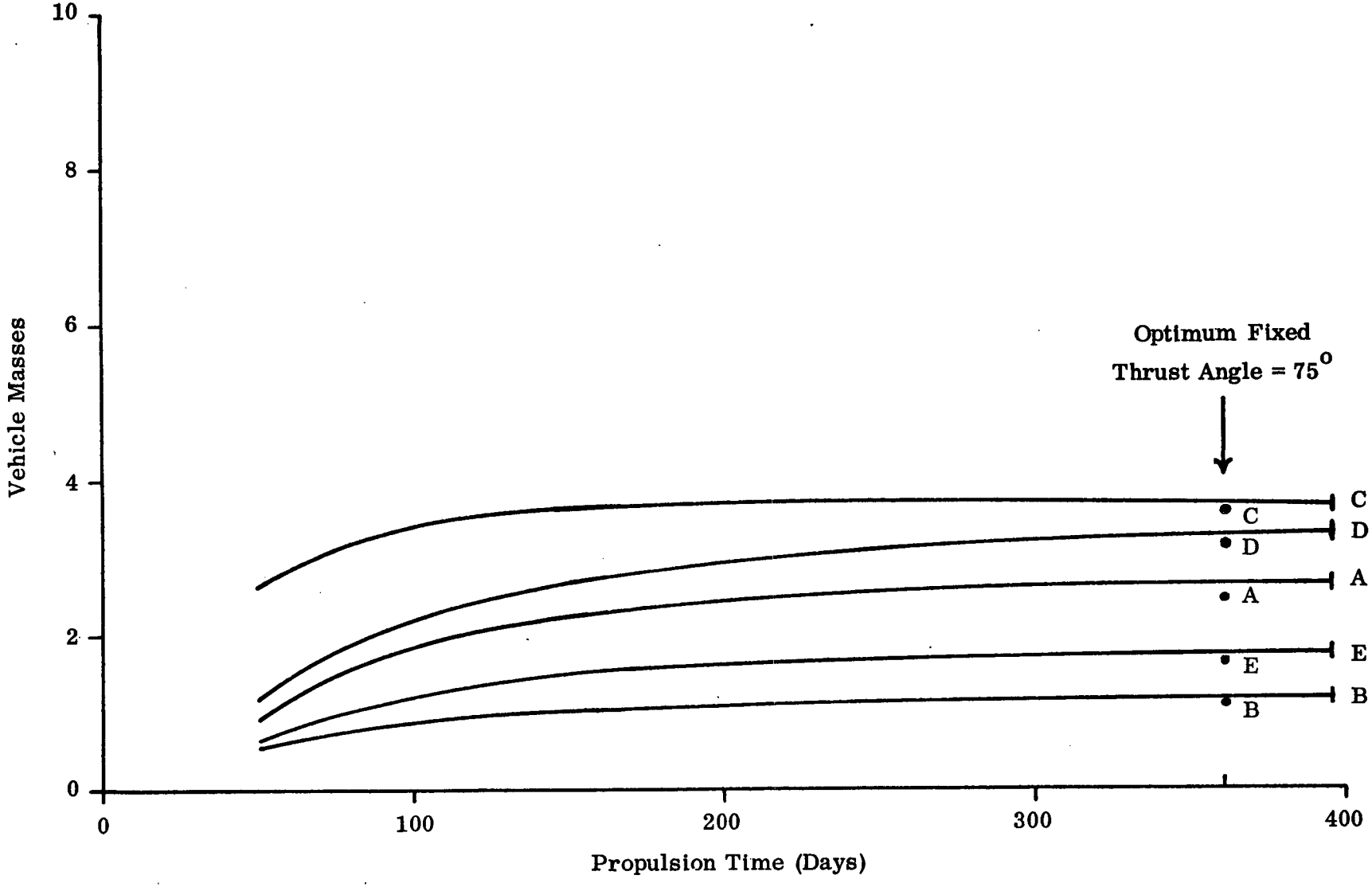

Fig. 17A Effect of Constrained Propulsion Time on Mode A Jupiter Orbiter Mission

F Reference Power (kw)/10
G Maximum Power (kw)/10
H Jet Exhaust Speed (m/sec)/10000
I Reference Thrust Acceleration/1. E-4

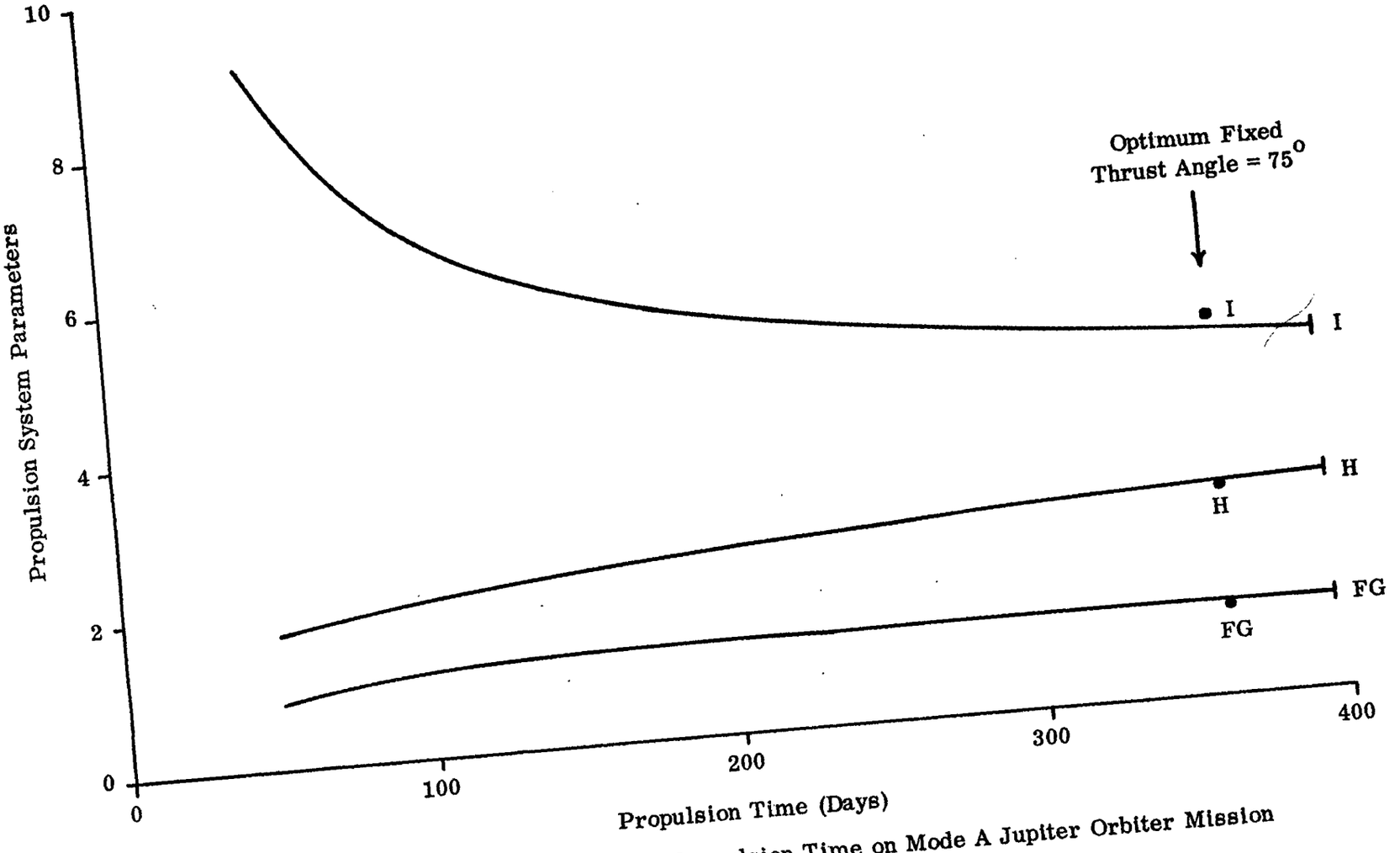

Fig. 17B Effect of Constrained Propulsion Time on Mode A Jupiter Orbiter Mission

K Maximum Solar Distance (au)
L Minimum Solar Distance (au)
M Heliocentric Travel Angle (deg)/100
N Launch Excess Speed (m/sec)/1000
O Arrival Excess Speed (m/sec)/1000
P Retro Incremental Speed (m/sec)/1000
R Launch Date (Days from 2444105)/10

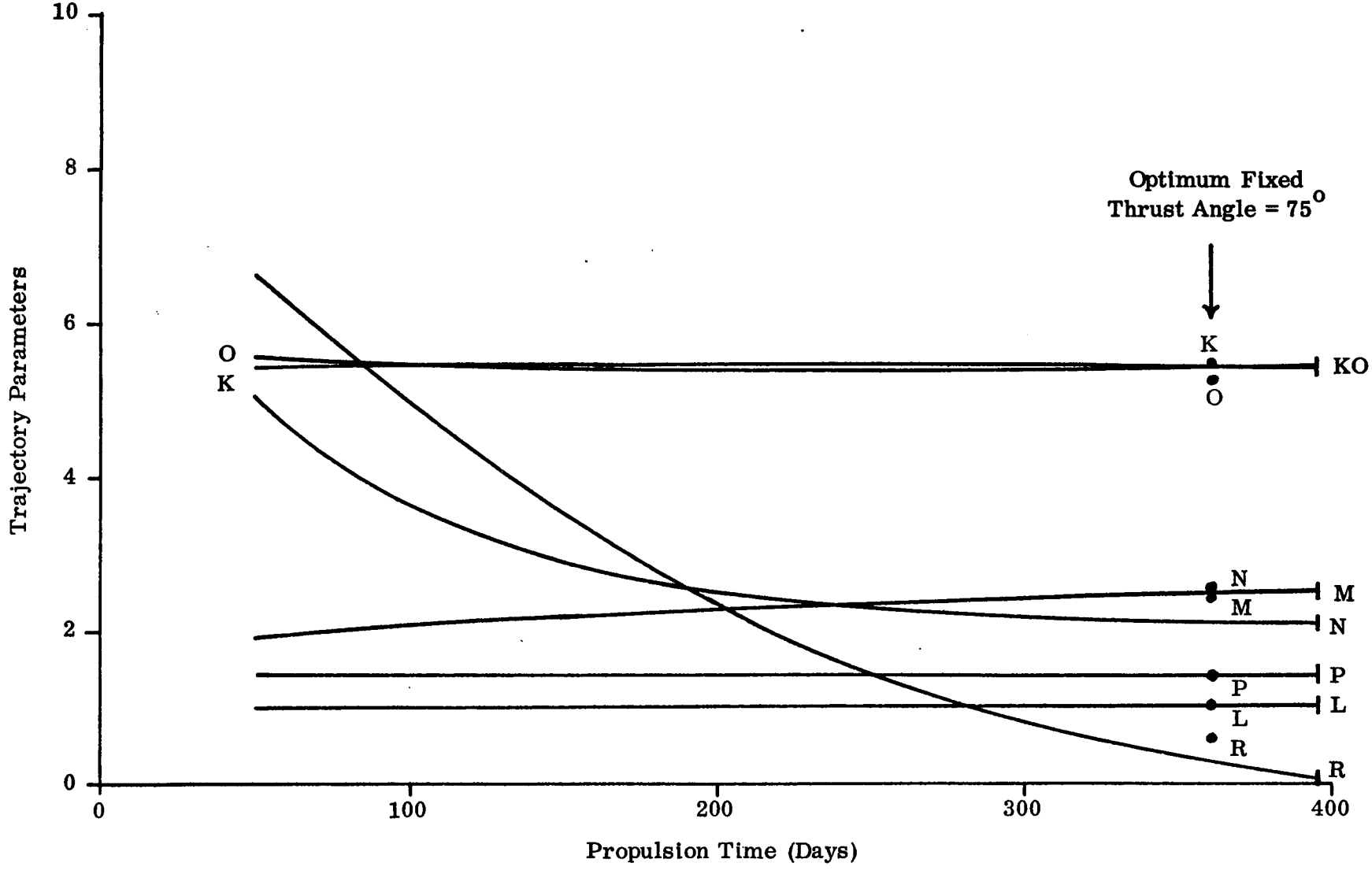

Fig. 17C Effect of Constrained Propulsion Time on Mode A Jupiter Orbiter Mission

T Propulsion Time Multiplier/1.E-1
U X-Component of Primer
V Y-Component of Primer
W Z-Component of Primer/1.E-1
X X-Component of Primer Derivative
Y Y-Component of Primer Derivative
Z Z-Component of Primer Derivative

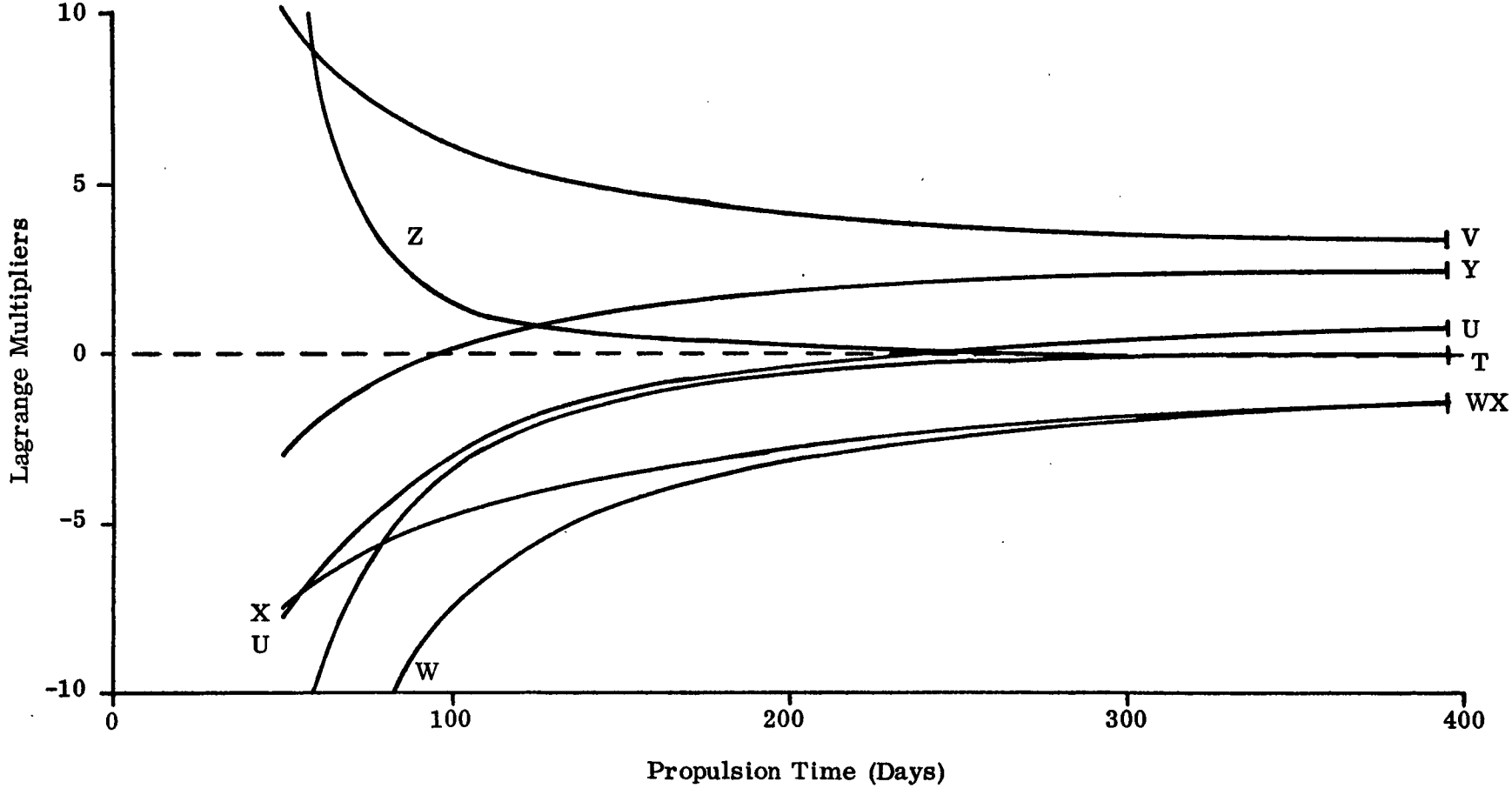

Fig. 17D Effect of Constrained Propulsion Time on Mode A Jupiter Orbiter Mission

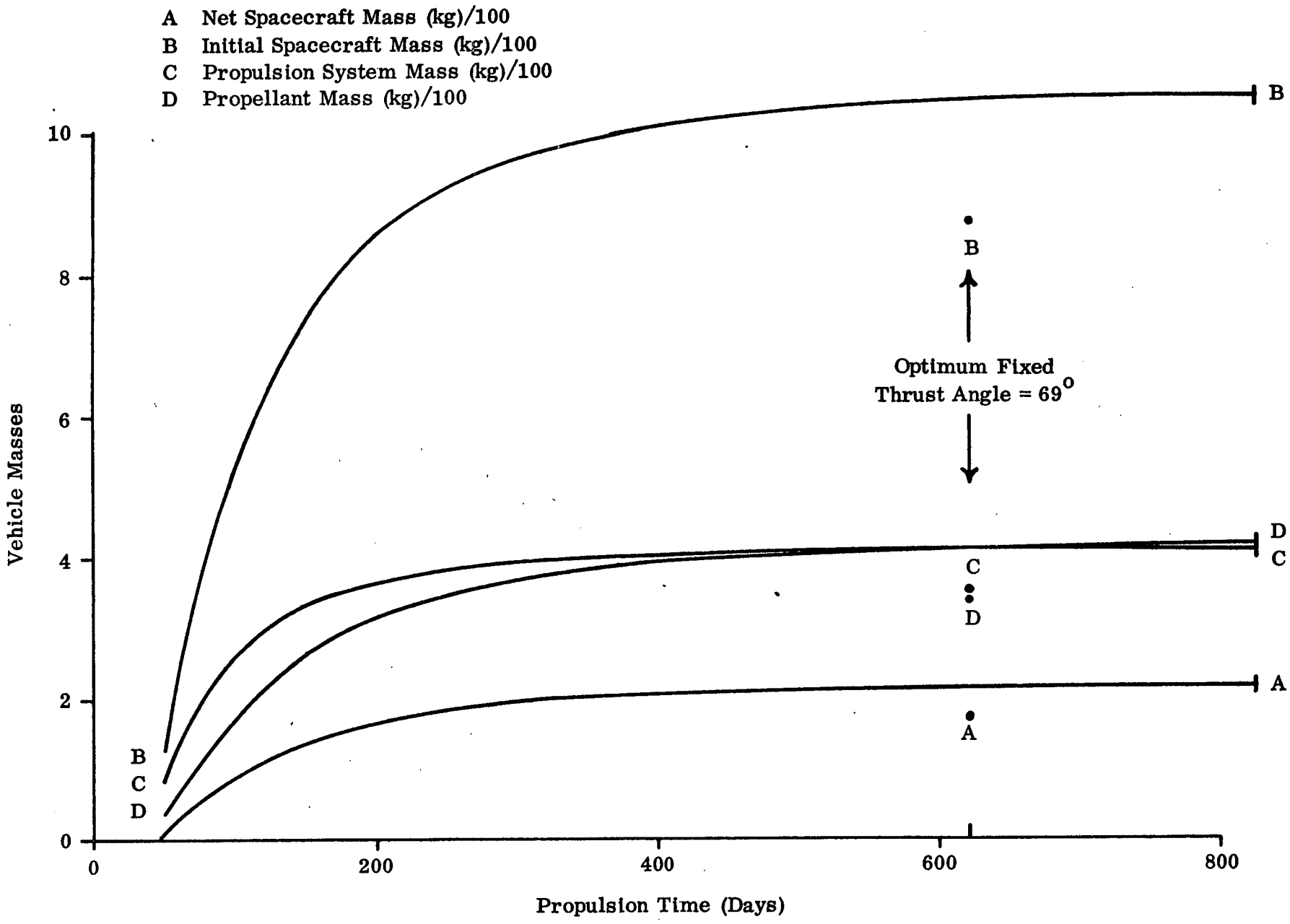

Fig. 18A Effect of Constrained Propulsion Time on Mode A Neptune Flyby Mission

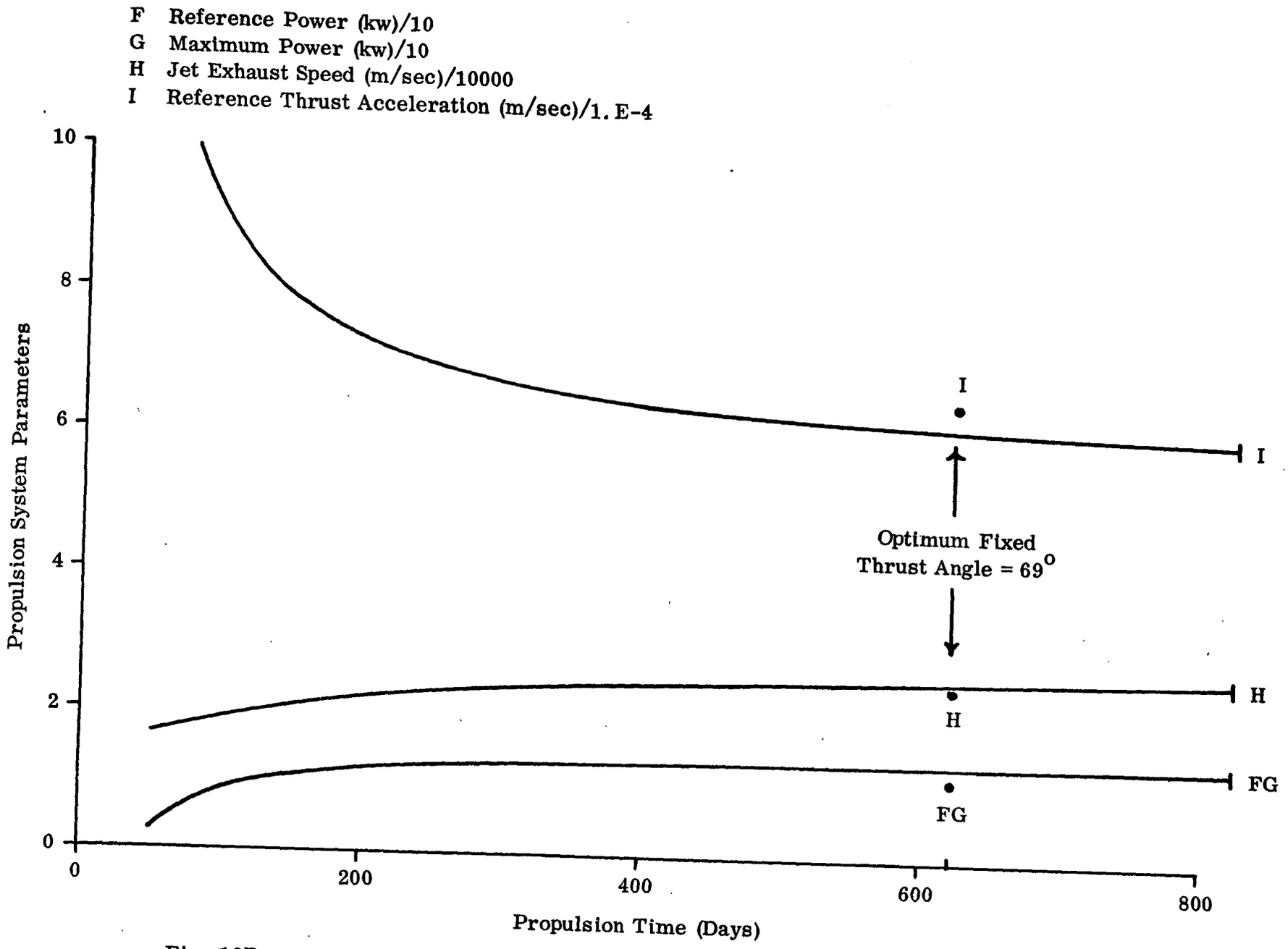

Fig. 18B Effect of Constrained Propulsion Time on Mode A Neptune Flyby Mission

K Maximum Solar Distance (au)/10
L Minimum Solar Distance (au)
M Heliocentric Travel Angle (deg)/100
N Launch Excess Speed (m/sec)/1000
O Arrival Excess Speed (m/sec)/1000
R Launch Date (Days from 2444186)/10

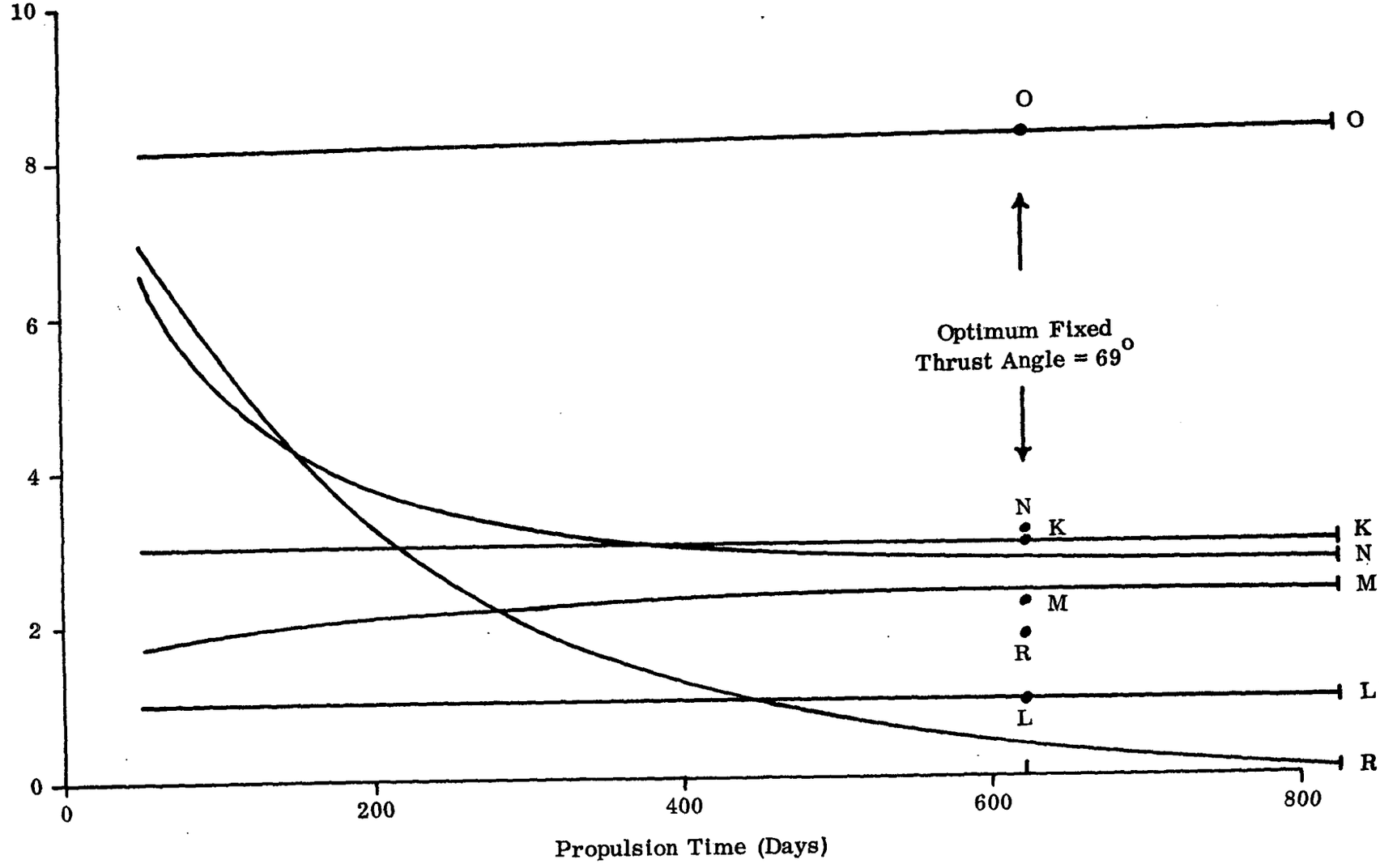

Fig. 18C Effect of Constrained Propulsion Time on Mode A Neptune Flyby Mission

T Propulsion Time Multiplier/1.E-1
U X-Component of Primer
V Y-Component of Primer
W Z-Component of Primer/1.E-1
X X-Component of Primer Derivative
Y Y-Component of Primer Derivative
Z Z-Component of Primer Derivative

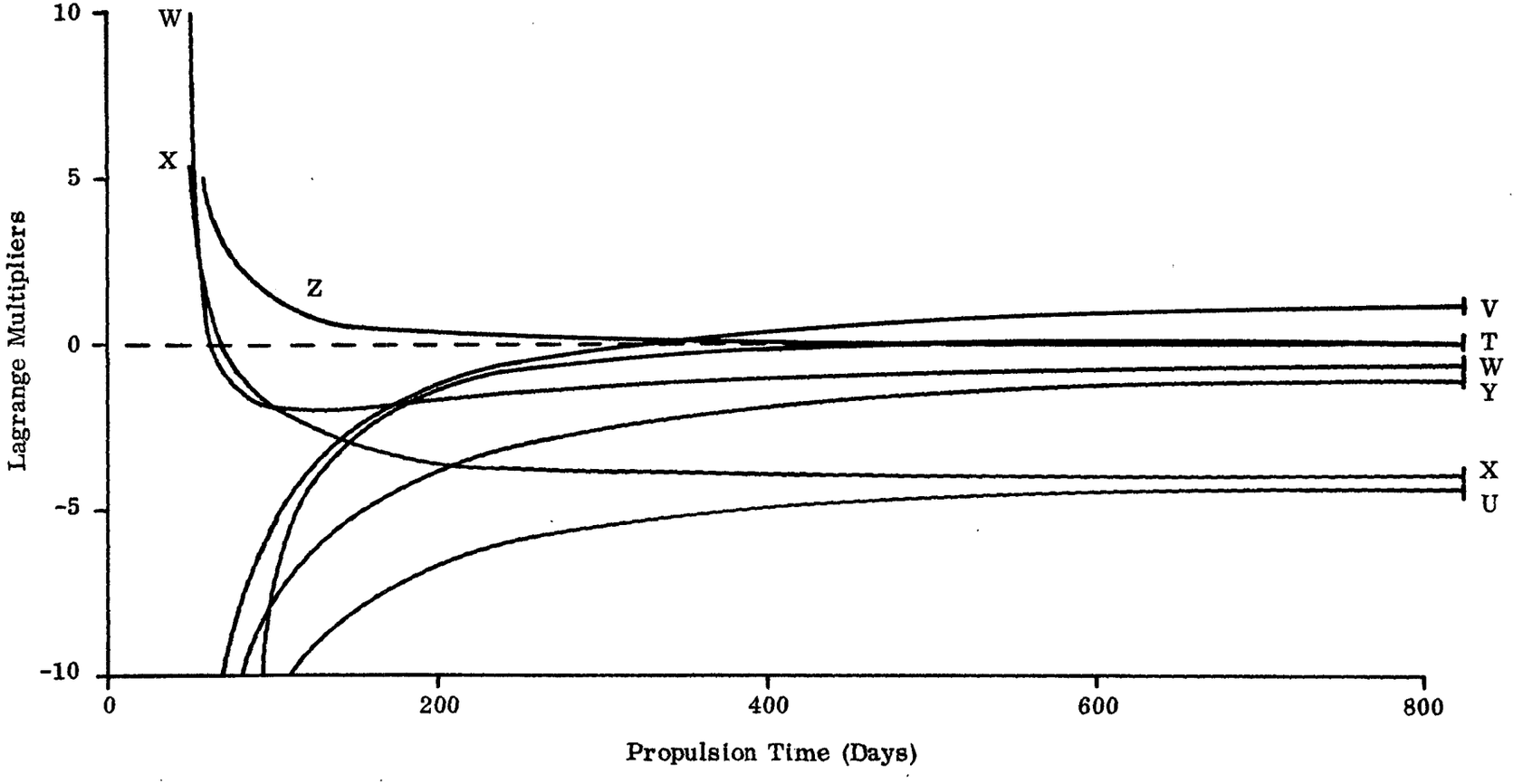

Fig. 18D Effect of Constrained Propulsion Time on Mode A Neptune Flyby Mission

A Net Spacecraft Mass (kg)/10
B Initial Spacecraft Mass (kg)/1000
C Propulsion System Mass (kg)/100
D Propellant Mass (kg)/100
E Retro Propellant Mass (kg)/100

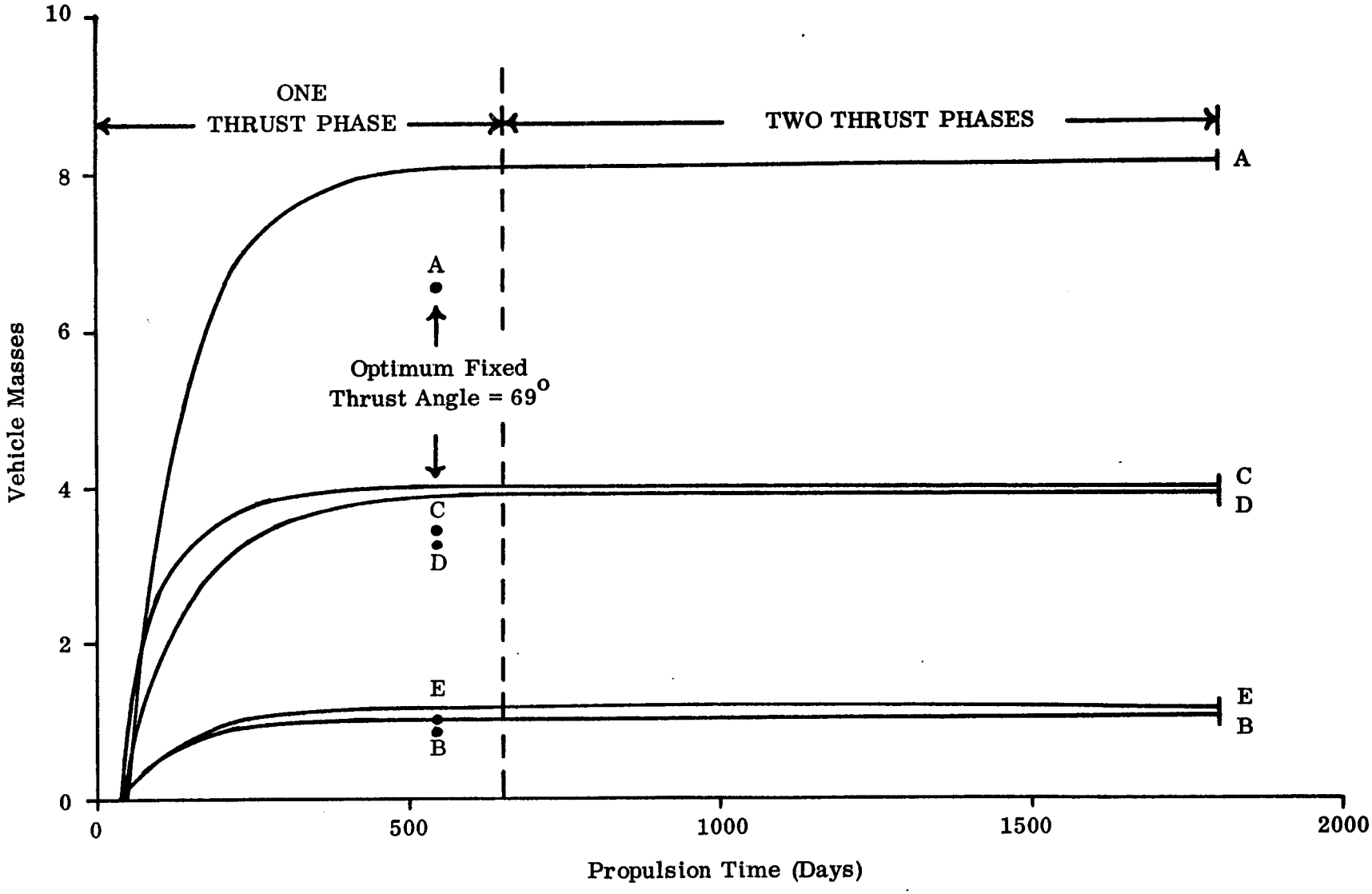

Fig. 19A Effect of Constrained Propulsion Time on Mode A Neptune Orbiter Mission

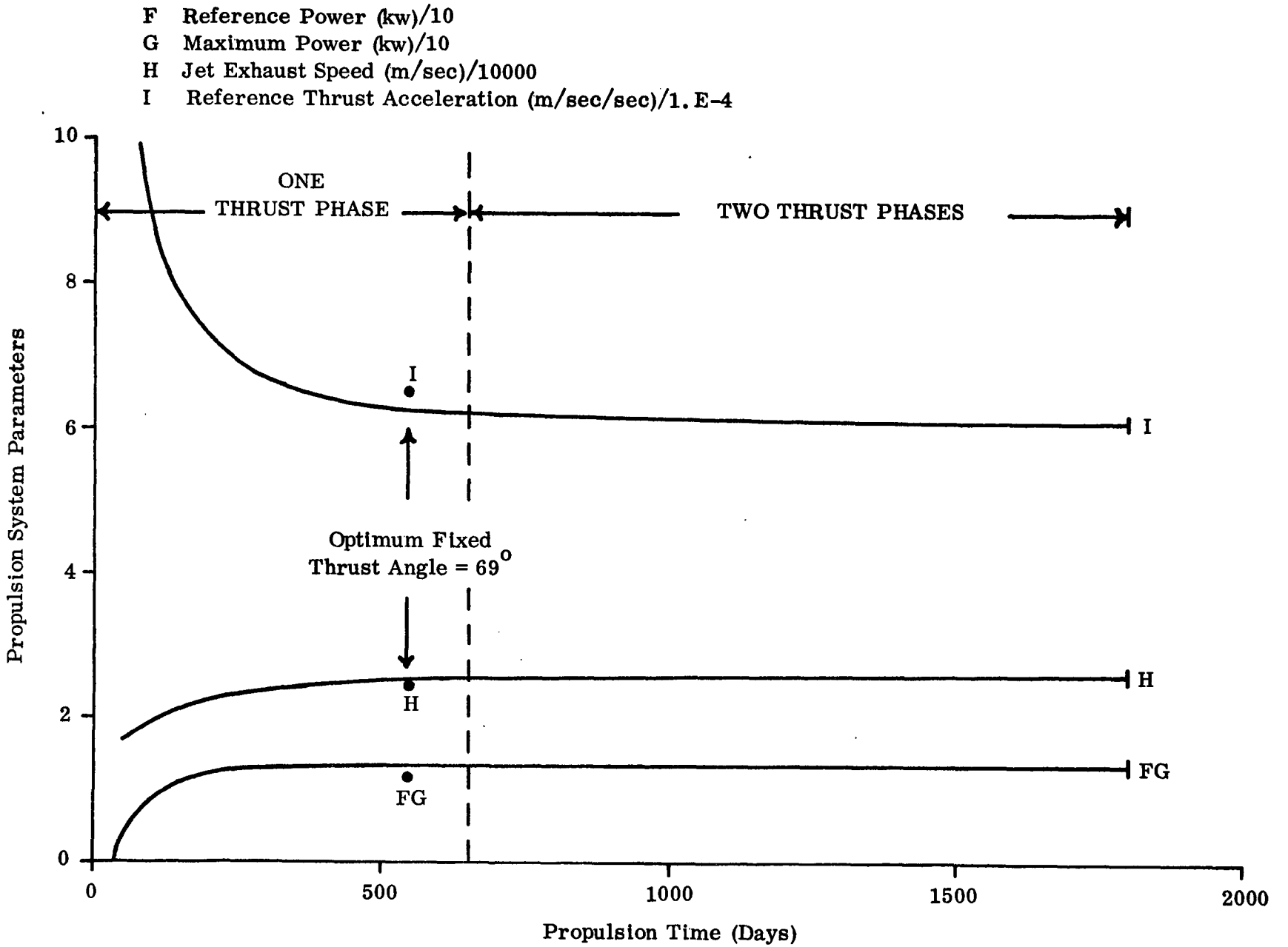

Fig. 19B Effect of Constrained Propulsion Time on Mode A Neptune Orbiter Mission

K Maximum Solar Distance (au)/10
L Minimum Solar Distance (au)
M Heliocentric Travel Angle (deg)/100
N Launch Excess Speed (m/sec)/1000
O Arrival Excess Speed (m/sec)/1000
P Retro Incremental Speed (m/sec)/1000
R Launch Date (Days From 2444190)/10

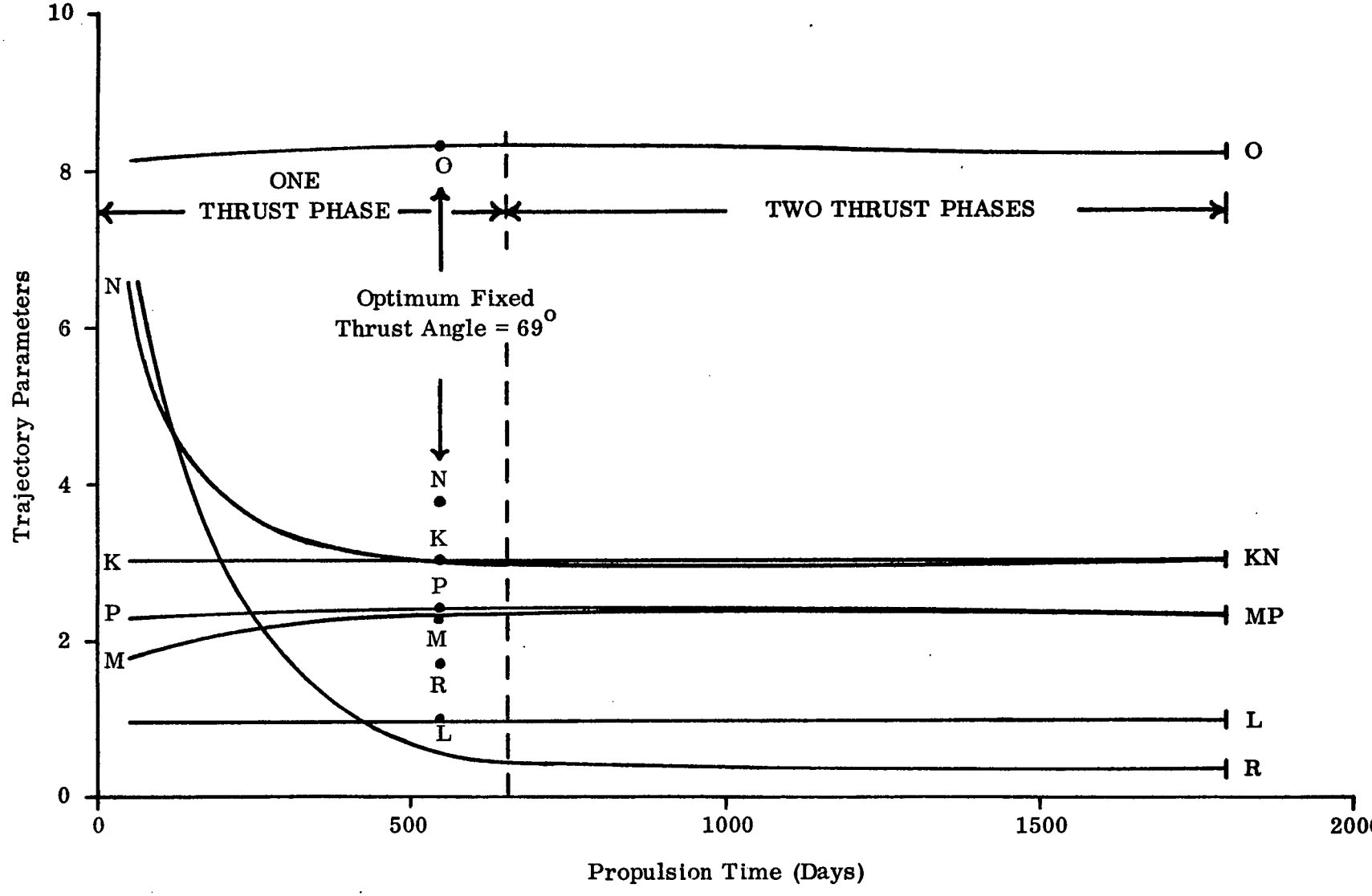

Fig. 19C Effect of Constrained Propulsion Time on Mode A Neptune Orbiter Mission

T Propulsion Time Multiplier/1.E-1
U X-Component of Primer
V Y-Component of Primer
W Z-Component of Primer/1.E-1
X X-Component of Primer Derivative
Y Y-Component of Primer Derivative
Z Z-Component of Primer Derivative

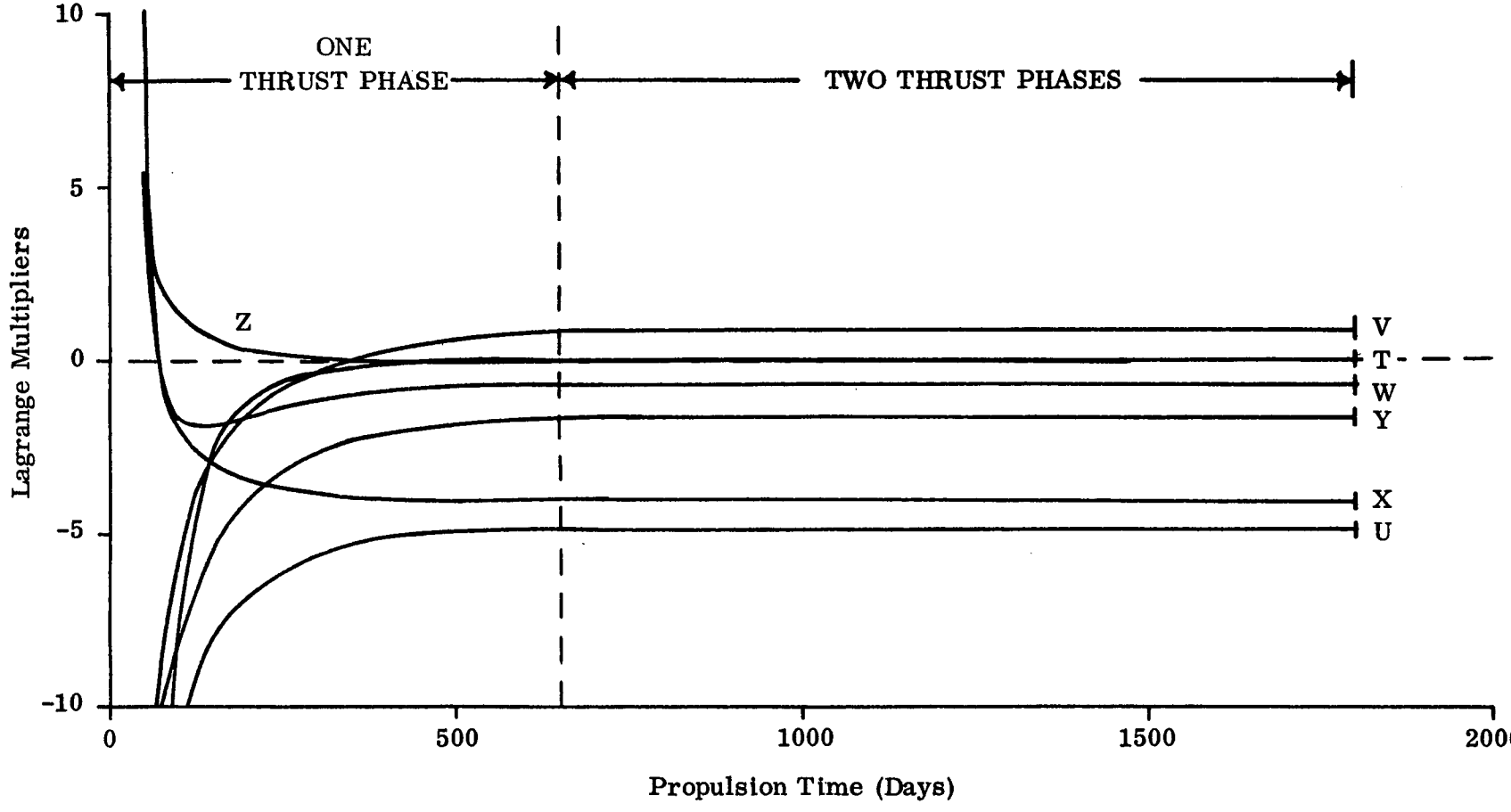

Fig. 19D Effect of Constrained Propulsion Time on Mode A Neptune Orbiter Mission

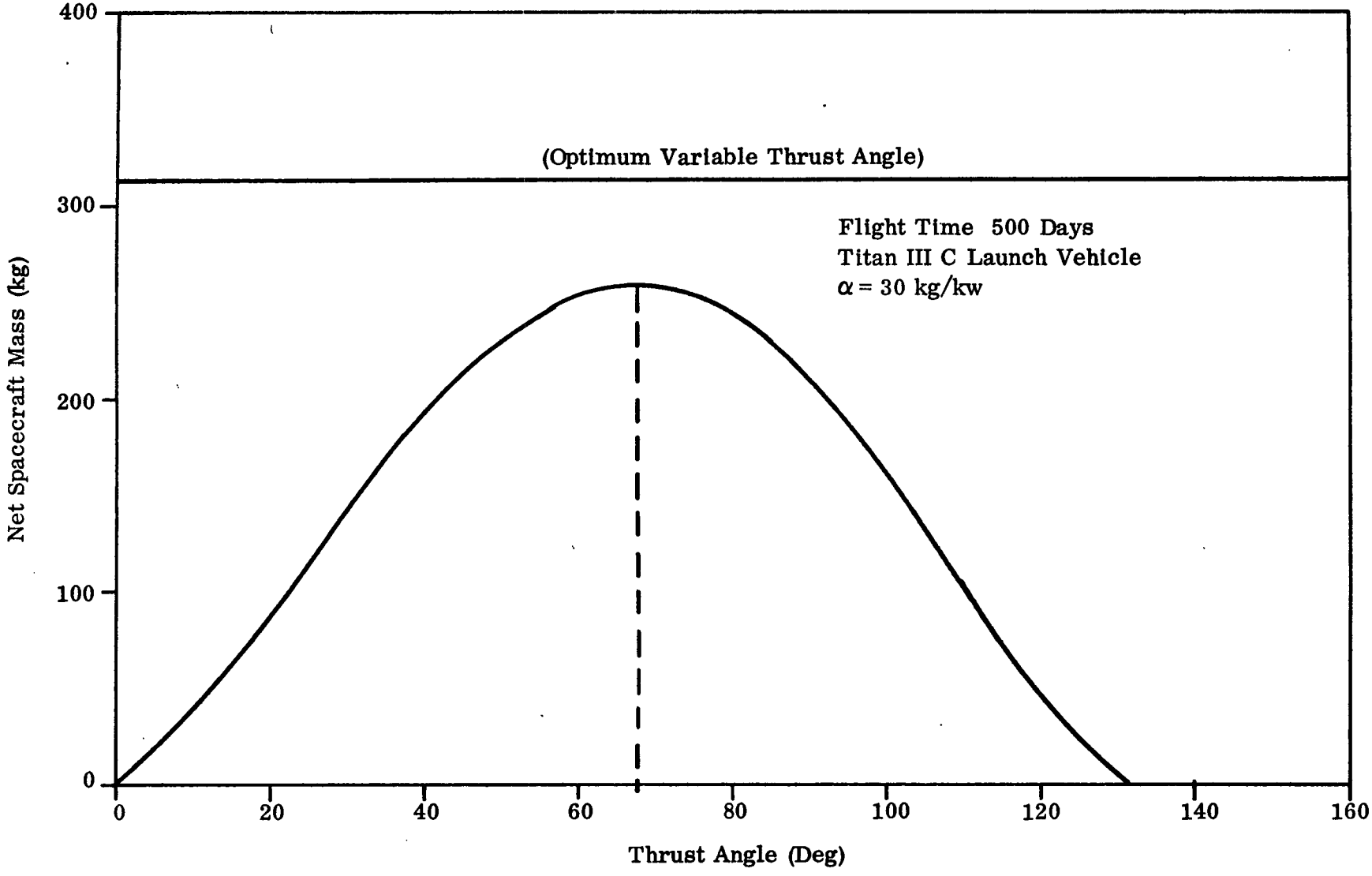

Fig. 20 Effect of Constant Thrust Angle on Jupiter Mode A Flyby Missions (2D)

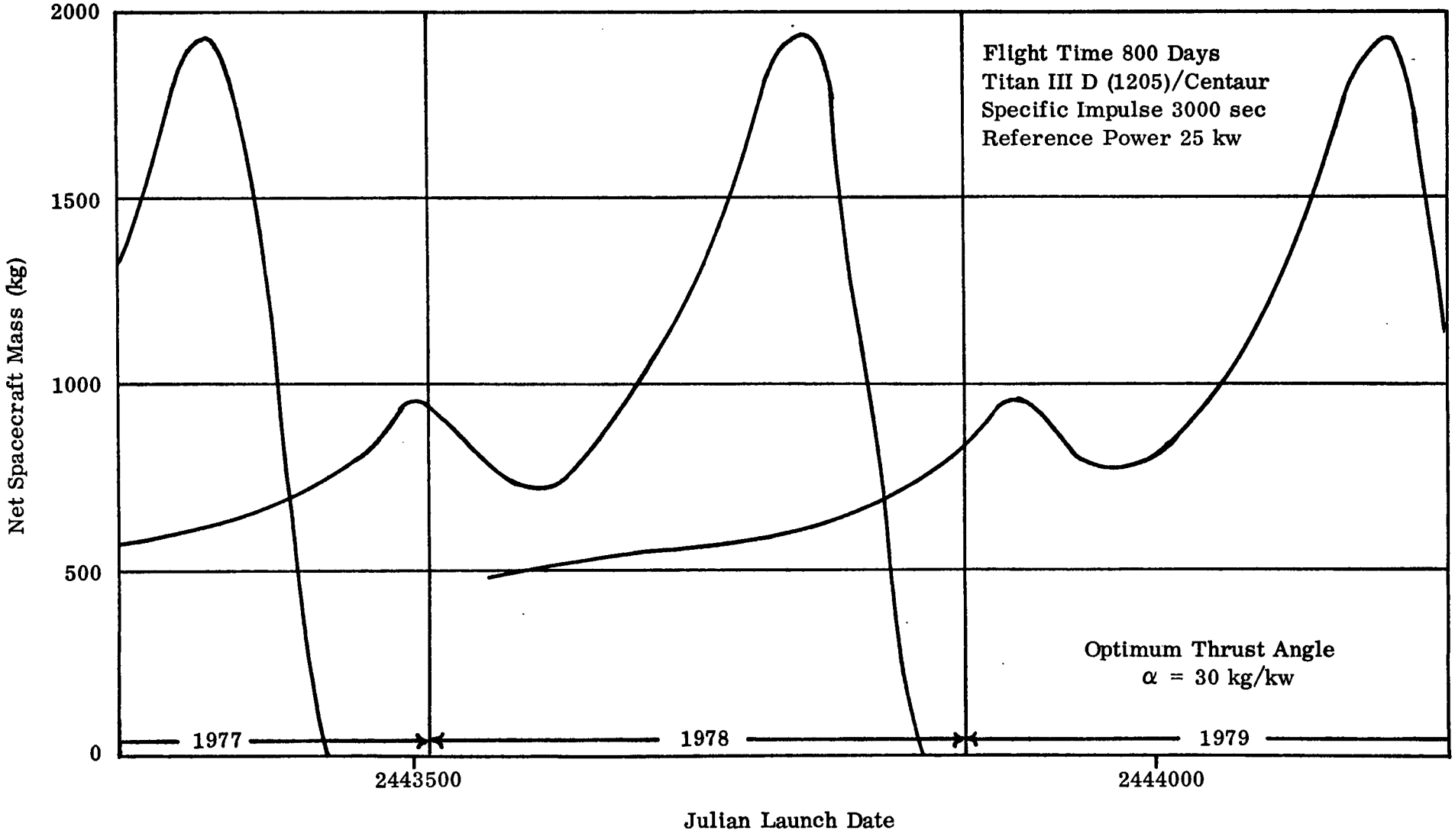

Fig. 21 1978 Jupiter Flyby Mission Window Performance Requirements

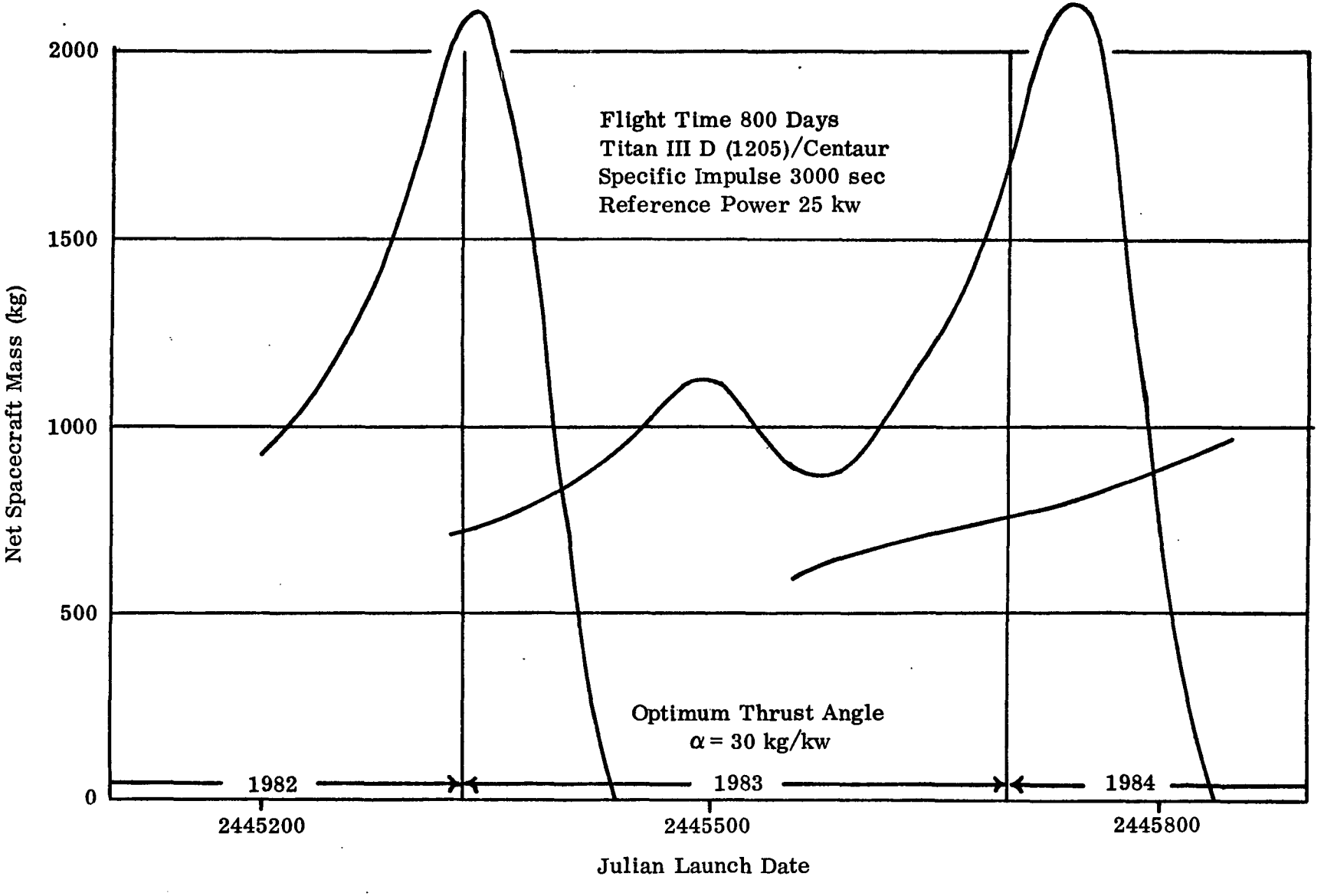

Fig. 22 1984 Jupiter Flyby Mission Window Performance Requirements

(Constructed From Figs. 21 And 22)

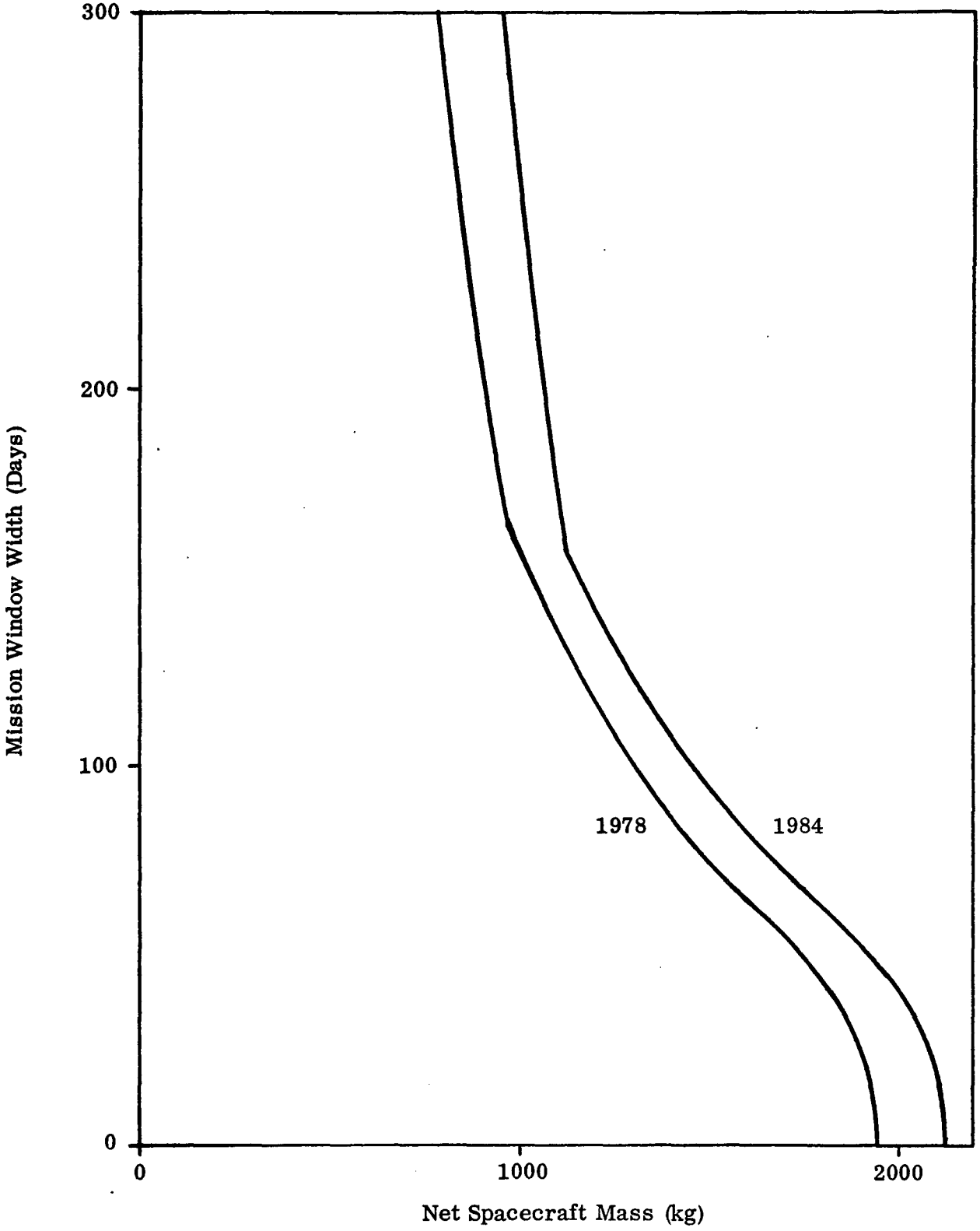

Fig. 23 Jupiter Flyby Mission Window Widths

Fig. 24 SEP MISSION PERFORMANCE CAPABILITIES

Net Spacecraft Mass (kg)

	Delta (2.5 kw) (Current)	Delta (4 kw) (Uprated)	SLV3C/C (8 kw)	Titan III C (15 kw)
800[d] Jupiter Swingby (1976)	96	154	308	575
1500[d] Jupiter Orbiter (1978)	83	133	266	498
400[d] 0.1 AU Solar Probe	50	80	160	300
510[d] Mercury Orbiter (1980)	90	144	288	540
730[d] Ceres Rendezvous (1976)	107	171	342	641
400[d] Eros Rendezvous (1979)	115	184	368	690
690[d] Icarus Rendezvous (1978)	57	91	182	340
650[d] Geographos Rendezvous (1977)	60	96	192	360
700[d] D'Arrest Rendezvous (1980)	48	77	154	288
700[d] Encke Rendezvous (1979)	83	132	264	495

Fig. 25 SEP PERFORMANCE PENALTIES DUE TO DESIGN CONSTRAINTS

Current Delta Launch Vehicle

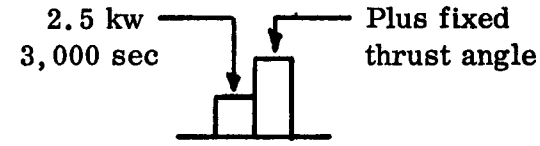

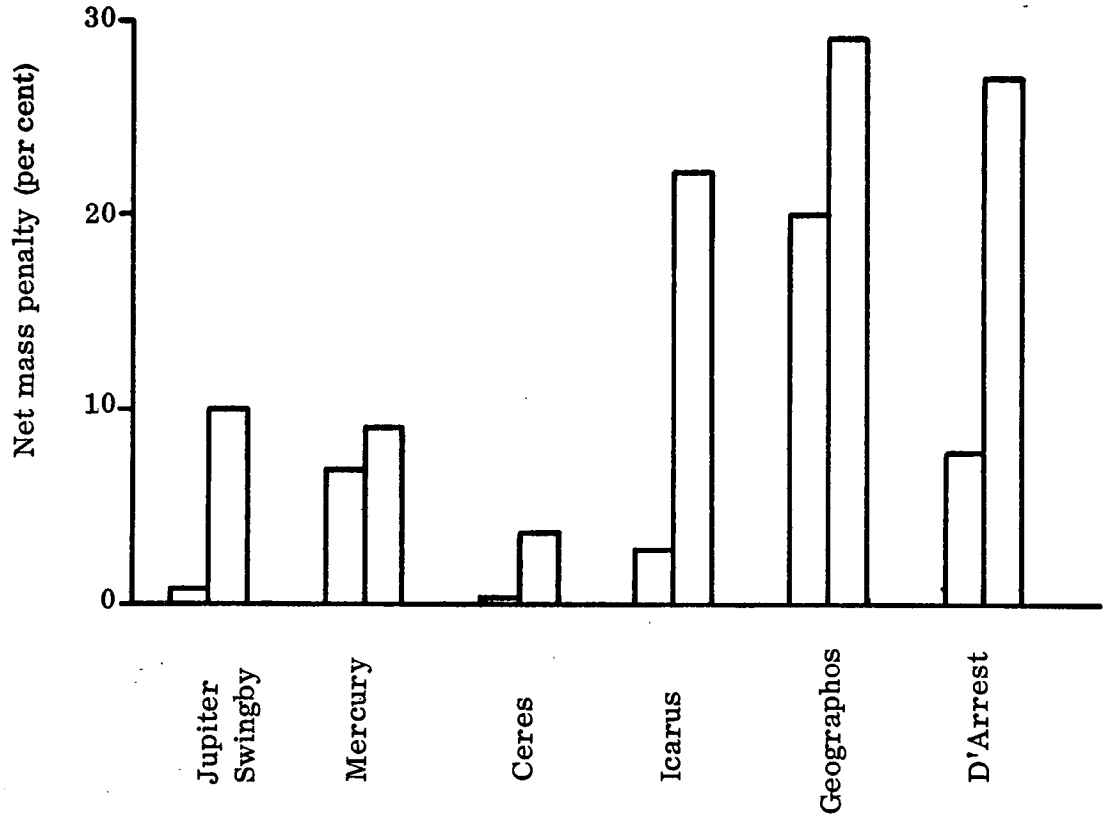

Fig. 26 730 DAY CERES RENDEZVOUS

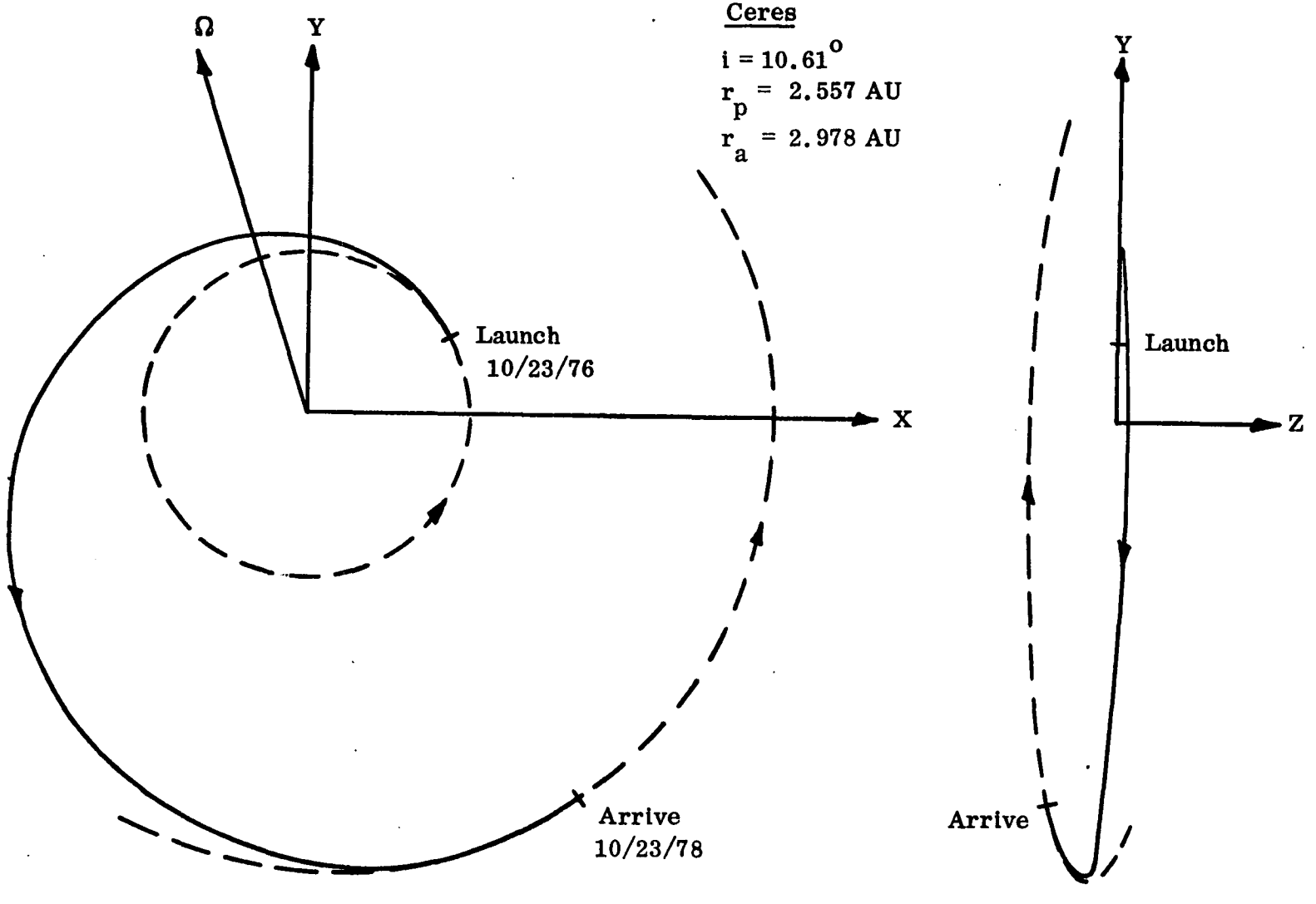

Fig. 27 400 DAY EROS RENDEZVOUS

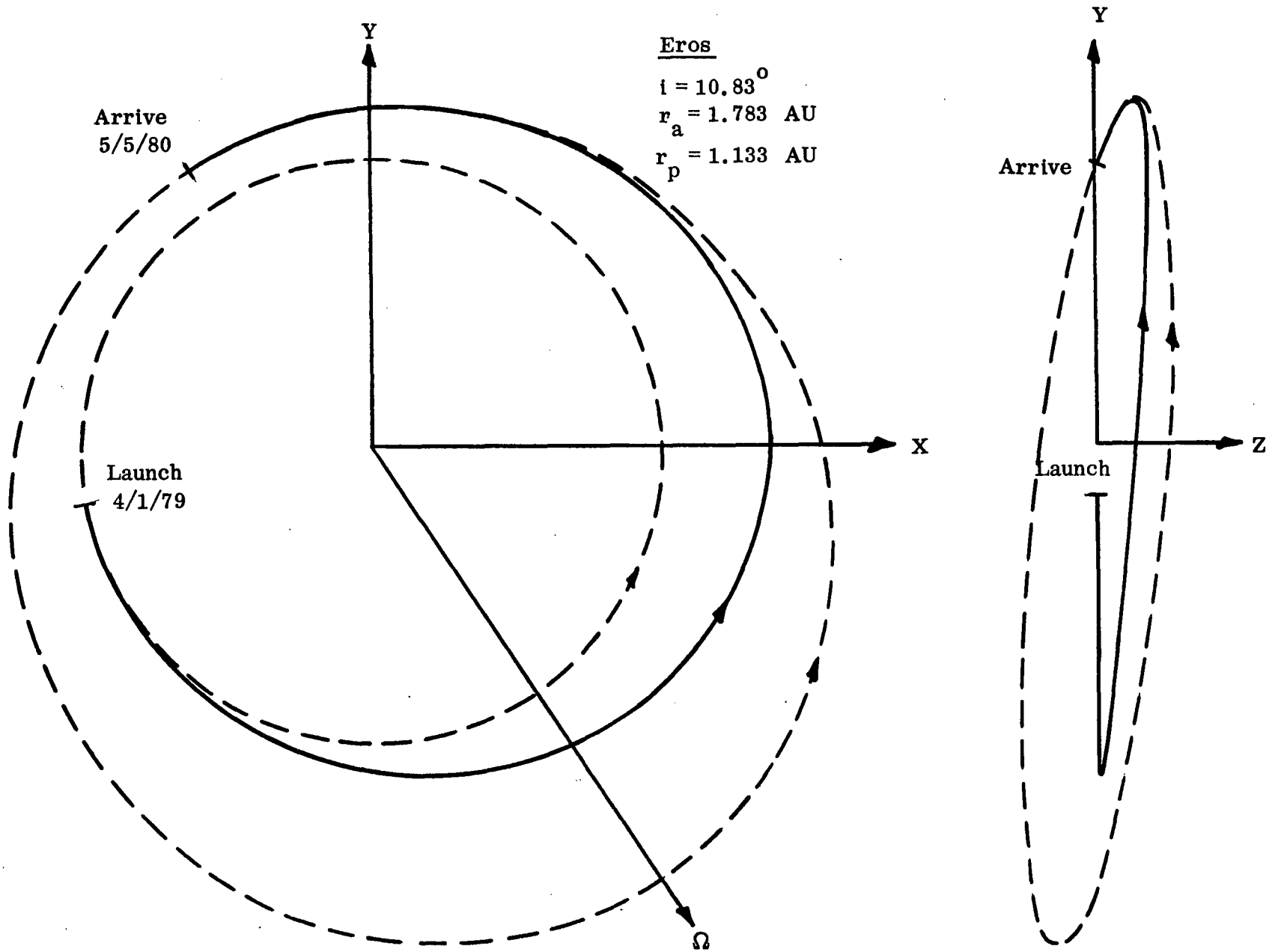

Fig. 28 650 DAY GEOGRAPHOS RENDEZVOUS

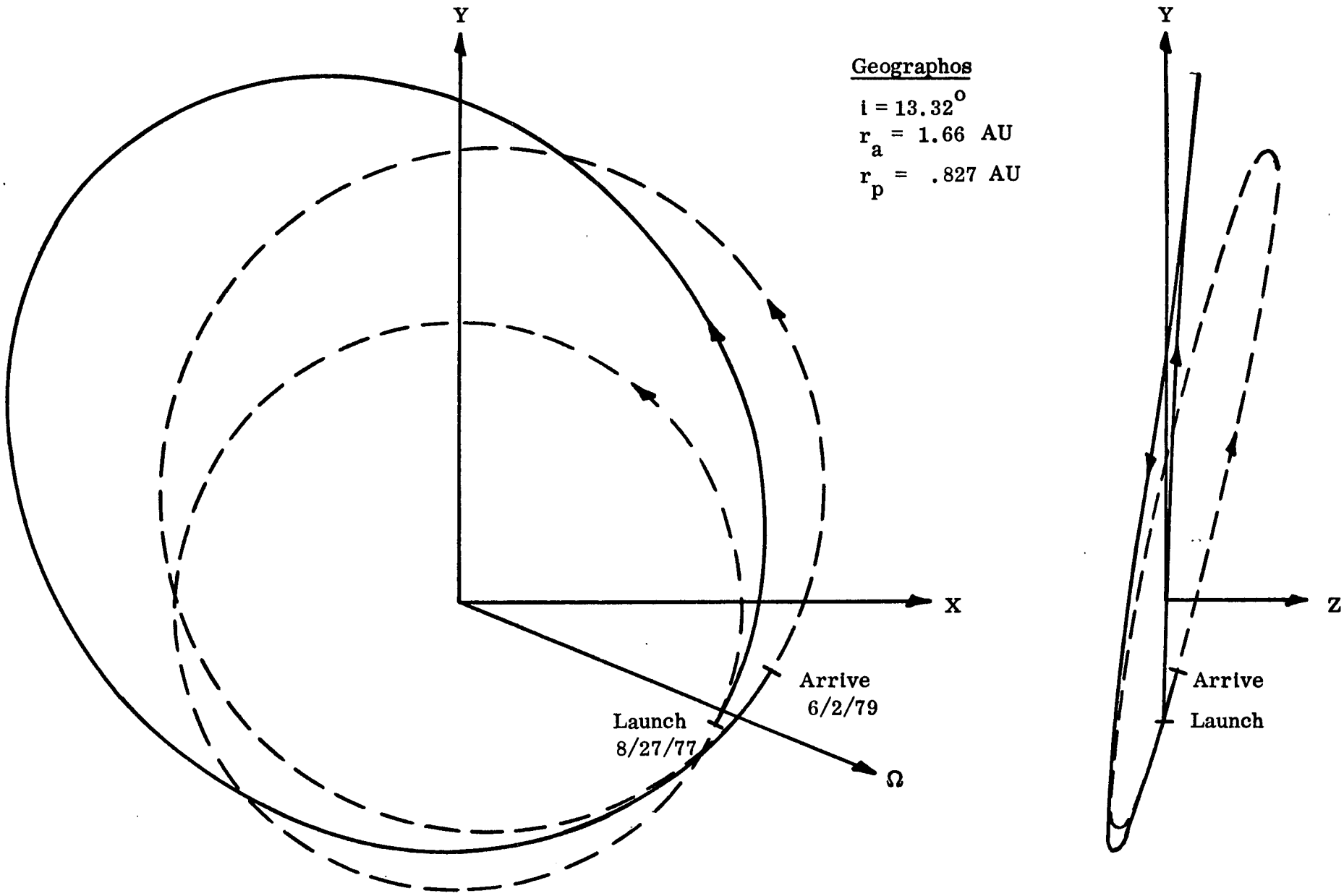

Fig. 29 690 DAY ICARUS RENDEZVOUS

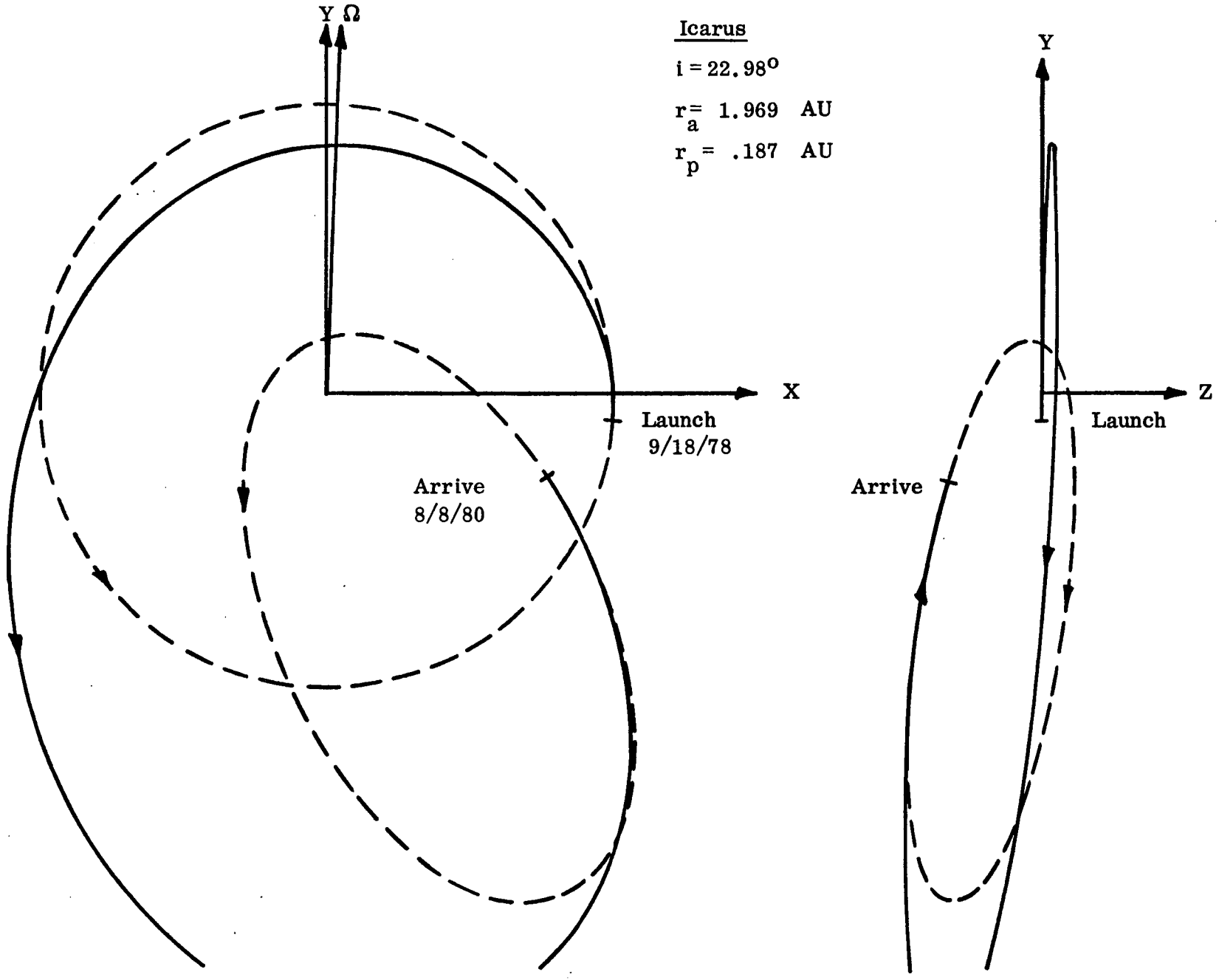

Fig. 30 700 DAY D'ARREST RENDEZVOUS

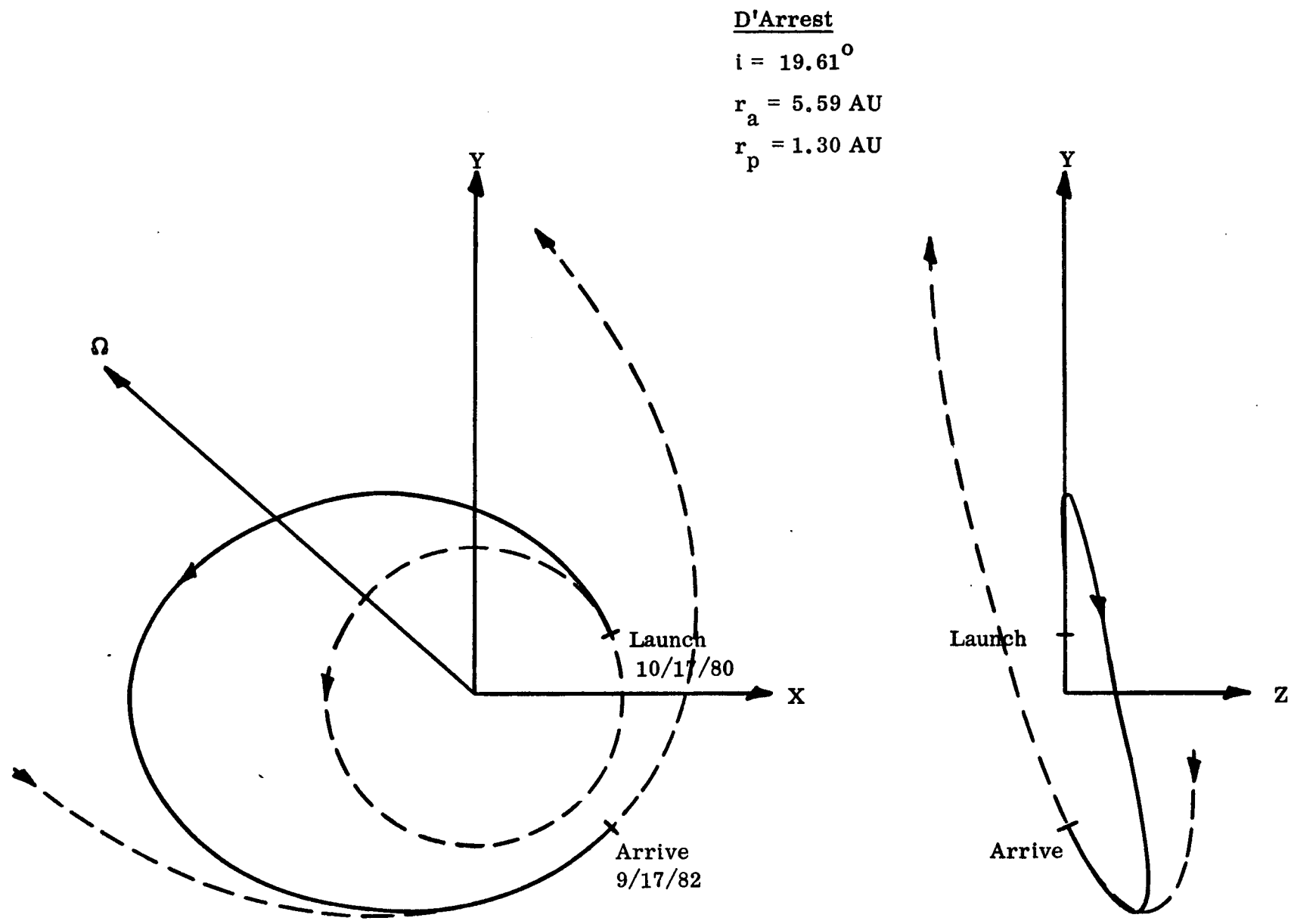

Fig. 31 700 DAY ENCKE RENDEZVOUS

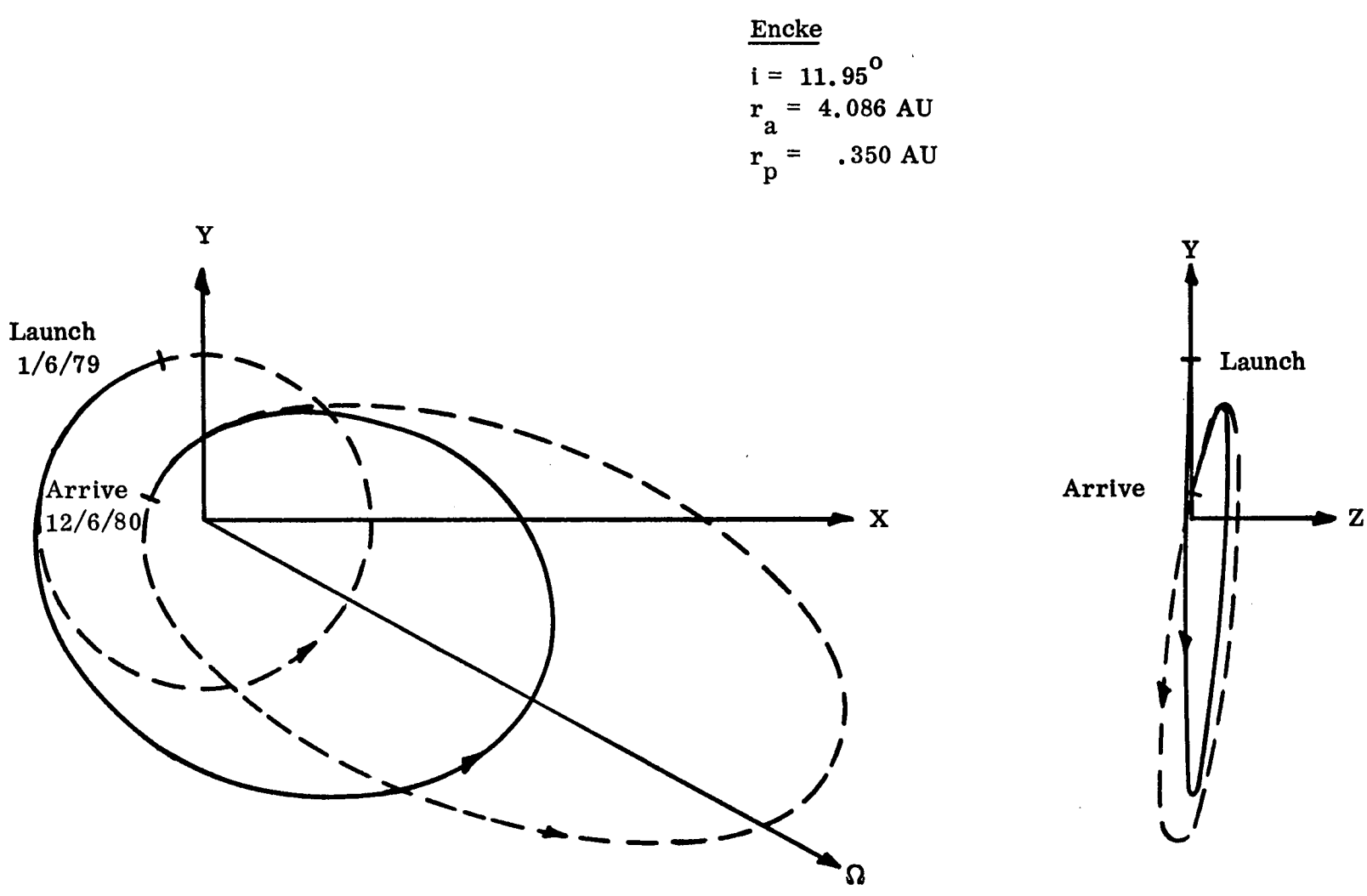

Fig. 32 510 DAY MERCURY ORBITER

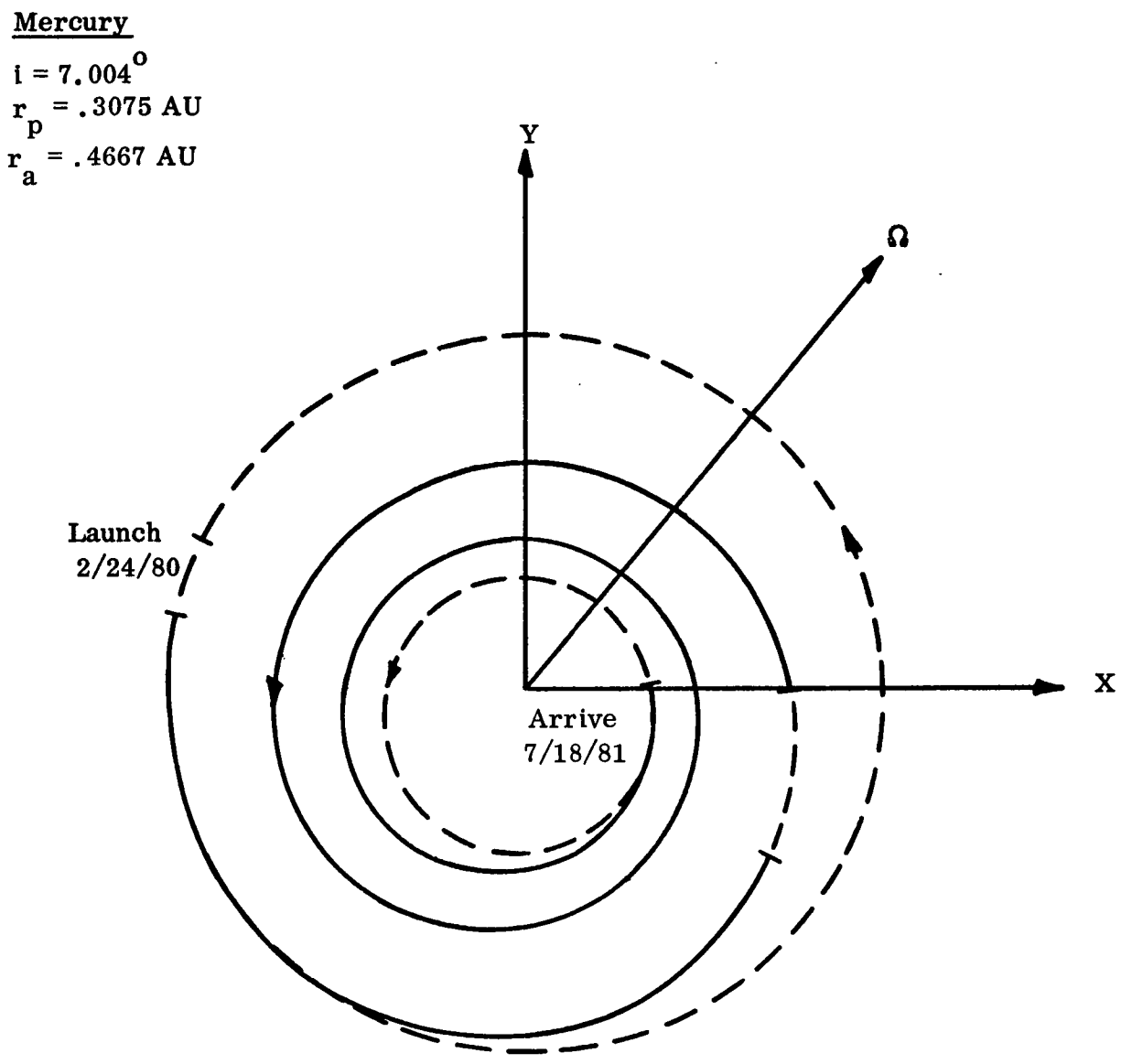

Fig. 33 400 DAY SOLAR PROBE TO 0.1 AU
$1\frac{1}{2}$ REVOLUTION SOLUTION

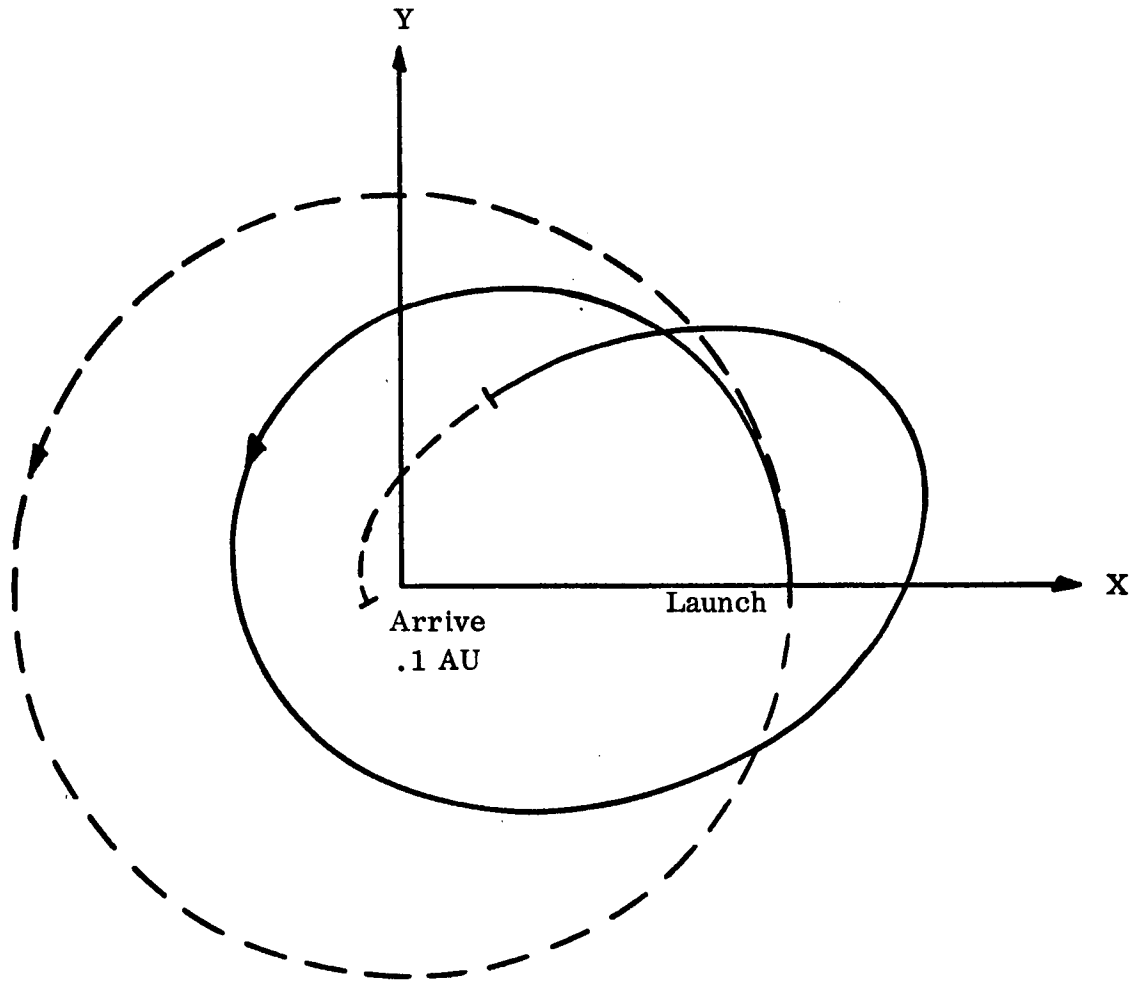

Fig. 34 GENERAL SWINGBY TRAJECTORY SCHEMATIC

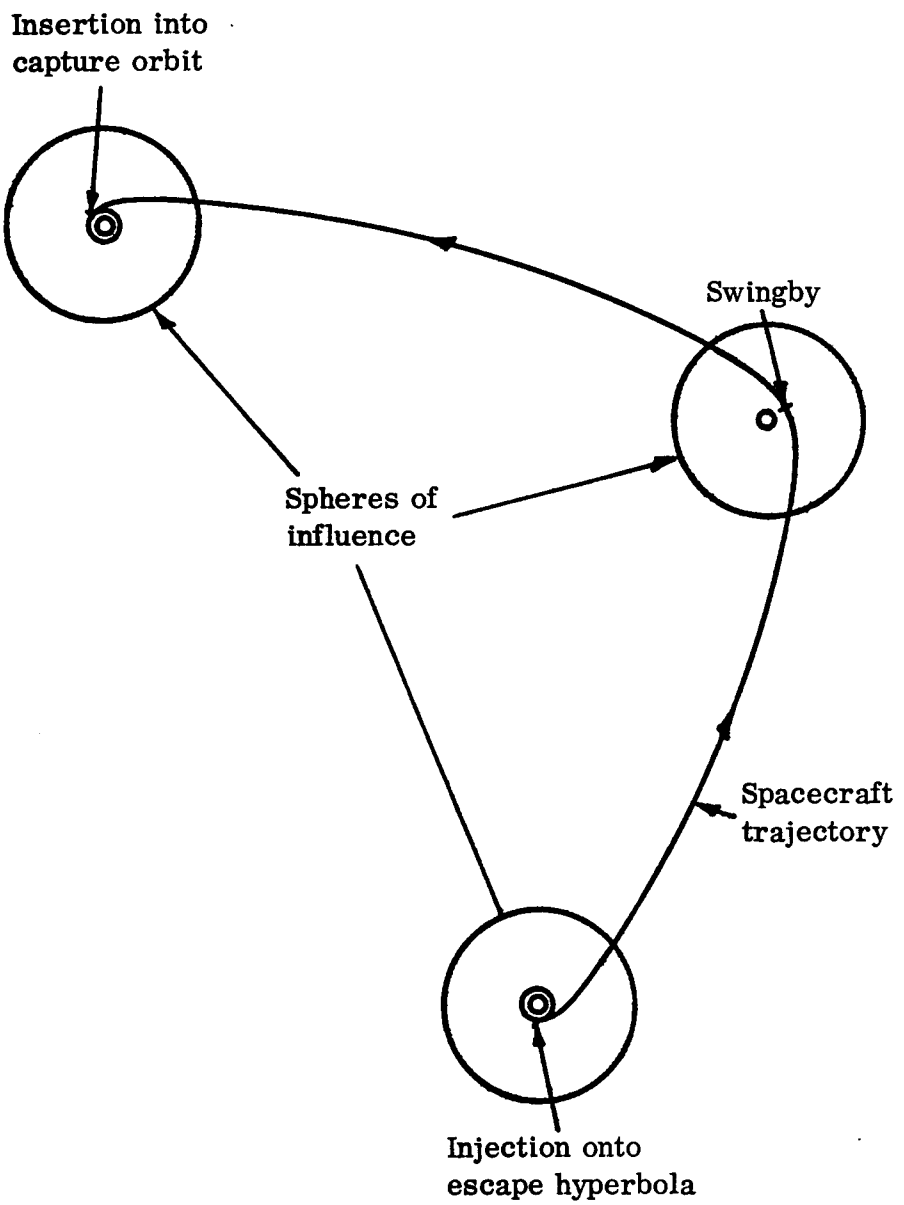

Launch July 31, 1977
(SOI = Sphere of Influence)

A - 2 Days - Leave Earth SOI, Engine On
B - 383 Days - Shut Down Engine
C - 624 Days - Enter Jupiter SOI
D - 684 Days - Pass Jupiter At 10.36 Radii
E - 744 Days - Leave Jupiter SOI
F -1349 Days - Enter Saturn SOI

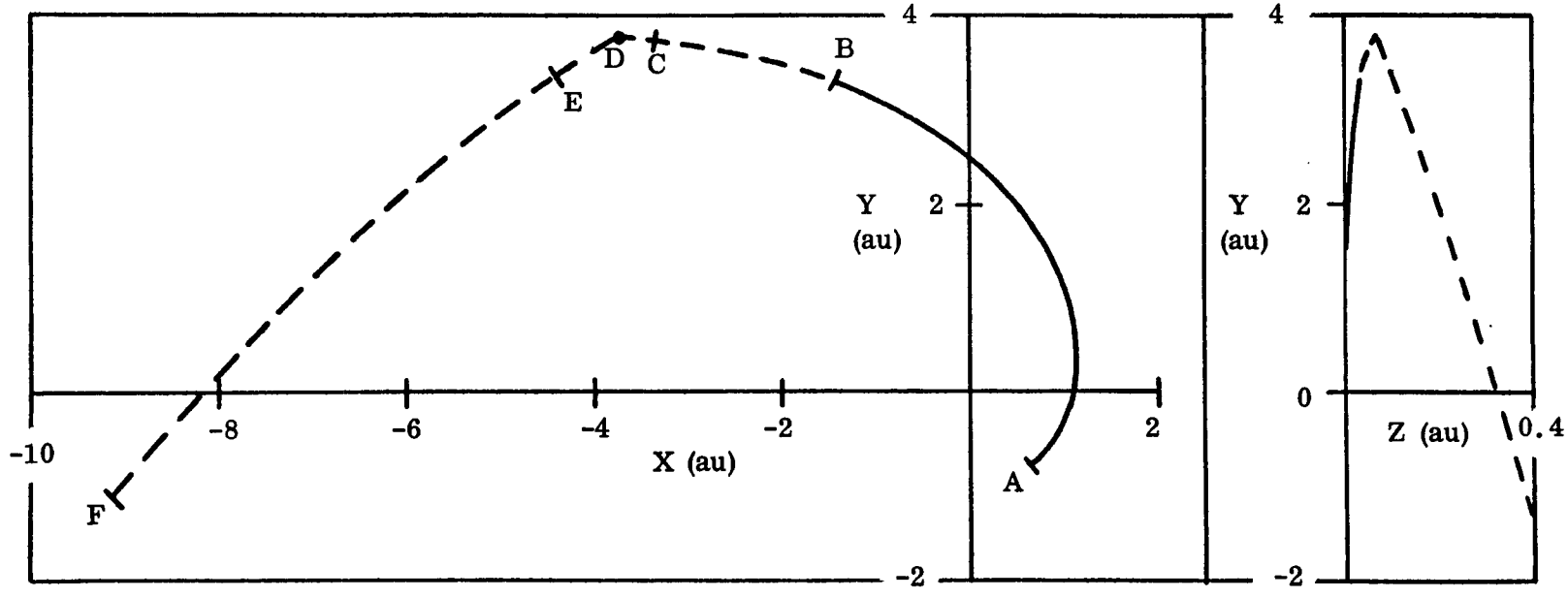

Fig. 35 1400 Day Earth-Jupiter-Saturn Trajectory

Fig. 36

NET SPACECRAFT MASS CAPABILITIES

FOR 1400 DAY SATURN MISSIONS

USING TITAN III D/CENTAUR

	Orbiter	Flyby
Direct - ballistic	406	838
Direct - SEP	702 (33.8)	1483 (36.7)
Jupiter Swingby - ballistic	271	975
Jupiter Swingby - SEP	470 (28.9)	1817 (34.1)

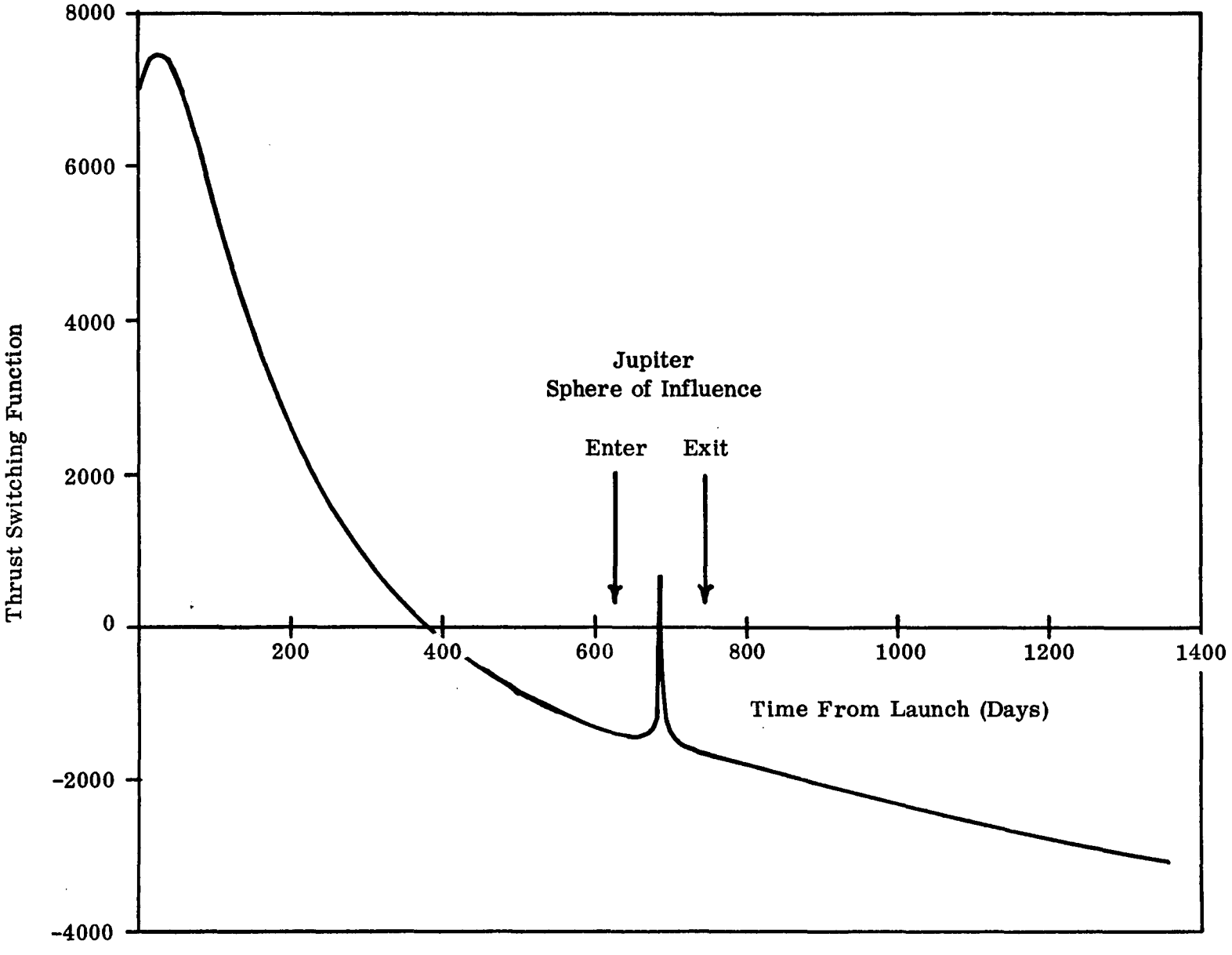

Fig. 37 Thrust Switching Function History On 1400 Day Earth-Jupiter-Saturn Trajectory

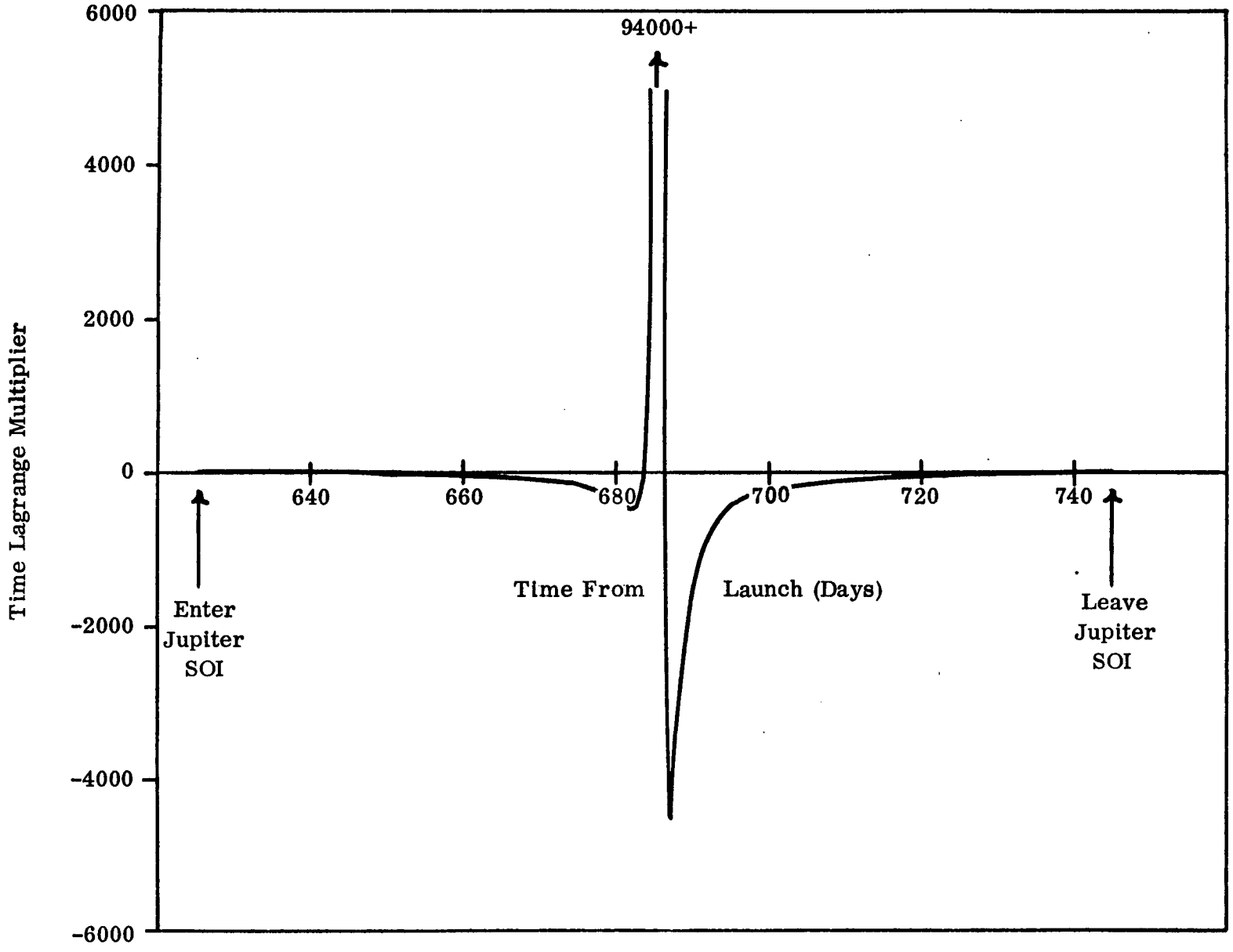

Fig. 38 Time Lagrange Multiplier History Inside Jupiter Sphere of Influence

REFERENCES

[1] J. L. Horsewood and F. I. Mann, "Optimum Solar Electric Interplanetary Trajectory and Performance Data," NASA CR 1524, April 1970.

[2] J. L. Horsewood and F. I. Mann, "Solar Electric Interplanetary Trajectory and Performance Data for Sub-Optimal Powered Spacecraft," NASA CR 112840, April 1970.

[3] J. L. Horsewood, F. I. Mann and P. F. Flanagan, "Solar Electric Performance Data for Extra-Ecliptic and Solar Probes and Ceres, D'Arrest, and Encke Rendezvous Missions," NASA CR 118312, December 1970.

[4] J. L. Horsewood and F. I. Mann, "Solar Electric Propulsion Mission Requirements Study," Analytical Mechanics Associates, Inc., Report No. 70-48, December 1970.

[5] F. I. Mann and J. L. Horsewood, "Optimum Solar Electric Interplanetary Mission Opportunities from 1975 to 1990," Analytical Mechanics Associates, Inc., Report No. 71-44, December 1971.

[6] J. L. Horsewood, P. F. Flanagan, and F. I. Mann, "HILTOP: Heliocentric Interplanetary Low Thrust Trajectory Optimization Program," Analytical Mechanics Associates, Inc., Report No. 71-38, November 1971.

[7] J. L. Horsewood and C. Hipkins, "SWINGBY: A Low Thrust Interplanetary Swingby Trajectory Optimization Program," Analytical Mechanics Associates, Inc., Report No. 71-10, March 1971.

[8] D. W. Hahn and F. T. Johnson, "Chebychev Trajectory Optimization Program (CHEBYTOP II)," The BOEING Company Report D180-12916-1, June, 1971.

[9] F. I. Mann, "Global Trajectory Targeting Via Computer Graphics," Analytical Mechanics Associates, Inc., Report No. 71-39, November 1971.

[10] M. H. Payne, "Truncation Effects in Geopotential Modeling," Analytical Mechanics Associates, Inc., Report No. 71-40, November 1971.

[11] F. I. Mann, "ADMAP (Automatic Data Manipulation Program) Computer Program Utilization Report," Analytical Mechanics Associates, Inc., Report No. 71-1, January 1971.

[12] "Launch Vehicle Estimating Factors," NASA Office of Space Science and Applications, January 1971.

[13] T. Barber, H. Meissinger, and J. L. Horsewood, "Simplified Techniques for Mission Analysis of Low Thrust Vehicles," Presented at AAS Seminar on Mission Analysis Techniques, Jet Propulsion Laboratory, Pasadena, California, May 1971.

[14] J. L. Horsewood, "Applications of Solar Propulsion for the Exploration of the Solar System," Presented at the 1971 Theoretical Mechanics Branch Astrodynamics Conference at the Goddard Space Flight Center, Greenbelt, Maryland, April 1971.